INTERSTELLAR MATTER, GALACTIC STRUCTURE, AND THE $l^{II} = 40^{o}$ REGION

by

William Andrew Sherwood

Ph. D.

University of Edinburgh

1973

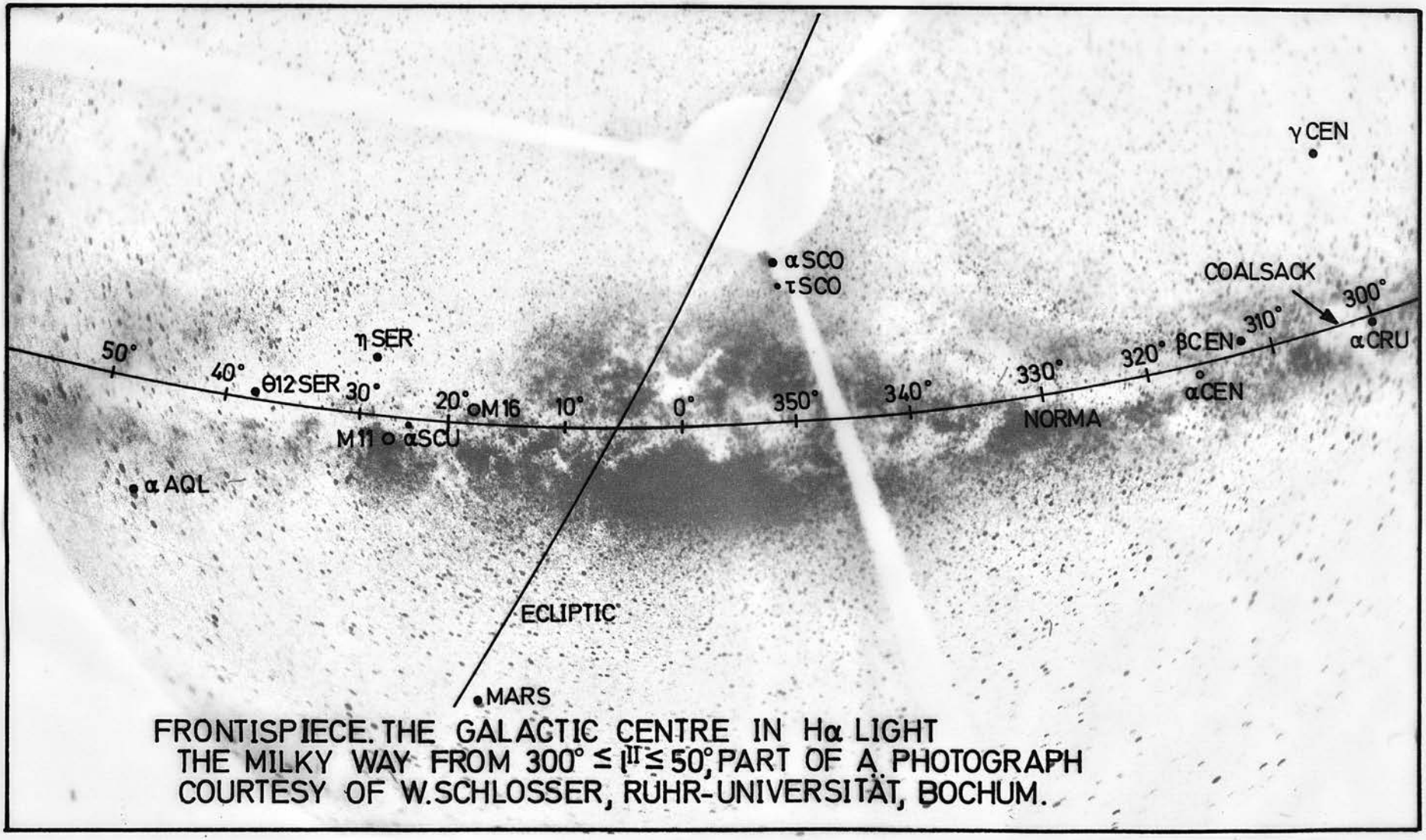

FRONTISPIECE. THE GALACTIC CENTRE IN Hα LIGHT
THE MILKY WAY FROM $300° \leq l^{II} \leq 50°$, PART OF A PHOTOGRAPH
COURTESY OF W. SCHLOSSER, RUHR-UNIVERSITÄT, BOCHUM.

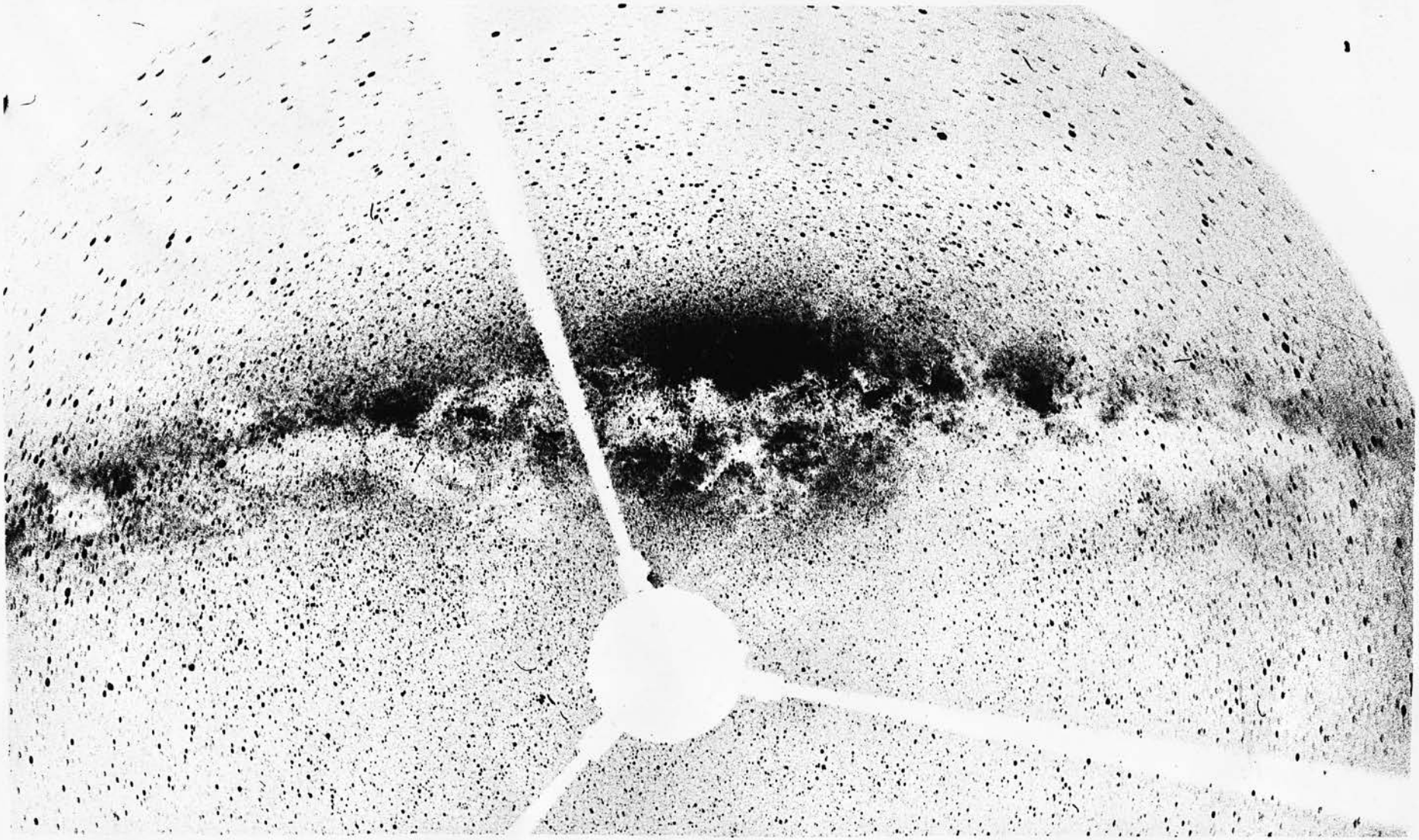

Abstract

Photoelectric and photographic observations of 400 stars and 3200 stars respectively have been used to determine the position of O-B2 stars and dust in a region centred at $l^{II}=40^{o}$, $b^{II}=0^{o}$. The photographic photometry was based on measurements by GALAXY. Objective prism spectra were used to classify several hundred of these stars.

The Sagittarius arm is traced from 30^{o} to 50^{o}; at $l^{II}=40^{o}$, it is more than 5000 parsecs from the Sun.

Some O-B2 stars in this direction belong to the Cygnus feature which is tentatively identified as a spur rather than an arm.

The dust is also associated with the Cygnus spur, lying between 300 and 1000 parsecs from the Sun. The greatest density occurs nearest the Sun with the obscuration reaching as much as 15 magnitudes/kpc. The total optical depth is about 6.

The dust does not share the same spatial distribution as the O-B2 stars although the neutral hydrogen is distributed similarly to the stars. There appears to be a population of late-type stars associated with the cloud, and while these stars may be pre-main sequence, they do not exhibit T-Tauri spectral characteristics.

The classification of galaxies is reviewed; gas, dust, and stars sometimes give quite different results.

In our Galaxy, it is possible that the optical classification might be earlier than the radio classification.

Acknowledgements

Some acknowledgements are perfunctory - not this one. I have travelled from Canada to study, at Edinburgh, data obtained in Italy and in Chile; the work was completed in Bochum, Germany. Everywhere I have made friends. Their interest and encouragement has made this labor worthwhile.

I would like to thank Professors Brück and Schmidt-Kaler for their hospitality in Edinburgh and Bochum, and for their generous allotments of observing time in Italy and Chile. Dr. Vincent Reddish, as my supervisor and friend, asked the questions which led to this thesis. In Italy, through the courtesy of Dr. G. Caprioli, I was able to measure several focus plates on the Becker iris photometer on Monte Mario. In Chile, through the courtesy of Dr. John Graham, I was able to take objective prism spectra at Cerro Tololo. Dr. Nancy Houk, then at Warner and Swasey Observatory, sent me low dispersion objective prism plates used in a preliminary survey. Dr. Mark Chartrand III, also at Warner and Swasey, measured some stars photoelectrically when it seemed that I would not be able to observe myself - these stars will be used in the calibration of the entire Schmidt field. Dr. Barry Turner sought OH in the cloud region, but nothing was found. Dr. W. Schlosser has allowed me to use his all-sky camera photographs of the Milky Way (Frontispiece and Plate 1)

which have been adapted for this thesis by Herr W. Hünecke. Messrs David Cooper and Joachim Kluke have been very helpful in explaining the various computing problems that I have had. Drs. Tony Moffat and Nikolaus Vogt have allowed me to use some of their programmes and Tony has allowed me to use his observations of OB stars between 40° and 50° l^{II}. Herr H. Brauer has drawn most of the fine figures; my wife Vicki has drawn the others. She has also typed this thesis - no mean achievement with thirty pages of tables and everything in my illegible script. I am especially thankful to her for her patience and understanding.

To Vicki and all my friends, I dedicate this thesis.

Table of Contents

Chapter 1

Introduction to Interstellar Matter and Galactic Structure

1.1 A General View

The Frontispiece shows the Milky Way, the projection of our Galaxy on the celestial sphere. It is a flat disc-like object with a bright nuclear bulge and an irregular surface brightness caused by the distribution of stars and dust. It is not clear from inspection what the multi-dimensional character of our Galaxy is really like. For this reason, I propose to begin with an examination of external galaxies and to compare them with our Galaxy. In particular, we are interested in the relationship between dust (presence, amount, distribution) and the structure of a galaxy.

In order to limit our search to galaxies which may be expected to resemble our own, we must first have a classification of our Galaxy. To do this, de Vaucouleurs (1970) has used six, basically radio, criteria:

i) multiplicity of spiral pattern
ii) inner ring diameter
iii) broken ring structure
iv) radio structure of nucleus
v) integrated spectral type
vi) HI diagram

From these, he found the Galaxy to be of type SAB(rs)bc where bc is the Hubble type Sbc, an intermediate spiral galaxy between Sb and Sc (Sandage, 1961); AB (A = absence, B = presence of a bar in the nucleus) denotes the partial formation of a bar; and rs (r = inner ring, s = spiral to the nucleus, ie. no inner ring structure) indicates partial ring structure. The central galaxy in de Vaucouleurs' Figure 1 illustrates the type.

Spiral structure has been (historically or traditionally) defined by optical features; viz. HII regions, dust lanes, and bright blue supergiants. Galactic structure is much more; it includes the spiral structure defined optically as well as the structure defined by other classes of objects which may be optically and physically invisible; eg. neutral hydrogen and dynamical qualities such as angular momentum and pressure. We should not expect **a priori** one class of object to fit the galactic structure derived from another class. Three examples will be given.

To date external galaxies, with a few important exceptions, have only been classified optically. Only recently have 21-cm observations mapped the distribution of neutral hydrogen with resolution sufficient for comparison with spiral features. Two of the best observed galaxies have been M31 and M33 (NGC 224, SASb and NGC 598, SAScd respectively).

In M31, Davis and Gottesman (Davis and Gottesman,

1970; Gottesman and Davis, 1970) found that the HII regions and blue supergiants (in associations) lie within the principal neutral hydrogen structure. Neutral hydrogen is deficient at the centre and in the inner arms as defined by the dust and also toward the optical limits of the galaxy. The maximum rate of star formation as a function of the distance from the centre of the galaxy and marked by the maxima in the distributions of HII regions and blue supergiants, is coincident with the maxima in the distributions of dust and neutral hydrogen. It may be noted that there is at least one instance in which dust has been separated from the gas - this will be important in considering the question of the gas-to-dust density ratio derived in Section 4.2.

In contrast with the good agreement among the distributions of the various classes of objects in M31, we find departures in M33. The neutral hydrogen has a broad distribution compared to the sharply peaked blue supergiant and HII distributions (Jaeger and Davies, 1971). The positions of the maxima of the three classes are also displaced from each other. The centre of the galaxy is defined by the blue supergiants and this should serve as a reminder that spiral structure is essentially defined by the distribution of this one class of object.

The differences between spiral and galactic structure are still greater in NGC 4258 (SAB Sbc)

which has been studied at 1415 MHz by Kruit et al. (1972). The blue continuum defines a two-armed spiral composed of narrow lines of knots of HII regions. At H_{α} these knots are again seen in the two arms but in addition there exist two other arms of smooth texture which are sharply inclined to the main arms. Since these arms are invisible in the blue, the source of ionization would appear not to be the radiation from OB stars. These "new" arms are clearly seen at 1415 MHz while the blue optical arms are very weak.

In summarizing the distinction to be made between spiral and galactic structure, we may say that spiral structure is defined by the radiation of bright OB stars while galactic structure is the sum of all components making up the galaxy.

The Hubble Atlas (Sandage, 1961) shows a number of Sbc galaxies which may be compared with our own; in particular, NGC 4216 (SAB(s)b, Plate 25) and NGC 4303 (SAB(rs)b, Plate 29) have much in common with our Galaxy (de Vaucouleurs, 1970; Sandage, 1961).

NGC 4216 is an intermediate Sb galaxy seen nearly edge-on. The nuclear bulge and the dust pattern are clearly visible. However, compared to the view of our Galaxy seen in the Frontispiece, NGC 891, a later Sb (also on Plate 25), is a better match. The nuclear bulge is somewhat smaller than ours; the surface brightness decreases rapidly between 8 and 10 kpc from the centre but the dust lane in the plane extends right

to the edge. The dust lane is rather irregular with several dense knots in the plane as well as extensions out of the plane silhouetted against the nucleus. The dust plane in NGC 891 is apparently warped or distorted relative to the luminous surface of the galaxy.

NGC 4303 (M61) is seen almost face-on and illustrates the classification criteria of the Milky Way quite well: the bar is not well-formed; there is some incomplete ring structure at the end of the bar; and the spiral arms are compact but irregular with faint branches. The arms are about 1500 pc wide. In contrast, the dust lanes near the centre are only 150 pc wide; the lanes lie along the inside of the two main spiral arms but dust can be seen whereever the star background is bright enough, even out to the edge of the galaxy. The brightness of a spiral arm appears to decrease along its length as opposed to its radial distance from the nucleus. About 8 to 10 kpc from the centre, there is a rapid decline in surface brightness.

In about three-quarters of the Sb and in half of the Sc galaxies, spiral structure can be traced out to 10 kpc. Undoubtedly, the structure may extend further (in M31, spiral features have been traced out to 22 kpc - Börngen et al., 1970) but to explain the low surface brightness it must be that blue supergiants and HII regions are not important components. That is to say nothing about dust which can only be seen against a bright background. For a theoretical discussion on the

decline of surface brightness in a galaxy seen edge-on (with and without self-absorption), see Pavlovskaya and Sharov (1971).

As the type of galaxy advances from Sb to Sc, the percentage of the mass of dust increases - perhaps in the same proportion as the gas which increases from 1% to 8% (Reddish, 1968). The dust is severely confined, usually along the inside of spiral arms in the plane of a galaxy. Connolly et al. (1972) found that the dust lies inside the HII spiral pattern of M81. Baade (1963) showed that the globular clusters of M31 were reddened only when they were directly behind a spiral arm. On the other hand, dust may also be out of the plane as in NGC 5383 (SBb(s),Plate 46) where only one of the two dust lanes cuts the bright central region. If the dust lies in the plane defined by the stars emitting the most blue light and is completely opaque, then the intensity of the light in the dust lane should be half of that on either side - the lane being filled in by stars lying above the plane. Lynds (1970) found, however, that the intensity in the dust lane was much lower: there was no difference in the size of the dust clouds when measured on red and blue plates implying very great optical depths from which she derived a lower limit of 3 magnitudes extinction. Lynds studied the distribution of dust in selected face-on Sc galaxies, three-quarters of which extend beyond 10 kpc in radius. The dust clouds ranged in size from 50 parsecs near the nucleus to 240 parsecs at 2 kiloparsecs

from the centre. Lynds measured only two dust clouds beyond 4 kpc from the centre - perhaps a selection effect imposed by the use of large scale"200-inch" plates of the centre region which would leave the outer regions underexposed.

It is apparent from studying the galaxies in the Hubble Atlas (and from determining the distance on the prints corresponding to 10 kpc) that the distribution of OB stars has usually begun to decline steeply by the Sun's distance from the centre of a galaxy. It is not clear whether the amount of dust undergoes a similar decrease (as it does in M31) or behaves differently. It is also apparent that the usual spiral tracers - bright blue stars, dust, and neutral hydrogen - may not reveal the same structure.

This section has revealed the general features to be expected in our Galaxy. We now turn to the integrated character of the Milky Way.

1.2 The Milky Way

It was a study of certain characteristics of the Milky Way that lead to choosing the longitude interval about $l^{II}=40^{o}$ as a region of special interest.

In the Frontispiece and Plate 1, the most obvious characteristic is the dust which divides and obscures the Galaxy. The dust has neither a smooth nor a symmetric distribution; there is more dust at low longitudes than at high (comparing either side of the nuclear bulge) and more above the plane than below. In particular, the longitude interval 20^{o} to 45^{o} appears to be the base of a large obscured region inclined some 50^{o} to the plane.

Another obvious feature shown in the Frontispiece and Plate 1 is the variation in surface brightness. There is the contrast between portions of the bright nuclear bulge and the dense features which cross it. But there is also the steady decrease in brightness away from the centre. The decrease is less dramatic in the plane but nevertheless the anticentre region becomes quite faint.

It might have been expected that the galactic distribution of spiral tracers would reflect the decrease in surface brightness. Figures 1.1 and 1.2 show this to be only partially fulfilled. The greatest numbers of supergiants (700 stars from Humphreys, 1970) and emission-line stars (5326 stars from Wackerling,

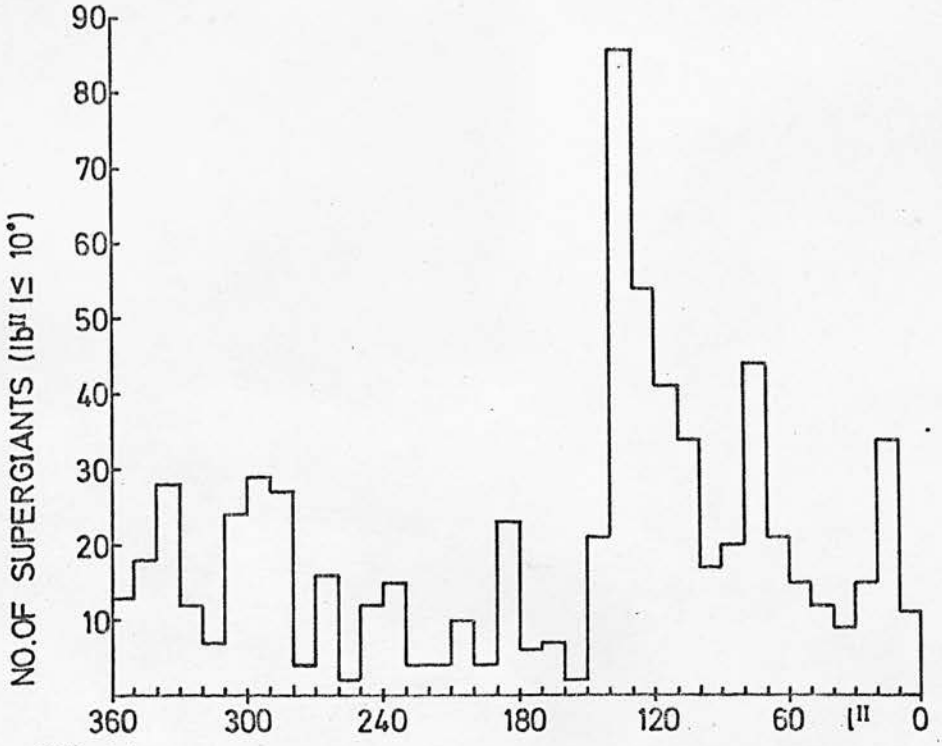

FIG. 1.1
GALACTIC DISTRIBUTION OF SUPERGIANT STARS

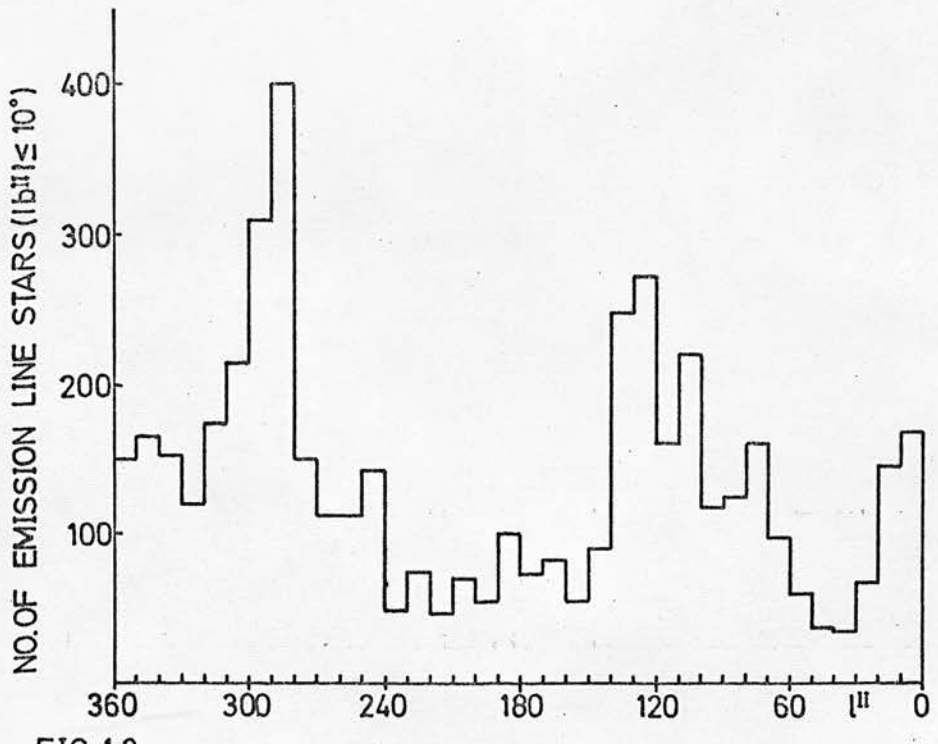

FIG. 1.2
GALACTIC DISTRIBUTION OF EMISSION LINE STARS

1970) occur not at the galactic centre but at 135° and 285°, in the Perseus and Carina associations, respectively. Between the two complexes, ie. from 140° to 280° the two distributions reflect the surface brightness of the area.

In comparison with the minima in the anticentre, the minima between 30° and 50° is rather insignificant. The surface brightness decreases between Scutum and Cygnus. We shall see in Chapter 3 that this is the result of heavy obscuration by dust clouds and has some consequences for galactic structure.

The distributions of OB stars and Wolf-Rayet stars in Figures 1.3 and 1.4 show the same minima and confirm that the one at $l^{II}=40°$, while small, is significant. The distribution of OB stars was determined from the catalogues of Luminous Stars of the Northern Milky Way produced jointly by Warner and Swasey and Hamburg Observatories and a similar catalogue of the Southern Milky Way (Stephenson and Sanduleak, 1971). The 133 Wolf-Rayet stars in Figure 1.4 were based on material from the afore mentioned catalogues as well as from Roberts (1962), Stephenson (1966), Smith (1968), and Wackerling (1970) (those stars with emission were included in Figure 1.2). No Wolf-Rayet stars are recorded between 34° and 54°. It is not clear to what extent this is a significant galactic feature. One faint emission-line object has been found during the course of this thesis but has not yet been classified -

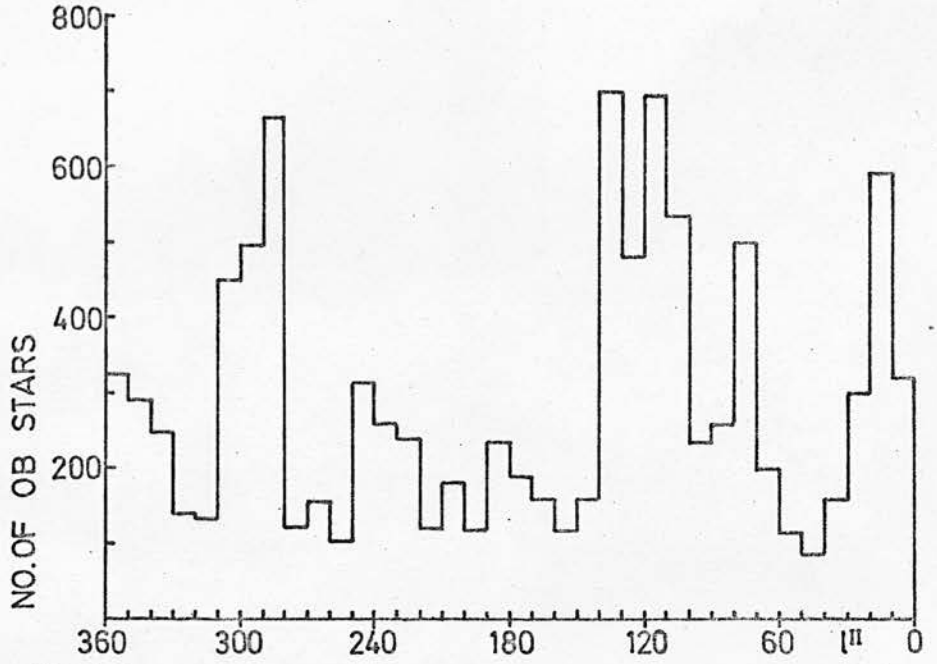

FIG. 1.3
GALALACTIC DISTRIBUTION OF OB STARS

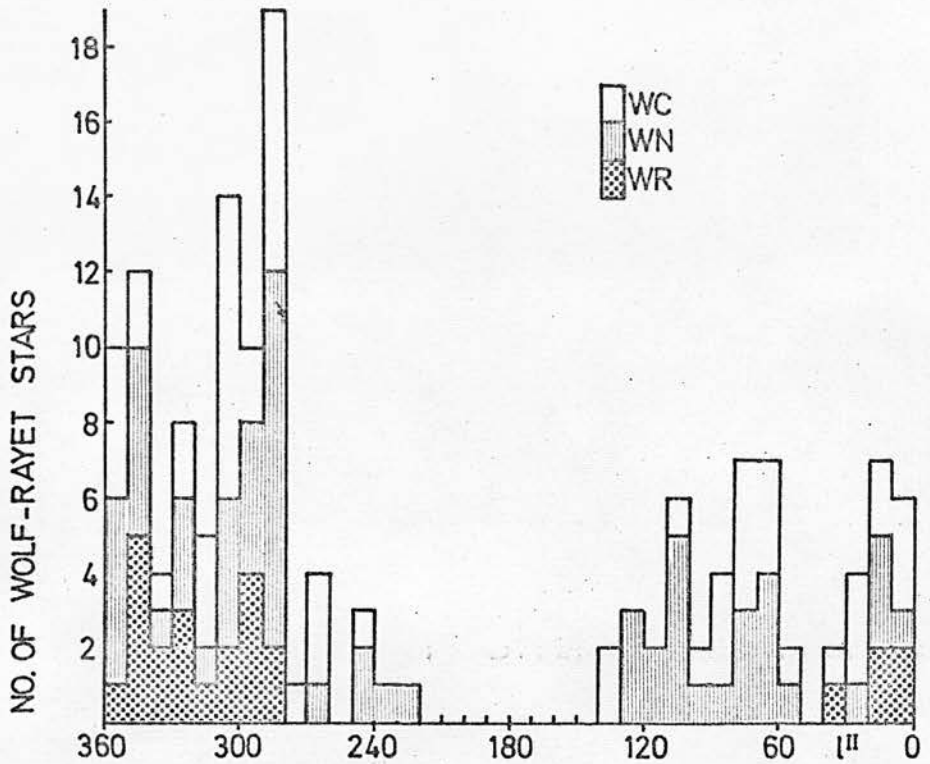

FIG. 1.4
GALACTIC DISTRIBUTION OF WOLF-RAYET STARS

it might be a very distant Wolf-Rayet star or a planetary nebula; photoelectric photometry suggests that it is variable. It will not be discussed further in this thesis.

For completeness, we include the HII distribution in Figures 1.5 a and b. The minimum at $l^{II}=40^{o}$ is less clearly seen in Figure 1.5b. Several HII regions have been detected but they are of small size, due either to being at great distances or highly obscured or both. One HII region, S74 (Sharpless, 1959), is studied in Chapter 3 and there it is found that both suggestions are correct.

The distribution of neutral hydrogen is continuous through $l^{II}=40^{o}$; it is declining from a great peak value toward the galactic centre to a low value in the anticentre. Kinematically derived distances indicate that the next spiral arm interior to the Sun has a continuous distribution of gas through $l^{II}=40^{o}$ with tangency near $l^{II}=50^{o}$.

The discontinuity in spiral tracers evidently is not due to a discontinuity in the gas distribution. It may however be due to heavy obscuration. What galactic structure can produce continuous distributions of gas and dust and discontinuities in early type stars? To investigate this question, a region near $l^{II}=40^{o}$ was selected for a photometric study.

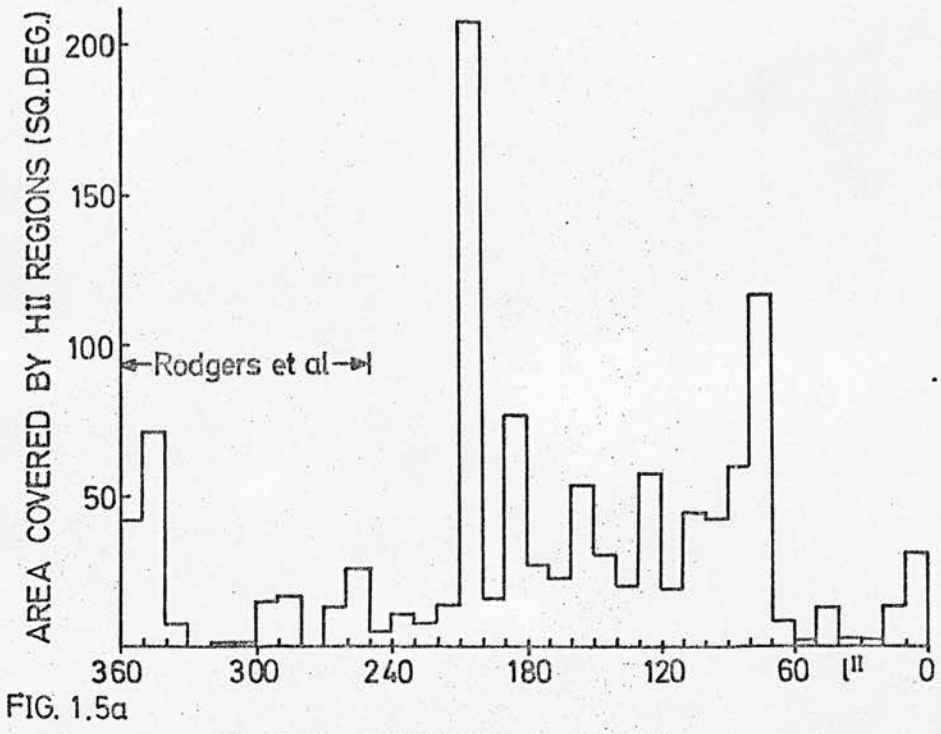

FIG. 1.5a

GALACTIC DISTRIBUTION OF HII

$\delta \geq -30°$ B.L.LYNDS APJ SUPPL. 12, 163, 1965.

$\delta < -30°$ A.W.RODGERS ET AL MN 121, 103, 1960

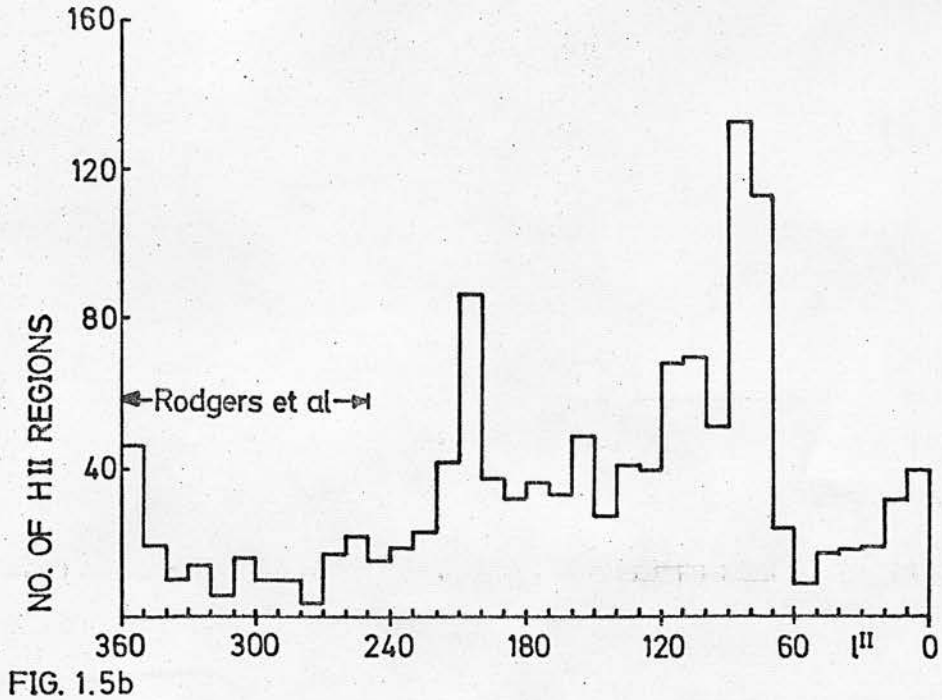

FIG. 1.5b

GALACTIC DISTRIBUTION OF HII REGIONS

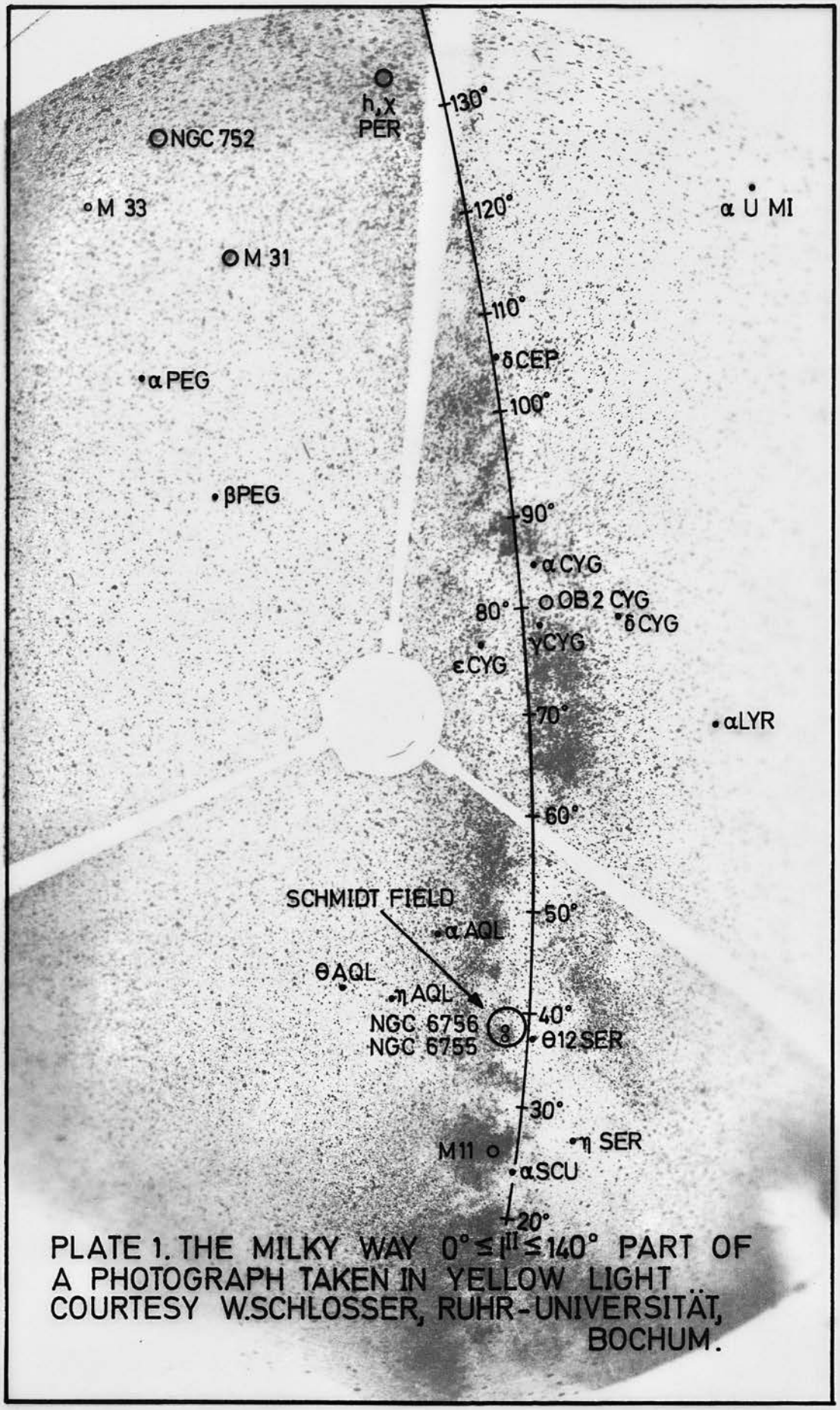

PLATE 1. THE MILKY WAY $0° \leq l^{II} \leq 140°$ PART OF A PHOTOGRAPH TAKEN IN YELLOW LIGHT. COURTESY W.SCHLOSSER, RUHR-UNIVERSITÄT, BOCHUM.

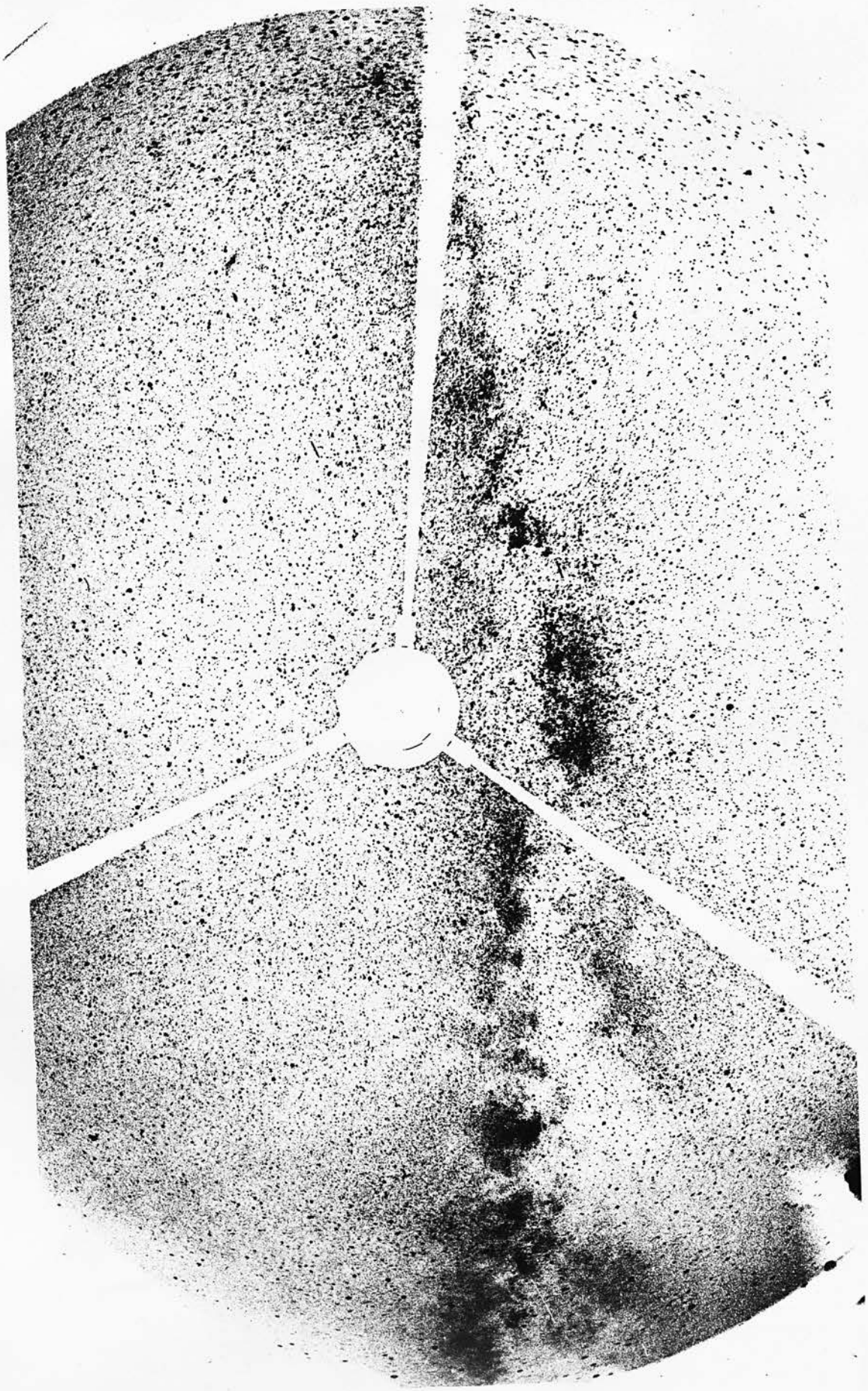

1.3 $l^{II}=40^{o}$

There have been few studies of any kind made of this area - there are few interesting objects to attract attention. The problem was to find an area where one could study the dust distribution and the few OB stars. The choice was narrowed by the requirement of a photoelectric sequence to calibrate the photographic photometry. The region finally chosen is described in Chapter 2. The initial number of photoelectric stars in the area was about 30, mostly in NGC 6755 (Hoag et al., 1961) (there are now several hundred).

Figure 1.6 shows the region being considered with the Schmidt field marked. For comparison, bright stars from LS II and IV have been plotted. The stars are nonrandomly grouped: more below the plane than above. The void above the plane is similar to the shape of the dust cloud shown in Plate 1.

Earlier work, eg. Weaver (1949), was hindered by the relatively bright limiting magnitude for OB star searches, by inaccurate means of calibrating plates (before the few photoelectric stars became available, photographic calibration was carried out by "transfer" methods from standard sequences), and by a lack of interesting objects to attract other workers (S74 has been known for a long time but is too faint for the interferometry techniques of Georgelin and Georgelin

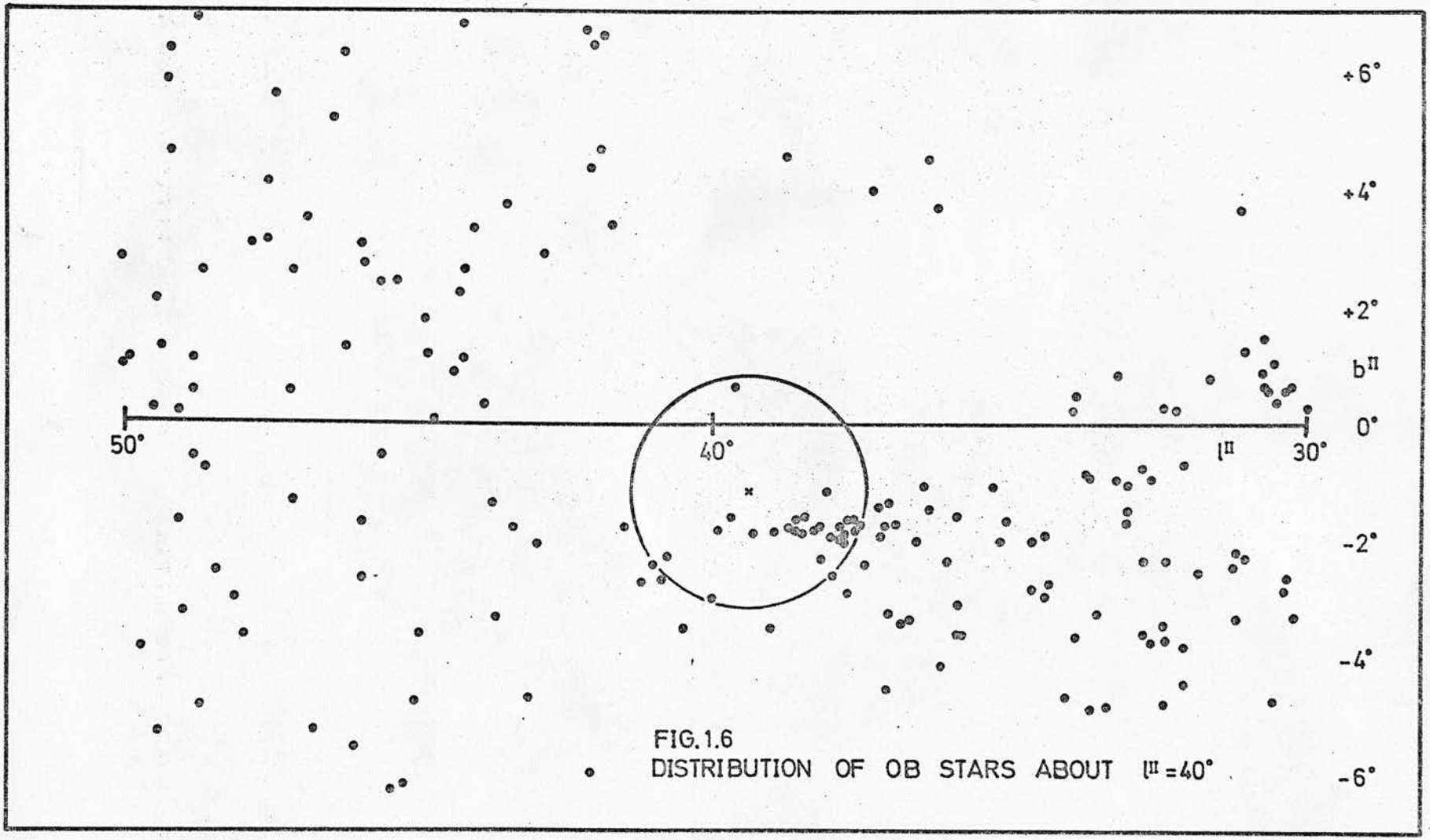

FIG. 1.6
DISTRIBUTION OF OB STARS ABOUT $l^{II}=40°$

(1970).

The present work has had the following advantages:

i) complete measurement of all stars in the region - invaluable for studies of absorption,

ii) a preliminary photographic study of reddening with distance which revealed some problems and hinted at the solution,

iii) generous amount of observing time in order to measure more than 100 OB stars from the Hamburg/Warner and Swasey catalogue; this revealed the spiral structure and served as the framework for the other studies,

iv) objective prism plates with a variety of exposure times taken before the photoelectric programme, and

v) time to discover early-type stars and observe them photoelectrically.

These advantages are described in detail in Chapter 2. In Chapter 3, the observations are given in Tables 3.1 to 3.3 and are analyzed in Section 3.2.

The relationships among the various components of galactic structure are described in Chapter 4. The direction for future work is also given. Chapter 5 presents a brief summary of the conclusions. As a convenience to the reader, details of some computer programmes are given in the Appendix; details of a surface photometry programme are also given there.

Chapter 2

Photometry

Photoelectric and photographic photometry is extensively used in this work. The photoelectric observations were made on the site of the European Southern Observatory, la Silla, Chile, at the outstation of the Ruhr University, Bochum, and were reduced in Bochum. The photographic observations were made in Monte Porzio, Italy, at the outstation of the Royal Observatory Edinburgh. They were measured in Edinburgh using GALAXY and were reduced partly in Edinburgh and in Bochum.

Objective prism spectrograms were taken at the Cerro Tololo Inter-American Observatory (CTIO).

Detailed descriptions of the photoelectric and photographic photometries are given in Sections 2.1 and 2.2, followed by a discussion of the results from GALAXY and a description of the spectroscopic material in Sections 2.3 and 2.4 respectively.

2.1 Photoelectric Photometry

A complete description of the Bochum 61-cm photometric telescope on la Silla has been given by Schmidt-Kaler and Dachs (1968). An EMI 9502 photomultiplier tube was operated at 1250 volts and was cooled by an alcohol bath containing dry ice. Dry ice was added to the cold box about two hours before the start of the

night and was replenished at the beginning of the night and approximately every three hours thereafter. The U and B filters were as described by Schmidt-Kaler and Dachs but the V filter was a 2-mm Schott OG 515.

A computer-orientated data acquisition system using programmes written at Bochum in the "BASIC" language for a Hewlett Packard 2114B computer was employed to record the data on punched paper tape. The observer identified the star as well as the filters and integration times to be used. The programme selected a gain step so that the intensity was between 8000 and 80000; it also noted during the observations the running mean intensity and its mean error as well as the sidereal time (to better than one second) at the midpoint of each observation. Full details about these programmes may be obtained from Dr. H. M. Maitzen at Bochum.

The observations were made between May 5 and August 5, 1972. The programme stars were observed on either side of the meridian between air masses 1.3 and 2.0. Ten-second integrations were used for stars of 7^{th} to 8^{th} magnitude increasing to 50 seconds for 15^{th} magnitude stars. The philosophy was to observe the brighter stars on one or two nights with about 2% accuracy for a single observation and the fainter stars on four to six nights to obtain an accurate mean (see Table 2.3).

Several methods were used to check the performance

of the photoelectric equipment in order to transform the observations to the UBV system. Every two or three hours during the night, a Cherenkov source mounted in the diaphragm slide was measured to check for amplifier drift. At the end of each observing run, a constant current source was used to determine the gain ratios for the amplifier. The ratios remained constant at the set values, nominally equal to ten.

Near the Schmidt field in Aquila, four UBV standard stars numbered 210, 222, 223, and 224 (Johnson and Morgan, 1953) were chosen as extinction stars and were measured every two or three hours. In addition, some stars in E-regions (Cousins and Stoy, 1962 and Cousins, 1971) were used to extend the range of air mass. Twenty-two other stars from Johnson and Morgan (1953) as revised by Johnson and Harris (1954) were also measured on most nights to transform the observations from the instrumental to the UBV system. The ranges in (B-V) and (U-B) for these stars were $-0\overset{m}{.}08$ to $+1\overset{m}{.}60$ and $-0\overset{m}{.}49$ to $+1\overset{m}{.}81$ respectively. Other standards were measured only two or three times.

The photoelectric reductions followed the method described by Hardie (1962). Mean primary and secondary colour coefficients and secondary extinction coefficients plus nightly primary extinction coefficients determined from the observations of standard stars were used to reduce the programme stars to the standard system. The coefficients used are listed in Table 2.1.

The rms error for a single observation is ±0.022, ±0.017, and ±0.042 in V, (B-V), and (U-B) respectively. This is the result from 540 measurements of standard stars on 23 nights, an average of 23.5 standard star observations per night.

Table 2.1

Primary (P) and Secondary (S) Extinction (E) and Colour (C) Coefficients Used to Transform the Instrumental System to the UBV System.

Colour	PE	SE	PC	SC
V	0.11	0.000	0.206	-0.033
(B-V)	0.15	-0.025	0.232	-0.084
(U-B)	0.25	-0.020	0.489	0.053

Among the programme stars were 59 stars measured independently by other observers: viz., Purgathofer (1969), Hoag et al. (1961), Hiltner (1956), and Moffat (Bochum, unpublished). The rms deviations between Sherwood and each of the others is given in Table 2.2.

The three faint Purgathofer stars (nos. 35, 36, and 37) which I observed only once (Table 3.3a) have been excluded as has been no. 5. This star was either subject to an atypically large measuring error or is a variable star for Purgathofer's one observation does not agree with my three observations which are consistent and agree also with the photographic values. On

Table 2.2

The RMS Deviation: Sherwood - Other.

Observer	No. of Stars in Common	σ_V	$\sigma_{(B-V)}$	$\sigma_{(U-B)}$
Purgathofer	24	0.035	0.040	0.076
Hoag et al.	7	0.044	0.044	0.098
Moffat	18	0.037	0.020	0.067
Hiltner	10	0.098	0.057	0.044
Johnson and Morgan Standard Stars	26	0.022	0.017	0.042

---

the average, the remaining stars were observed twice by each of us.

In NGC 6755 (Table 3.3b), there are seven stars in common with Hoag et al. (1961) (eight stars in V). Neither of us observed these stars often enough to reduce the scatter.

There are 18 stars in common with Moffat (unpublished) chosen from LS II and LS IV. The observations were made in 1970 with the same telescope and photometer used here. The observations have not yet been reduced to their final form and, when used in the analysis in Chapter 3, zero-point corrections of -0.020 and -0.045 were made to his V and (U-B) respectively.

Hiltner's stars are common to the list LS IV.

Figure 2.1 shows the individual differences plotted against my photometric values. It seems clear from the figure and the size of the errors in Table 2.2

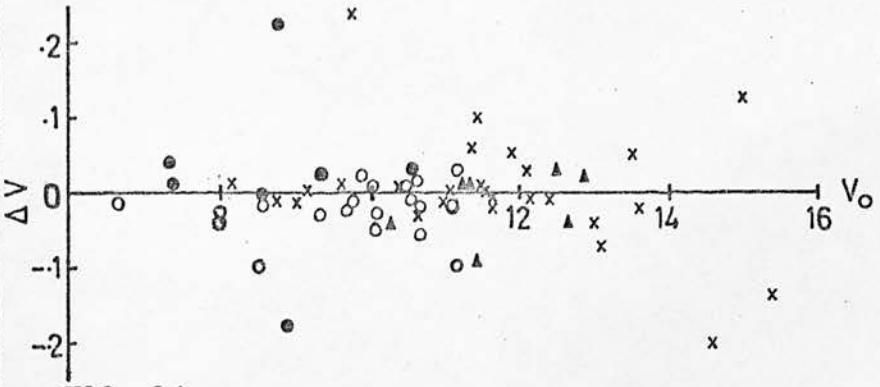

FIG. 2.1a

ΔV VS. V_o. $\Delta = Pe_{OBS.} - Pe_{PUB.}$. $V_o = V_{OBS.}$

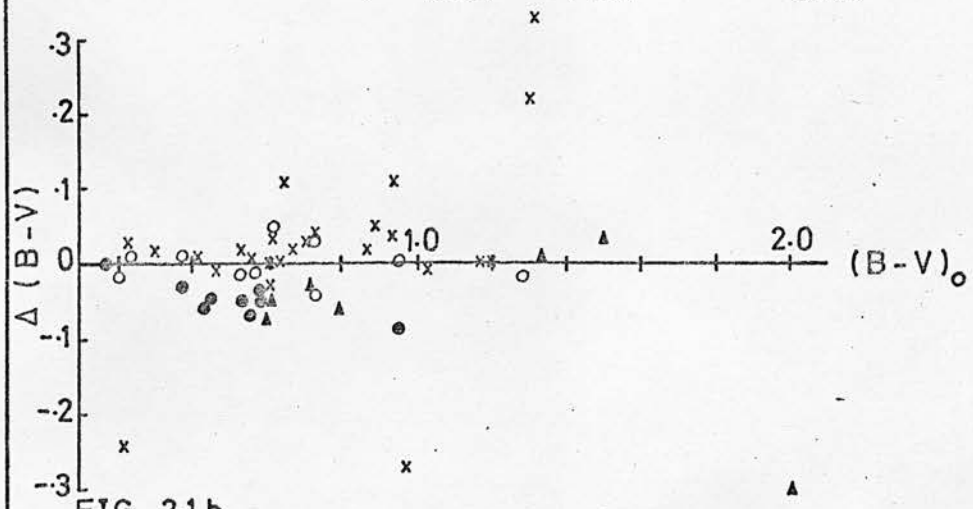

FIG. 2.1b

Δ (B - V) VS. $(B-V)_o$.

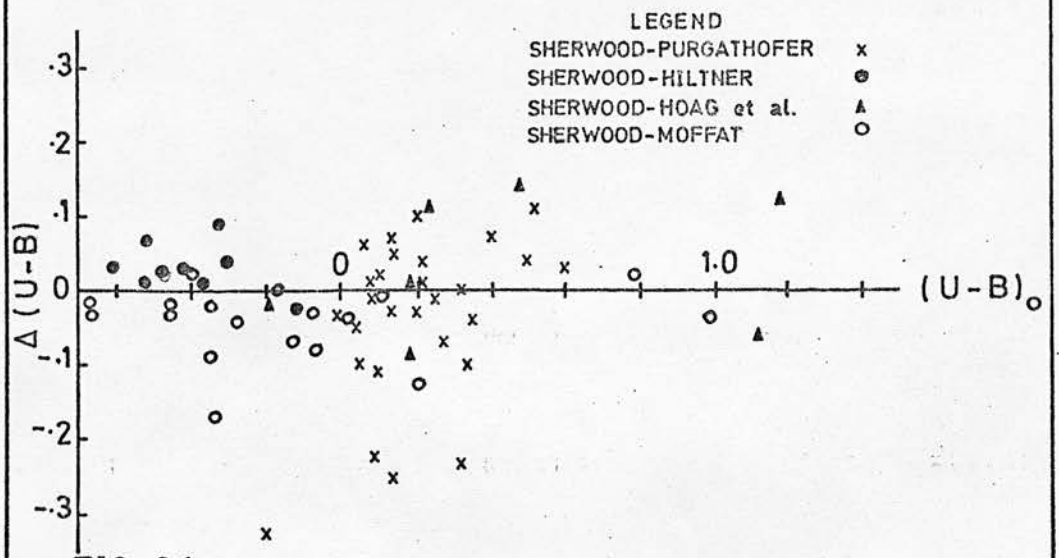

FIG. 2.1c

Δ (U - B) VS. $(U-B)_o$.

that there are some rather large discrepancies. It is not possible to account for the differences at the present time unless the photometric errors are larger than the usually published ones. See Lawrence and Reddish (1965) for an additional discussion of this point. It should be noted that Purgathofer and Hoag both made their observations in part at the Lowell Observatory and yet the agreement between them through my observations is not very good. There may be some errors not considered in the measurements associated with such a crowded field as NGC 6755.

As mentioned earlier, the error of a single observation increases rapidly with increasing magnitude. Combining several observations of low weight uses the telescope more efficiently and provides more information than one long integration of a star on only one night. Table 2.3 shows the error of the mean for fourteen programme stars in Table 3.2 fainter than V = $12^{m}.0$ which have been observed four or more times.

Table 2.3

The Error of the Mean for Stars with V $\geq$ $12^{m}.00$ Observed Four or More Times. Stars Are from Table 3.2 Identified in Chapter 3.

Star No.	V	B-V	U-B
101-1	$\pm$0.01	$\pm$0.01	$\pm$0.06
190-12	0.04	0.08	0.18
190-8	0.04	0.02	0.06
190-7	0.04	0.03	0.13
190-11	0.04	0.04	0.14
190-5	0.03	0.03	0.13
182-6	0.02	0.01	0.04
182-5	0.03	0.04	0.18
182-7	0.02	0.02	0.09
182	0.02	0.02	0.05
182-8	0.02	0.03	0.16
182-1	0.02	0.03	0.06
182-3	0.03	0.03	0.03
182-4	0.02	0.02	0.08

2.2 Photographic Photometry

The 40-60-cm Schmidt telescope at the Edinburgh outstation just south of Rome, Italy was used to obtain the direct plates for the photographic photometry. The optical alignment of the telescope was checked by means of a Dewhirst test (Dewhirst and Yates, 1954) about once a week for the period of about two months during which the observations were made and on each occasion the telescope was found to be correctly adjusted. Focus plates were taken every night that photometric plates were taken; the focus was determined for five positions on each plate (centre and two-thirds of the way to the edge of the plate along each axis) and found to be constant. Although the focus plates could not in general be measured until the end of the observing session, the values in the mean agreed with the one adopted for usage. The exposure times and, for the ultraviolet plates, the choice of emulsions were influenced by the frequent occurrence of atmospheric dust which scattered light from Rome and fogged some plates. The plates which were used and their characteristics are listed in Table 2.4. The plates were developed and fixed horizontally at 20°C.

GALAXY - the idea, the mechanics, and the process of operation - has been described by Reddish (1970), Walker (1971), and Pratt (1971) and need not be repeated here.

Table 2.4

Photographic Data for Plates Measured by GALAXY.

Colour	Date	Plate No.	Emulsion	Filter	Exposure Time min.	Hour Angle at Start hr min
V	9. 7.69	1060	IIaD	GG14	15	+0 13
	12. 7.69	1069	"	"	10	+0 48
	7.10.69	1165	"	"	15	+2 13
	7.10.69	1166	"	"	15	+2 37
B	12. 7.69	1067	IIaO	GG13	10	+0 06
	17. 7.69	1099	"	"	12	+0 05
	20. 7.69	1112	"	"	13	-1 00
	20. 7.69	1115	"	"	12	+1 09
U	13. 7.69	1075	IIaO	UG2	45	+0 17
	16. 7.69	1090	IaO	"	20	-0 36
	16. 7.69	1092	"	"	20	+0 31

The region measured by GALAXY is an approximately circular field (the plates are round) of two degrees radius centred on the star BD $+4^{\circ}3979$ at RA = $19^{h}4^{m}53^{s}$, DEC = $+5^{\circ}8'24''$ (1950.0) and $l^{II} = 39.^{\circ}4$, $b^{II} = -1.^{\circ}2$. The initial distribution of stars on the UBV system was limited to the cluster, NGC 6755, and an area near the edge of the field. Consequently, only 3.8 square degrees have been calibrated for photometry to date.

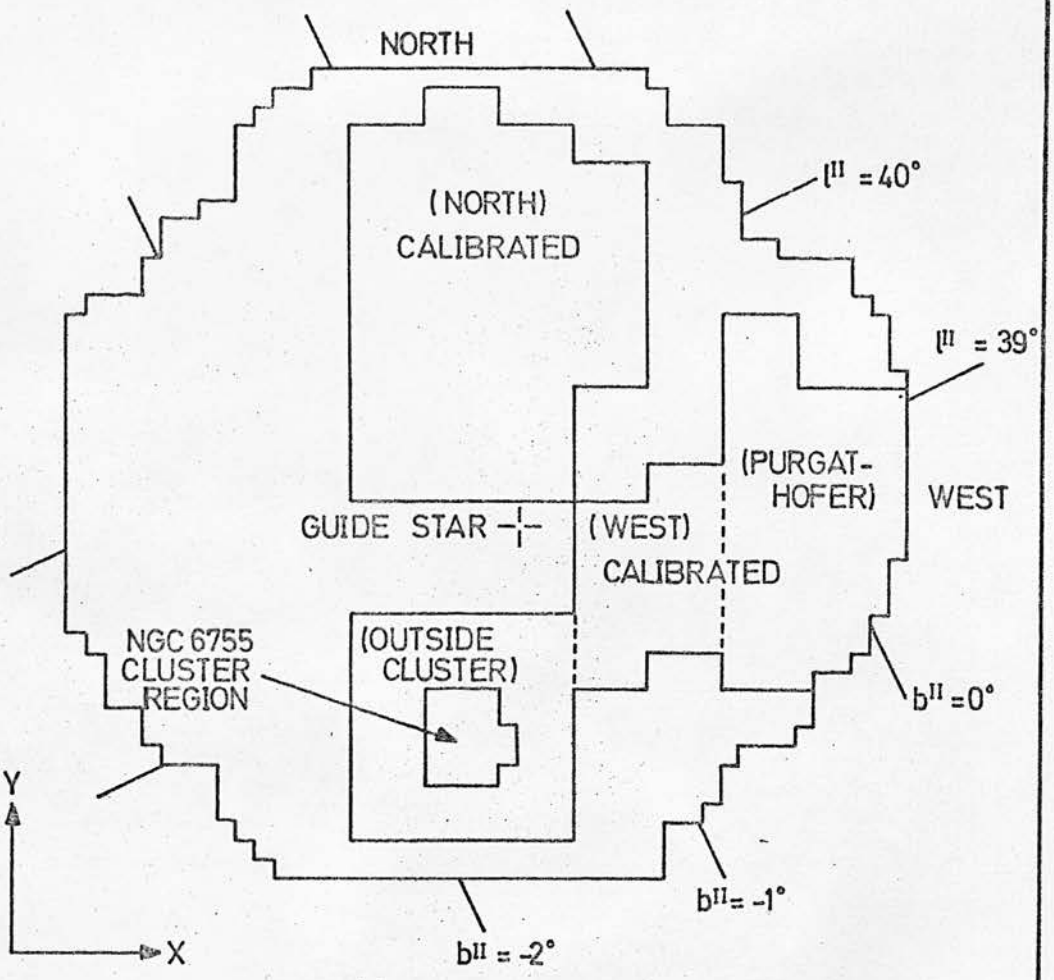

FIG. 2.2
REGION MEASURED BY GALAXY WITH THE IDENTIFICATION OF THE AREAS CALIBRATED.

That area is shown in Figure 2.2 relative to the region measured by GALAXY. The scale is such that 1 cm in the figure corresponds to 8.192 mm on the photographic plate (or 18.43 arc min.). A "+" denotes the position of the guide star. See also Plates 2 and 3 in Chapter 3. The plates were calibrated with sequences by Hoag et al. (1961) in NGC 6755, by Purgathofer (1969) in the field at the west edge of the plate (Plate 2), and by me (stars marked by a "c" in Table 3.2). It was decided to calibrate separately the cluster region (marked in the figure) in order to avoid the additional problem of background fog (at this time GALAXY had no facility to determine it).

It was found that about half of the stars in the sequence by Hoag et al. were affected by crowding. In order to have an adequate number of stars to calibrate this area of the plate, the photographic sequence also measured by Hoag et al. was used. Stars which were affected by crowding or had uncertain photometric values marked by ":" were rejected.

The scatter among the V and B magnitudes showed a colour dependence which was removed for the final results:

$$V' = V + 0.1(B-V) \qquad \text{if } (B-V) > 1.00$$

$$B' = B + 0.1(B-V) - 0.07 \qquad \text{for all } (B-V).$$

For the cluster, the zero point for the last equation

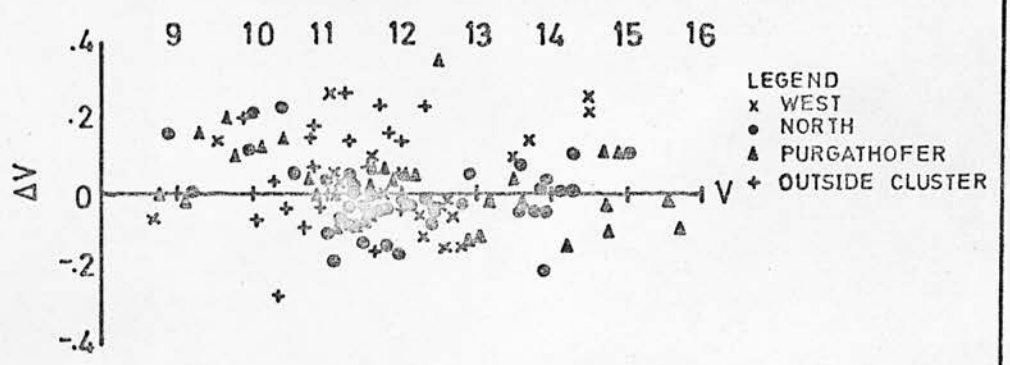

FIG. 2.3a

$V_{pe} - V_{pg}$ VS. V_{pe}.

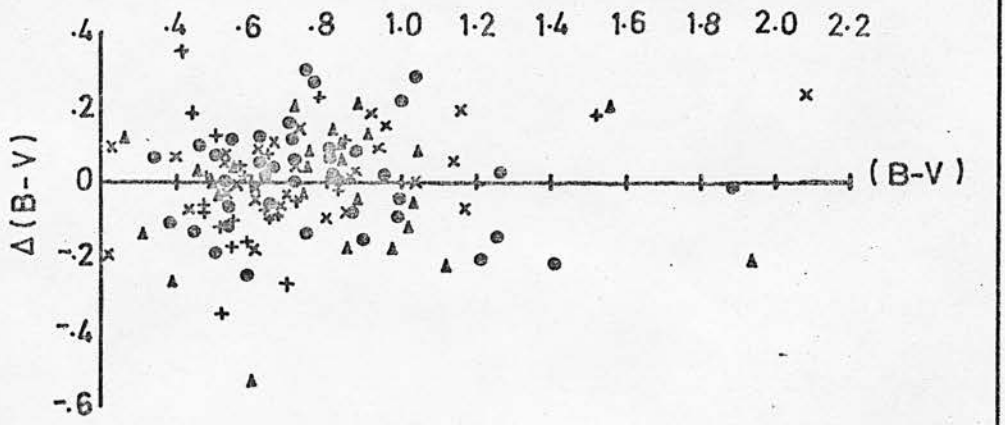

FIG. 2.3b

$(B-V)_{pe} - (B-V)_{pg}$ VS. $(B-V)_{pe}$.

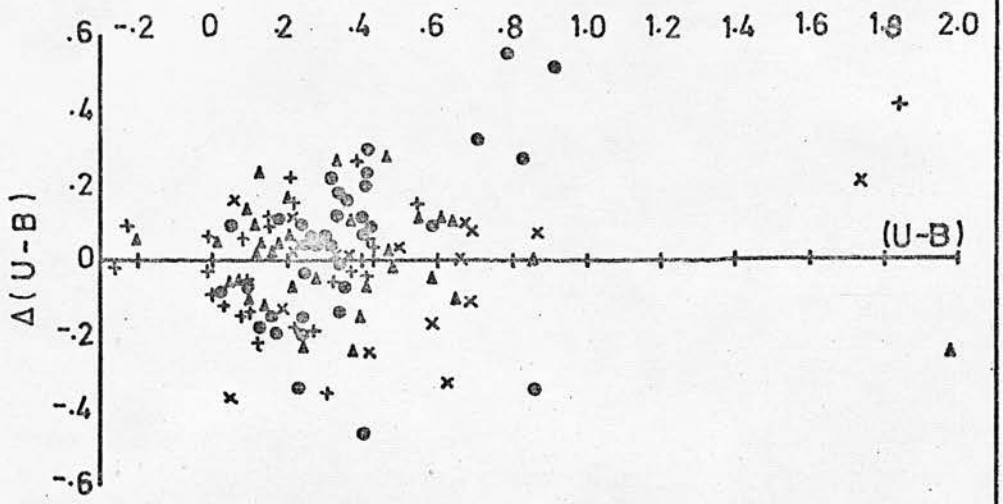

FIG. 2.3c

$(U-B)_{pe} - (U-B)_{pg}$ VS. $(U-B)_{pe}$.

was -0.10.

The differences between GALAXY and either the photoelectric or the Hoag photographic values as a function of magnitude and colour are shown in Figures 2.3 and 2.4 respectively. The errors are tabulated in Table 2.5

Table 2.5

Comparison of the GALAXY Photographic Measures with a) Photoelectric Measures and b) Photographic Measures by Hoag et al (1961).

Colour	a No. of Stars	a Pe-GALAXY	b No. of Stars	b Pg-GALAXY
V	134	±0.107	101	±0.093
(B-V)	134	0.137	76	0.122
(U-B)	133	0.172	65	0.198

The large error in (U-B) results from a poorly determined U magnitude due to a machine fault which occurred while GALAXY was measuring plate 1092; only the east half of the plate was measured. Therefore, on the west half, U magnitudes are based on the average of only two plates.

For the purpose of computing stellar statistics and of testing the possibilities of doing surface photometry with GALAXY (Appendix B), the rest of the

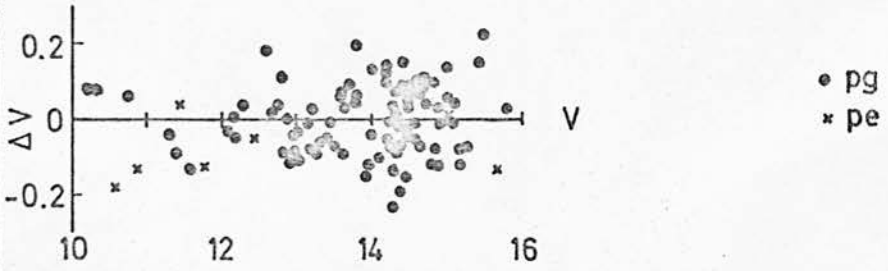

FIG. 2.4a

$V_H - V_{GAL.}$ VS. V_H

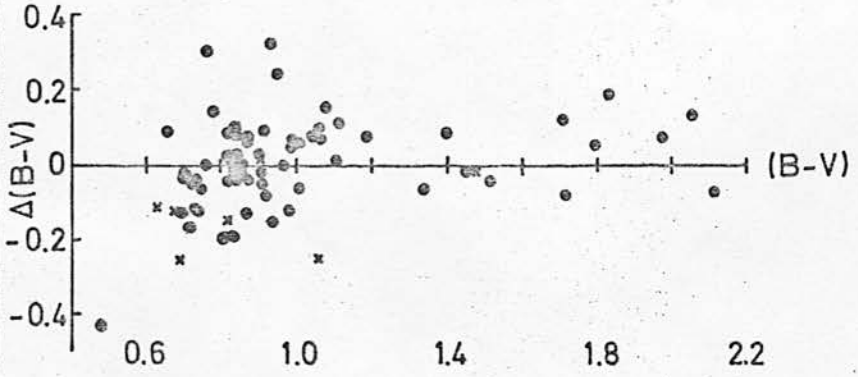

FIG. 2.4b

$(B-V)_H - (B-V)_{GAL.}$ VS. $(B\ V)_H$

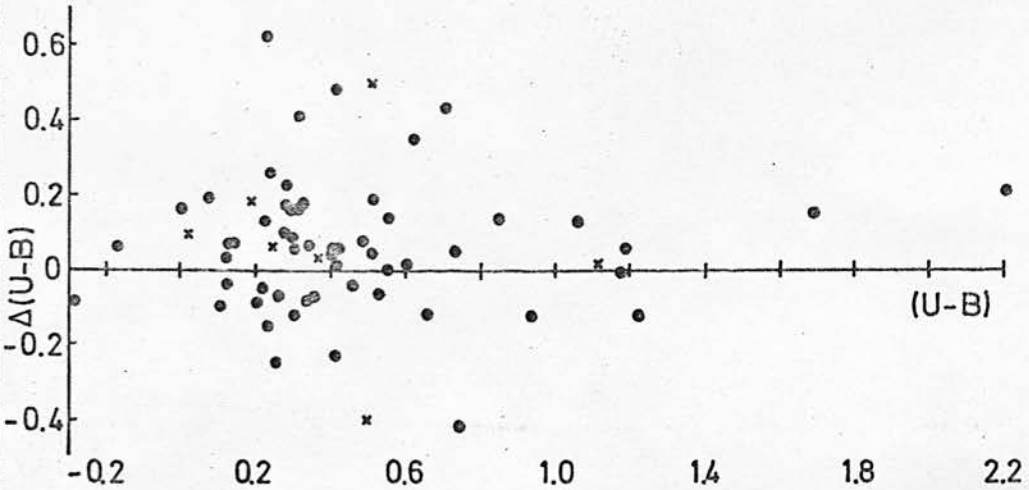

FIG. 2.4c

$(U-B)_H - (U-B)_{GAL.}$ VS. $(U-B)_H$

region measured by GALAXY has been calibrated using the Purgathofer sequence. It will be subject to systematic errors up to $0^m.5$ but should be adequate for discussion purposes.

The range of magnitude (faintest measured value minus brightest) for stars measured on two or more plates is shown in Figure 2.5. It shows the increase in the internal scatter as a function of magnitude. The data has been taken from the Purgathofer and cluster areas. It is estimated that the limiting magnitudes in V, B, and U are $16^m.75$, $17^m.75$, and $16^m.0$ respectively.

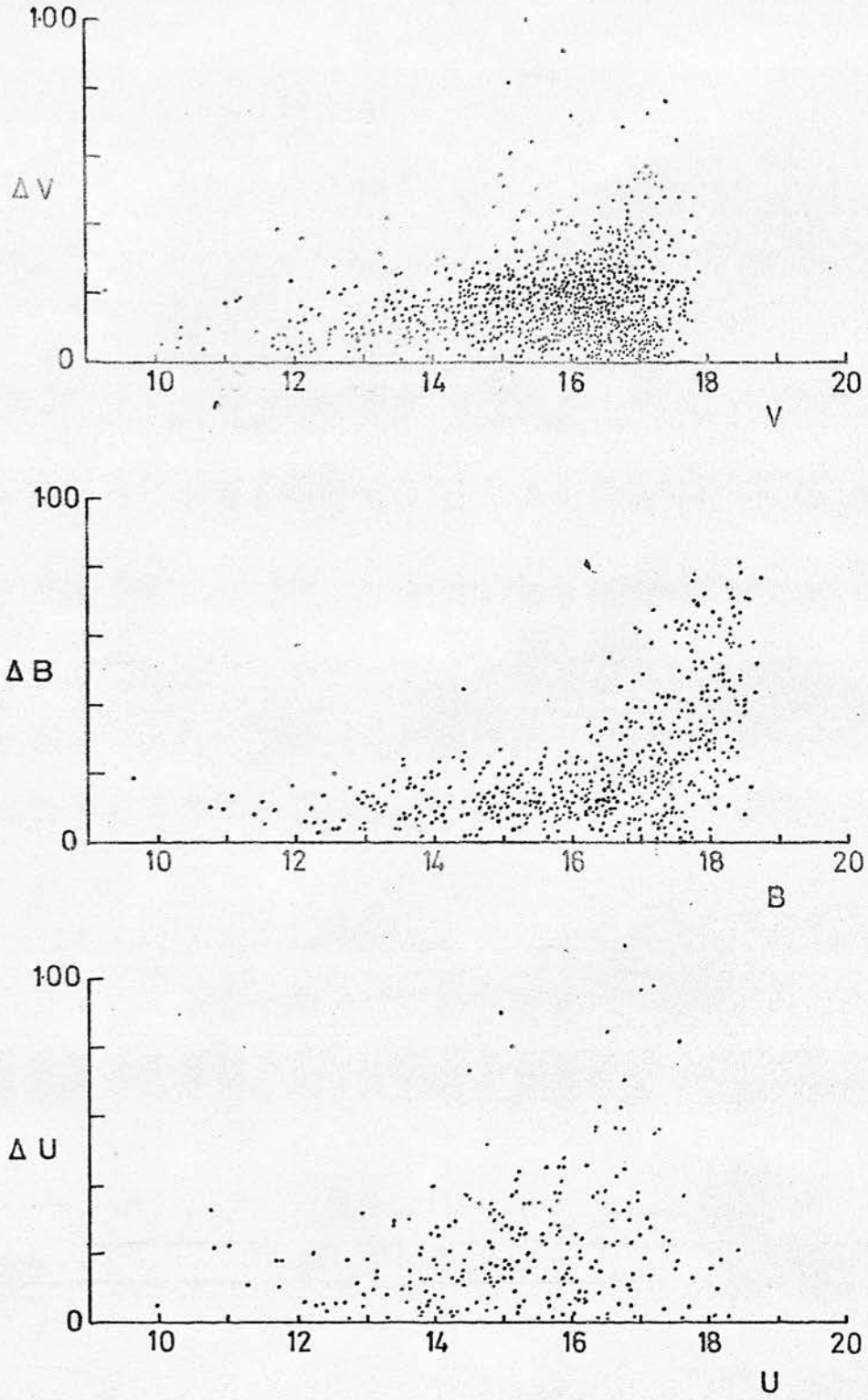

FIG. 2.5
INTERNAL SCATTER AS A FUNCTION OF V, B AND U MAGNITUDES.

2.3 GALAXY Measurements - Completeness

GALAXY was operated in such a manner as to measure objects above a certain minimum density set by the background fog level. Quite often, these objects were just chance configurations of photographic grains. To reduce the number of spurious star counts, an object was defined as a star if it were on two or more plates. Ideally, a real star would be measured on all plates on which it appeared, but changes in limiting magnitude will make some stars too bright or faint while changes in seeing will alter the effects of nearby images and may distort an image to the point where it will be rejected by GALAXY. Finally, GALAXY has only a probability of measuring any given star. This section deals only with this probability, its absolute value, and its dependence on apparent magnitude, colour, and surface density.

2.3.1 Comparison with Counts by Eye

A portion of the plate V1060 (good seeing, limiting magnitude $> 17^{m}.1$) containing stars measured by Purgathofer (low surface density of stars) was enlarged and reproduced as a negative print. Seventy stars were counted after inspection of the print. GALAXY found only fifty objects in the same area on the same plate; one object could not be identified with anything on the

original plate and was too large to be noise. Of the twenty-one stars missed, eight were between 12th and 15th visual magnitude and should not have been missed.[1] Near the plate limit, GALAXY was expected to find only about 50% of the stars due to grain noise. Table 2.6 summarizes the results of visual and automatic counts of stars. The POSS red print of the area was used as an independent identification of stars for both counts.

Table 2.6

Completeness of GALAXY Counts Relative to Visual Inspection for a Small Region of Low Star Density on V1060.

	GALAXY	Eye
Number of Stars Counted	49 (70%)	70
Number of Bogus Objects (not plate defects)	1 (2%)	-
Number of Stars Missed	21 (30%)	-
Number of Important Omissions	8 (11%)	-

If the omissions are random, then the probability of a star being missed on all four plates is $(0.1)^4$, ie. 10^{-4}.

In two regions, one about 15 arc minutes south of NGC 6755 and the other east of Purgathofer star P-2 and north of P-4 (west side of Plate 2), star counts were

1 I have been informed that since this work was carried out, the failure of GALAXY to find and to measure all the stars was traced to an error in the electronic logic which has now been corrected.

made to B=$20^{m}.5$ on the POSS blue print and to B=$17^{m}.7$ on the plates (Appendix A). The logarithm of the number of stars per square degree brighter than the magnitude m was plotted against m (Figure 3.10). The point from the POSS count lies on the extrapolation of the GALAXY counts. One may conclude from this that the GALAXY measures are statistically complete down to B=$17^{m}.7$ when four plates are used.

2.3.2 Dependence of Counts on Magnitude and Surface Density

Two hundred and fifty stars were selected at random from three fields of high, medium, and low star surface density. (A high surface density has more than fifty stars per twenty-one square arc minutes while a low surface density has fewer than twenty stars in the same area. The plate scale is 135 arc seconds per millimetre.) In each of V and B, four plates were measured; three U plates were measured except in the low star density region on the west side of the field where only two plates were completely measured.

The percentage of stars measured on one to four plates was calculated for each magnitude interval and the results smoothed before being plotted in Figure 2.6.

Stars much brighter than 10^{th} magnitude have images physically too large to be measured with the GALAXY optical system being used and were too few in

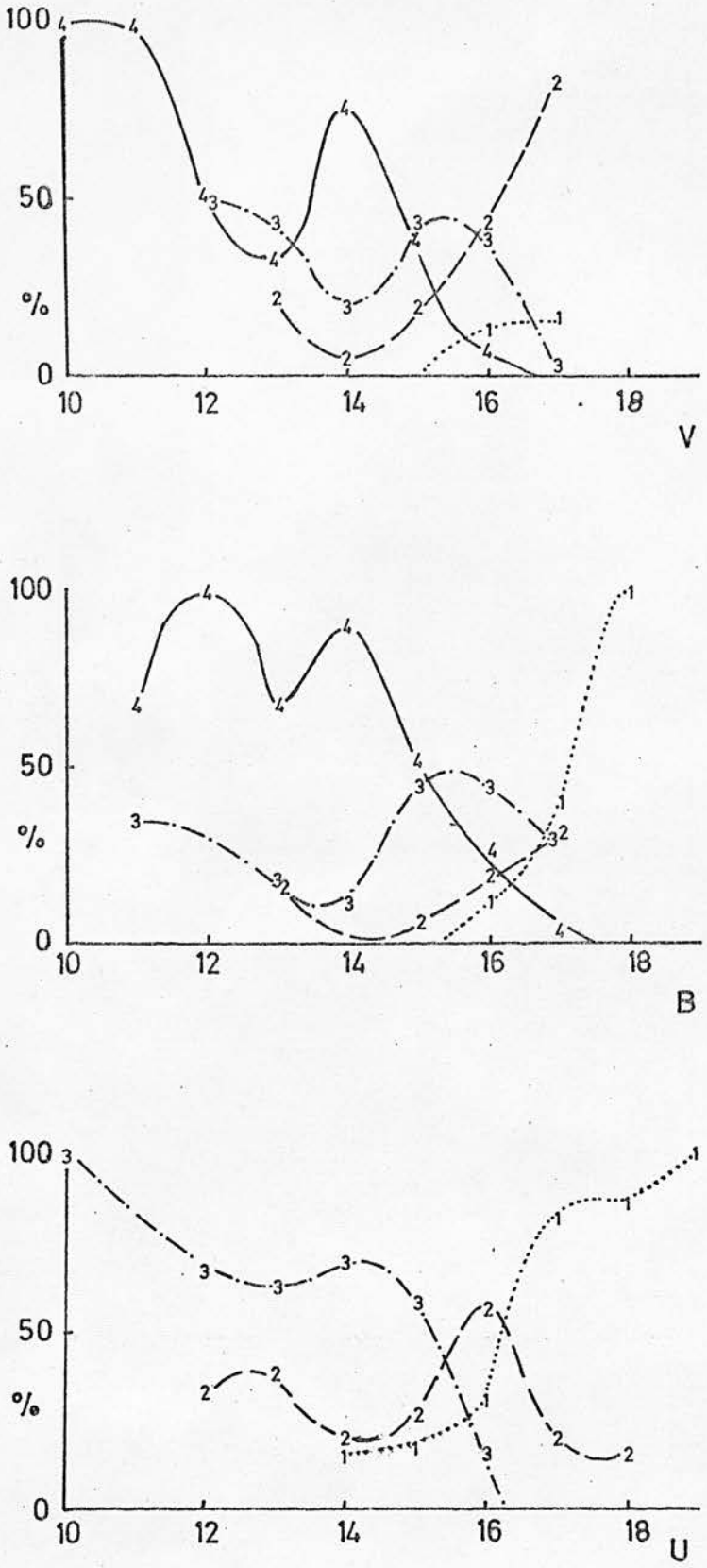

FIG. 2.6
PERCENTAGE OF STARS MEASURED ON 1 TO 4 PLATES AS A FUNCTION OF MAGNITUDE IN THE HIGH STAR DENSITY REGION.

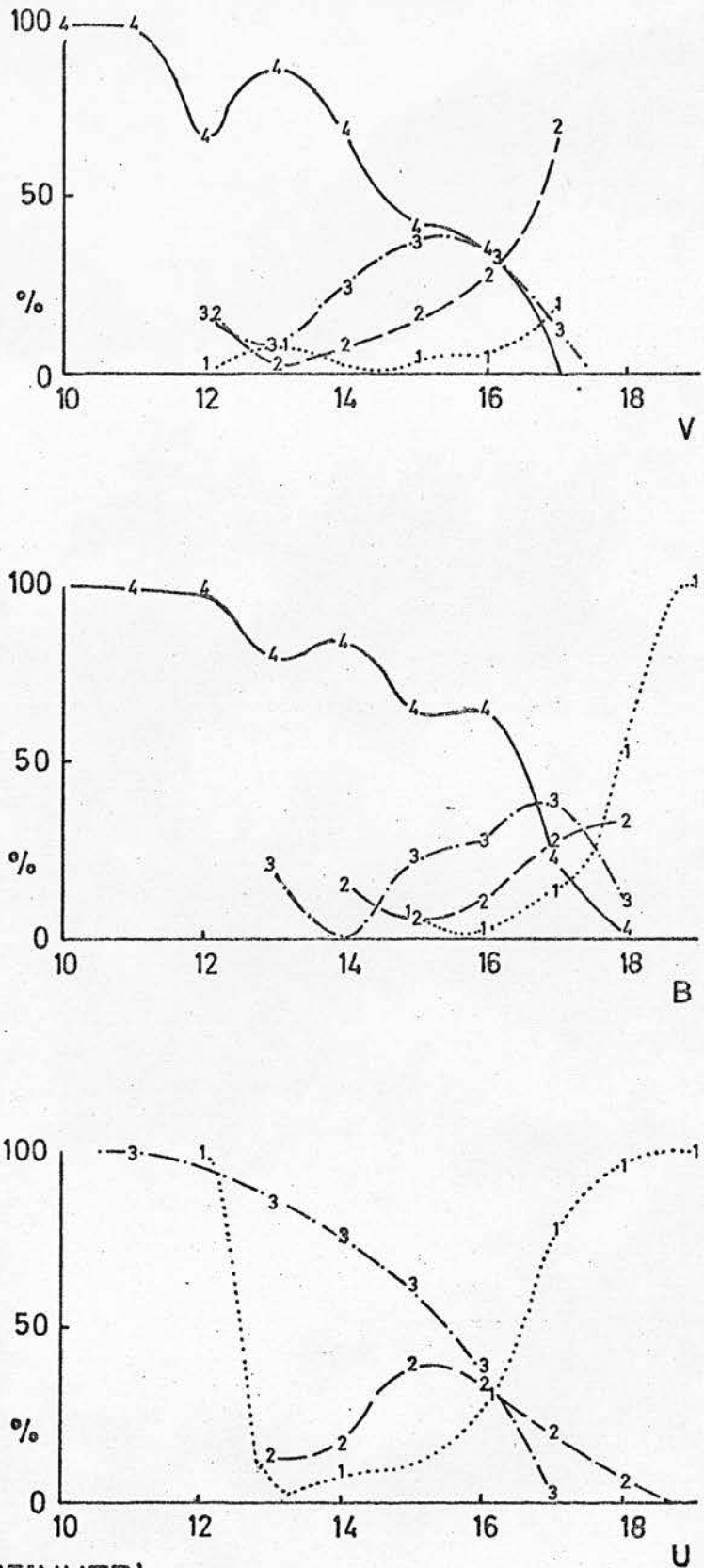

FIG. 2.6 (CONTINUED).
MEDIUM STAR DENSITY REGION.

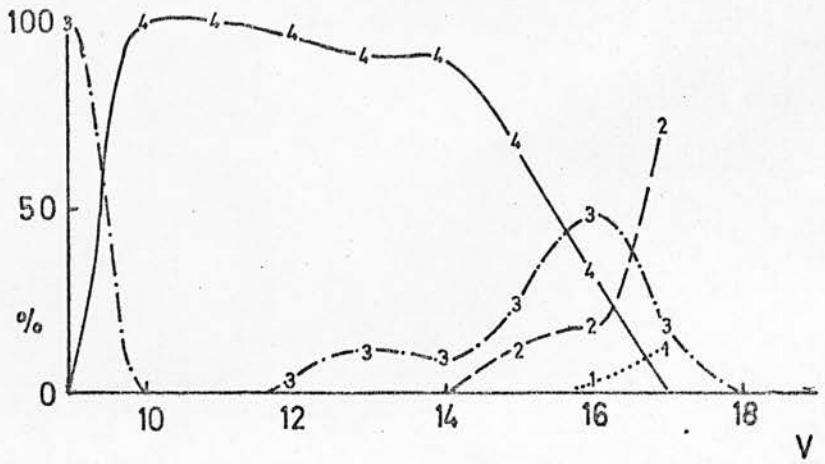

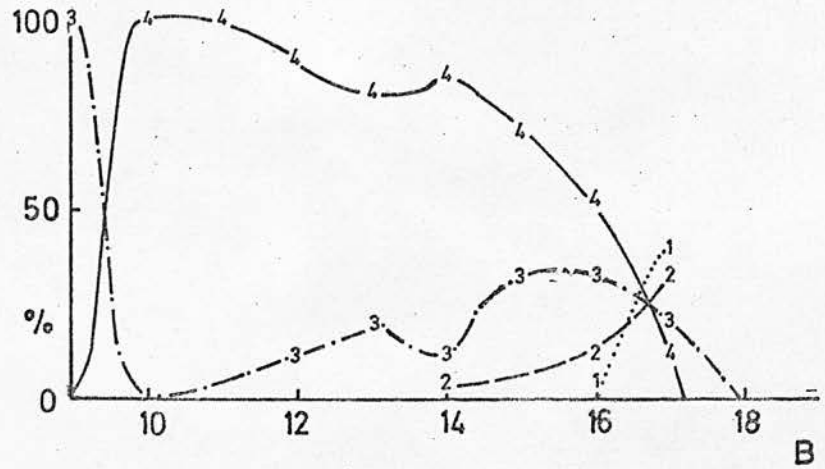

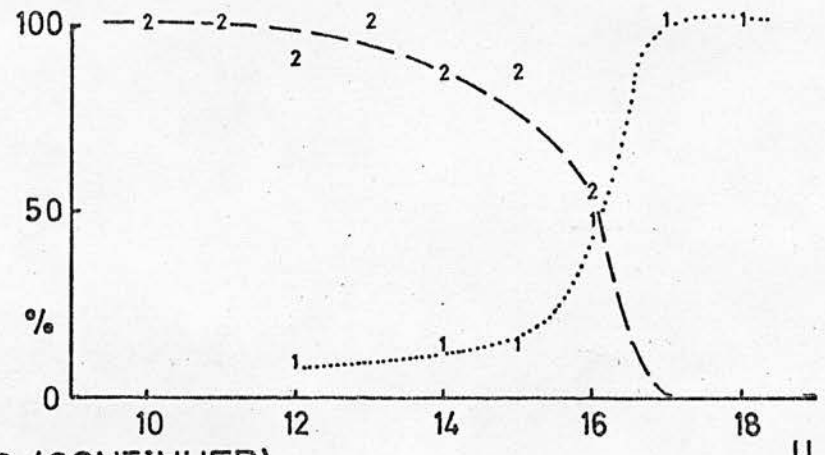

FIG. 2.6 (CONTINUED).
LOW STAR DESITY REGION.

number for analysis. (There are other systems more suitable for the large images of astrographic reflectors and refractors.) Bright stars have been measured when the plates were not exposed so long or were exposed under better seeing conditions.

Poor seeing may affect the measuring ability of GALAXY in crowded regions. This may explain what is seen when the high surface density V and B diagrams are compared with those of the low density region: there is a dip at about 13^{th} magnitude where the star images are still "large" and the number of such stars is also large enough for the problem of overlapping images to be serious.

At faint magnitudes on the yellow plates, there is a rapid rise in the number of stars measured on only two V plates - the result of defining a star as an object measured on two or more plates. This selection effect does not appear so marked on the B or U diagrams because other selections are more important; for example, the reddening in this region means that we do not detect "blue" stars, stars below the V limiting magnitude but not below the B limit, and a large number of red dwarfs will often be too faint in B to be measured but will appear in the V counts. This argument also applies to heavily reddened OB stars. The increase in number of faint stars counted in V suggests that many of the objects measured once were really stars and that the limiting magnitude in V was

greater than 17th magnitude.

The selection of objects described as stars has already been discussed. A prior selection of objects was made in the preparation of the GALAXY magnetic tape catalogue; for example, all stars with m-numbers less than a certain value were rejected. It is felt that for a number of plates, this selection was too severe. On one ultraviolet plate, fifty thousand stars were measured on a Becker iris photometer compared to the five thousand stars with one or more ultraviolet measures by GALAXY. It is not possible that 90% of the objects seen by eye were specks of dirt for the positions agreed with those of stars on the blue finder charts.

In conclusion, it may be said that crowding and seeing have marked effects on the measuring capability of GALAXY on Schmidt plates of small scale (135 arc seconds per millimetre).

2.3.3 Colour and Surface Density

To see how the measurement of stars varies with colour, one can first isolate the problem by studying only those stars which have been measured on all four V and on three or two U plates; this effectively guarantees that the stars used are neither too bright (blue) nor too faint (red) to be measured on the blue plates and that serious crowding has been eliminated. Multiple histograms, Figure 2.7, have been drawn for high, medium, and low surface densities for the cases where three and two U plates were measured. The bottom histogram is the total number of stars selected; immediately above is the number of stars measured on three of the four blue plates (measurement missing on one plate); further above are the numbers of stars missing on two and three blue plates. Stars selected in this way were always measured on at least one blue plate. Subtracting the sum of the stars in the top three histograms from the sum in the bottom one yields the number of stars measured on all four B plates.

Plaut (1964) has used the binomial probability distribution for computing completeness factors which can be modified to determine the probability of GALAXY measuring a star image. Let N be the number of stars measured on all V and U plates and p be the probability that a star which has been measured on all V and U plates will not be measured on a blue plate. Let n be

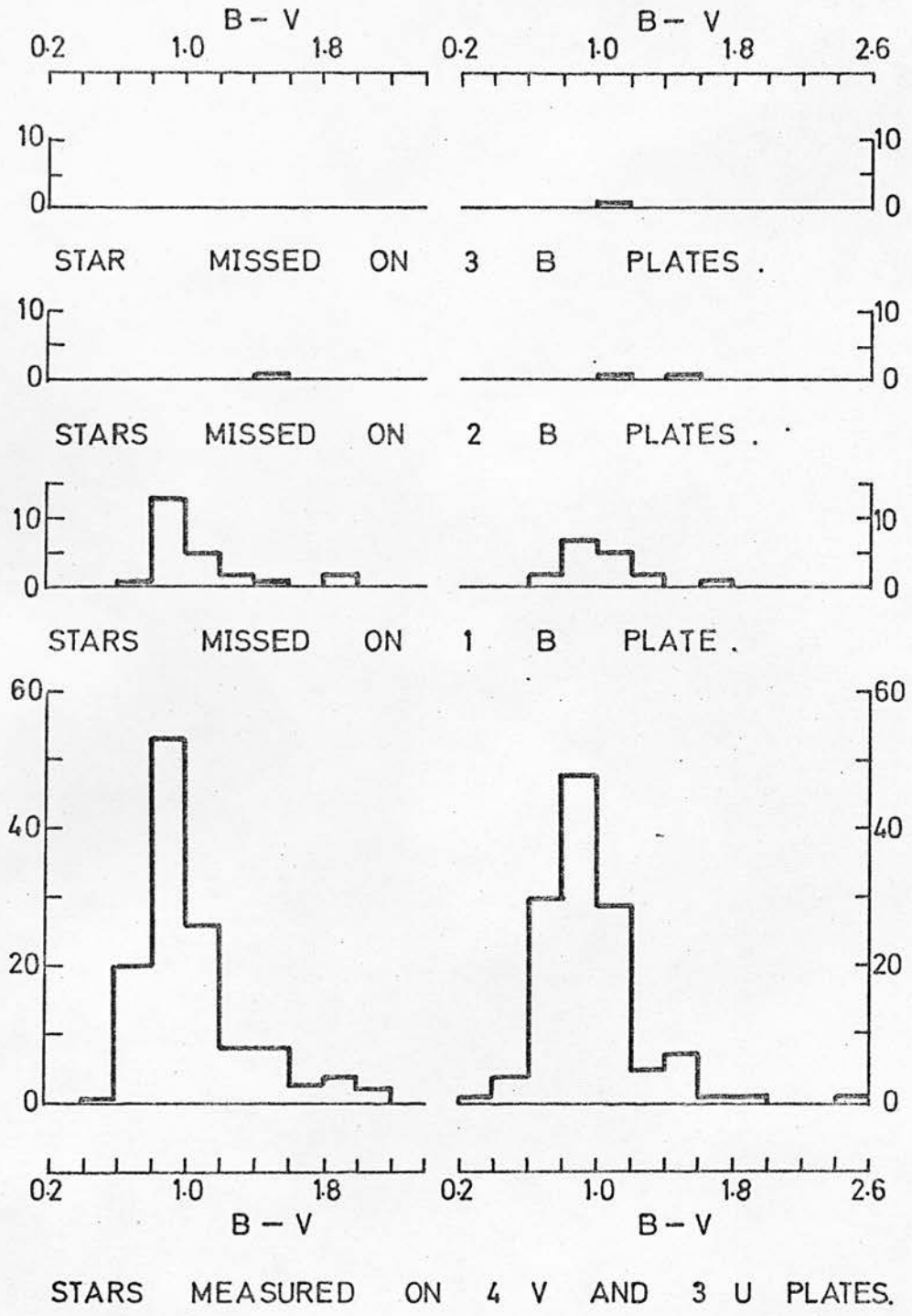

FIGURE 2.7. DISTRIBUTION OF STARS FOUND (LOWEST HISTOGRAM) AND MISSED ON THE B PLATES AS A FUNCTION OF COLOUR AND SURFACE DENSITY . HIGH SURFACE DENSITY (LEFT) MEANS MORE THAN 50 STARS PER 21 SQUARE ARC MINUTES ; MEDIUM SURFACE DENSITY (RIGHT) MEANS BETWEEN 20 AND 50 STARS PER 21 SQUARE ARC MINUTES .

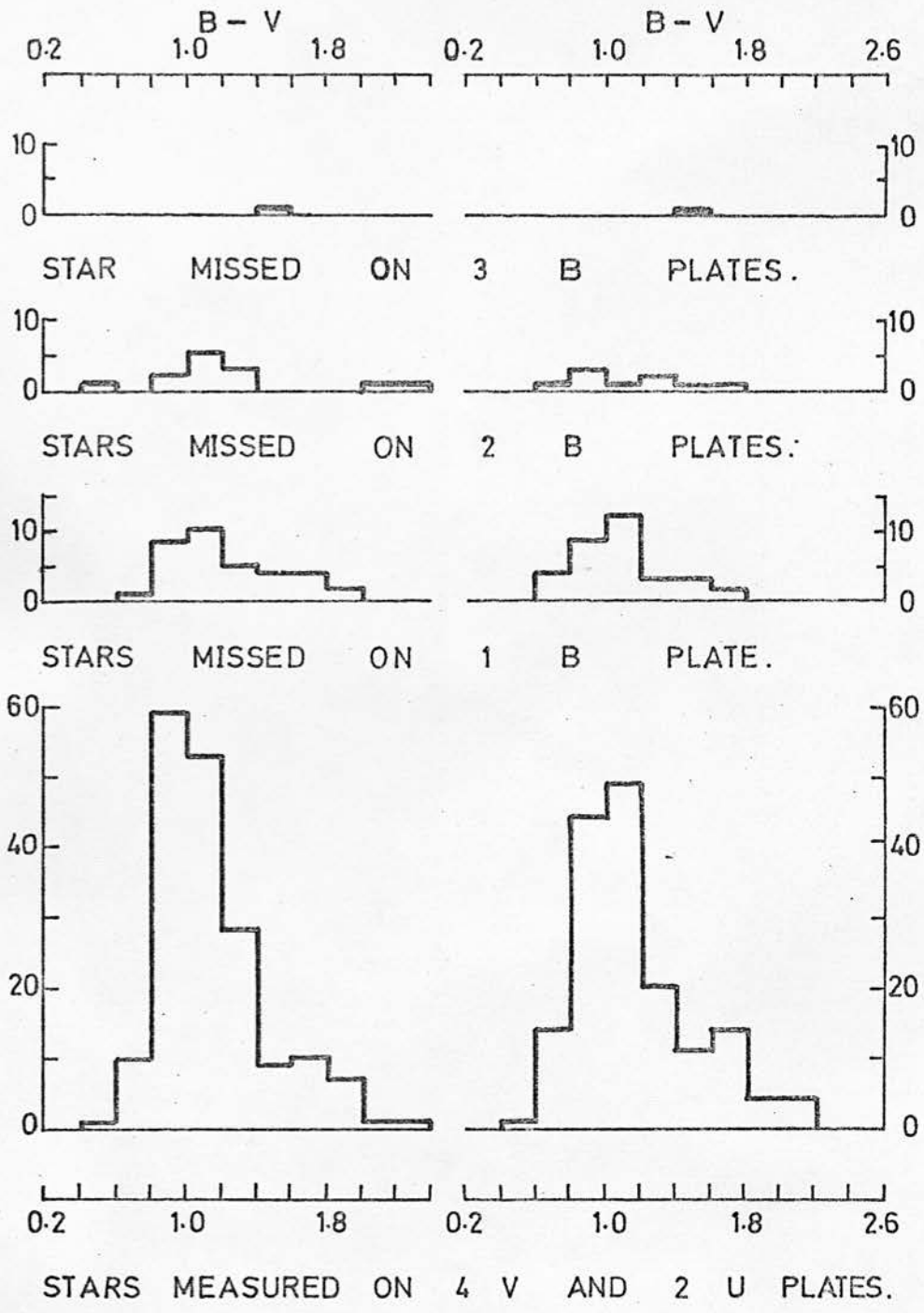

FIGURE 2.7 (CONTINUED)

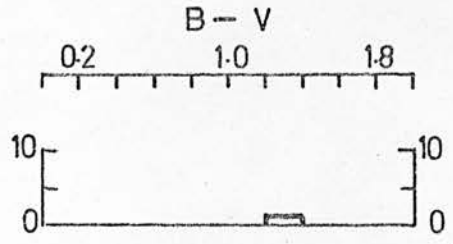

STAR MISSED ON 3 B PLATES .

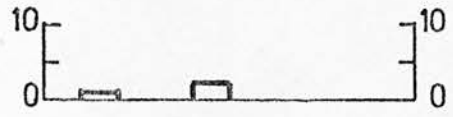

STARS MISSED ON 2 B PLATES .

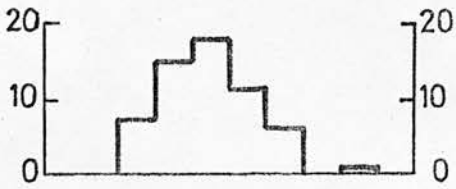

STARS MISSED ON 1 B PLATE .

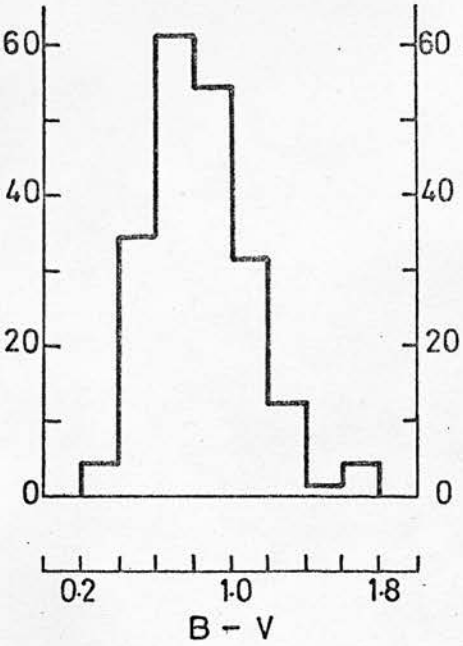

STARS MEASURED ON 4 V AND 2 U PLATES IN LOW SURFACE DENSITY (CLOUD) REGION . LOW SURFACE DENSITY MEANS LESS THAN 20 STARS PER 21 SQUARE ARC MINUTES .

FIGURE 2.7 (CONTINUED)

the number of blue plates. Then one expects a star to be missed 0, 1, 2, ..., n times.

$$m(0) = N(1-p)^n \qquad \text{missed zero times}$$
$$m(1) = N(1-p)^{n-1}pn \qquad \text{missed once}$$
$$m(2) = N(1-p)^{n-2}p^2\frac{n(n-1)}{2!} \qquad \text{missed twice}$$
$$\vdots$$
$$m(n) = Np^n n \qquad \text{missed n times}$$

where $N = \sum_{n} m(n)$.

The total number of stars missed is N-m(0); the average number of times a star was missed is

$$\frac{m(1) + 2m(2) + ... + nm(n)}{m(0) + m(1) + m(2) + ... + m(n)} = np \ .$$

From the histogram, the m's are known and n=4, the number of blue plates measured. The histograms are summarized in Table 2.7.

The value of p is essentially the same for high and medium star counts for the 4V-3U selection. There are three ways of missing a single U measure of a given star from three plates and therefore, one might estimate p to be three times greater in the 4V-2U selection. It is significant that it is much less than this. It may be that a factor, such as crowding, which causes a star to be missed on at least one B plate continues to affect to some degree the measuring capability on the U plates. This would explain why the 4V-2U selection has a greater probability of missing a

B image.

From Figure 2.7 and Table 2.7, we see that GALAXY measures stars equally well in high and low star concentrations. In Table 2.8, the data is combined to study the effect of colour on the ability of GALAXY to measure images. It is evident that the image structure does not depend on colour; this is an important point to note in considering Schmidt astrometric problems.

Table 2.7

Summary of Figure 2.7.

	4V-3U Plates		4V-2U Plates		
	high	medium	high	medium	low
N	125	128	178	162	201
m(0)	100	109	130	119	139
m(1)	24	16	34	33	58
m(2)	1	2	13	9	3
m(3)	0	1	1	1	1
m(4)	0	0	0	0	0
p	0.052	0.045	0.088	0.083	0.083

It should be noted in Figure 2.7 and Table 2.8 that stars with $(B-V) < 0.6$ are to be found only in the low surface density regions. This unusual effect will be met again in the next chapter and will be discussed in Chapter 4.

Table 2.8

Number and Percentage of Stars Missed on One or More Blue Plates as a Function of (B-V).

4V-3U Plates

(B-V)	0.2	0.4	0.6	0.8	1.0	1.2	1.4	1.6	1.8	2.0	2.2	2.4	2.6
No. Missed	0	0	3	20	12	3	3	1	2	0			0
% Missed			6	20	22	23	20	25	40				
% Error			4	4	4	16	14	25	28				

4V-2U Plates

(B-V)	0.2	0.4	0.6	0.8	1.0	1.2	1.4	1.6	1.8	2.0	2.2	2.4	2.6
No. Missed	1	8	21	42	39	20	10	8	2	1	1		
% Missed	25	22	25	26	29	33	48	28	18	20	100		
% Error	25	8	6	4	5	6	16	9	18	20			

2.4 Objective Prism Data

The Curtis Schmidt telescope (60-90-cm) at the Cerro Tololo Inter-American Observatory was used with the 4° prism to obtain objective prism spectrograms. The spectra were made on Kodak 103a0 emulsion without filter at a dispersion of 280 Å/mm at Hγ and were widened 0.2 mm. The plate scale is 96.6 arc sec/mm and the clear field of $5^{\circ}.1$ (side) has the same centre as the Monte Porzio Schmidt field and so completely covers the area measured by GALAXY. The plates were developed vertically in a nitrogen bubble tank and both fixed and washed in air bubble tanks.

Table 2.9

Photographic Data for the Objective Prism Spectrograms

Plate No.	Emulsion	Exposure Time min.	Hour Angle at Start hr min
11225	103a0	1	+1 23
11226	"	40	+0 18
11227	"	20	-0 35
11228	"	10	-1 05
11229	"	5	-1 55

Table 2.9 lists the plates taken, all on one night

(15/16 June, 1972) with good seeing. There is however a clear gradient in image quality from excellent in the North to poor in the South (aggravated also by crowding) so that some of the stars could not be classified as well as they might have been at this dispersion.

The plates were examined in Chile enabling a better selection of early and F type stars to be made for photoelectric observations. Most of the stars so observed were reclassified in Bochum and included those stars unaffected by crowding which were brighter than $B=13^m$ in Tables 3.1, 3.2, and 3.3.

Stars to be classified were compared with three sources of MK data: i)with those stars in the field which previously had been classified by Nassau and Stephenson (1963) in LS IV (limiting magnitude $B=12^m$), ii)with the standards in the atlas by Abt et al. (1968) taken with a grating slit spectrograph at 128 Å/mm, and iii)with Seitter's atlas (1970) of standards taken with an objective prism spectrograph at 240 Å/mm. The Abt atlas was better for early-type stars and the Seitter atlas was better for late-type stars but there really ~~were~~ was not an adequate number of standards on the plate. Objective prism spectra depend critically on the quality of the seeing and render the usual comparison technique rather impotent in contrast with intercomparison of slit spectrograms.

Chapter 3

Observations and Results

3.1 Observations

In the first chapter, it was shown that a discontinuity in young spiral tracers exists near $l^{II}=40^{o}$. In order to study the development of the feature, photoelectric observations were made of high luminosity stars between $30^{o} \leq l^{II} \leq 45^{o}$ with $|b^{II}| \leq 5^{o}$ chosen from LS IV (Nassau and Stephenson, 1963). In a few cases, other stars nearby were inadvertently observed because the coordinates coincided with a star other than the one on the finder chart[1] (eg. $+3^{o}5$ and $+3^{o}5.1$) or the star was a visual double at the telescope. In this way, 143 stars were selected. Table 3.1 contains the mean values of the observations and the number of nights, N, on which a star was observed.

Moffat observed stars between $40^{o} \leq l^{II} \leq 50^{o}$ taken from LS II (Stock et al, 1960) and LS IV (loc. cit.). These observations will be published elsewhere.

The data both from Table 3.1 and from Moffat (of stars not included in Table 3.1) are shown in the two-colour diagram of Figure 3.1. The observations from the table and from Moffat are distinguished by an "x"

1 The finder charts are in LS IVa but a few of these stars are within the Schmidt field and have been identified on Plates 2 and 3.

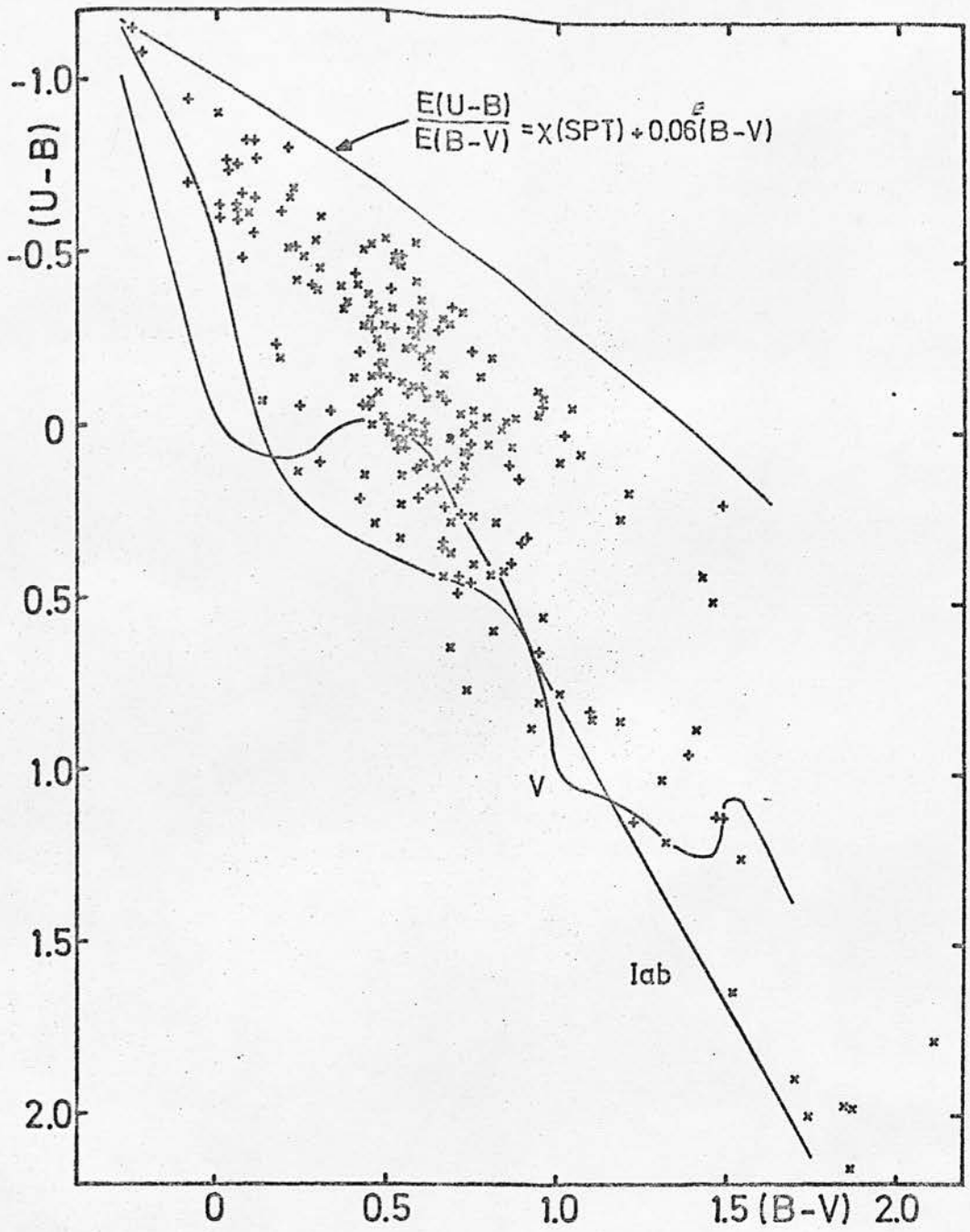

FIG. 3.1

OBII STARS BETWEEN $30° < l^{II} < 50°$ FROM LSII AND IV

OBSERVED BY SHERWOOD (×) AND MOFFAT (+).

Table 3.1

Photoelectric Observations of OB Stars: $30^{\circ} \leq l^{II} \leq 45^{\circ}$.

OB No.	OB Class	SpT	V	(B-V)	(U-B)	N	R
- 4°32		A7Ib	10.18	0.92	0.86	3	1
33		WN8	11.03	0.46	-0.34	3	9
- 3°16	OB		12.00	0.49	-0.03	2	
17	OB^-		10.18	0.57	-0.12	2	
18	OB		11.67	1.85	2.26	1	
- 2°13	OB^-		10.17	0.54	-0.13	3	
14	OB		11.60	0.66	-0.20	2	
14.1			12.10	0.63	0.08	1	
16	OB		11.22	0.86	0.05	3	
17	OB		10.43	0.94	-0.12	1	
18	OBh		11.09	0.80	-0.21	2	
19	OB		10.56	0.84	-0.03	3	
20	OB		11.20:	0.70	0.17	2	
21.1			10.70	1.87	1.96	2	
22		B9Ib	9.84	0.80	0.42	2	1
23	OB		11.14	0.38	-0.36	2	
24	OB	B0.5p	9.07	0.42	-0.51	1	R
			8.60	0.44	-0.53	1	
25	OB		9.79	0.56	-0.33	2	
26	OB		10.82	0.45	-0.32	2	
- 1° 4	OB^+r	B8II	9.20	1.42	0.42	3	6
5	OB		10.75	0.87	-0.04	3	
6	OB^-	B5	7.70	0.44	-0.38	3	3
7	OB	B1V	7.85	0.29	-0.53	3	1
8	OB	B8	9.86	0.56	-0.24	3	3
9	OB		11.48	0.45	-0.07	3	
10	OB		10.66	0.49	-0.54	2	
11		B8II	9.34	0.66	0.42	2	1
12	OB		11.63	0.48	-0.19	2	
13		B7II	9.06	0.45	-0.01	2	1
14	OB^-		10.32	0.21	-0.52	1	
15.1			12.02	1.54	1.24	1	

Table 3.1 (continued)

OB No.	OB Class	SpT	V	(B-V)	(U-B)	N	R
- 1°16	OB		11.96	0.47	-0.25	1	
17	OB⁻		10.43	0.30	-0.46	1	
18	OB⁻		11.25	0.43	0.14	1	
- 0° 4	OB		11.37	1.06	0.06	1	
5	OB	B7II?	10.61	1.40	0.86	1	1
6	OB⁻	B5	8.61	0.49	-0.29	1	3
7	OB⁺	O8	9.98	0.58	-0.52	1	1
8	OB⁻		11.15	0.61	0.11	1	
9	OB⁻		11.21	0.72	0.10	1	
10	OB⁻		11.36	0.79	-0.04	1	
11	OB⁻		11.24	0.48	-0.23	1	
12	OB⁻		11.24	0.48	-0.10	1	
13	OB		11.18	0.30	-0.60	1	
14	OB		11.46	0.25	-0.49	1	
15.1			10.18	0.54	0.03	1	
+ 0° 2	OB⁻	B5	7.95	0.66	-0.16	2	3
3	OB⁺(h)	B0	11.64	-0.00	-0.90	1	4 R
4	OB⁻		11.41	0.81	0.26	1	
5.1			11.89	2.11	1.77	1	
6	OB	B3V	7.39	0.09	-0.61	2	1
7	OBr		10.18	1.45	0.48	2	
8	OB		9.97	0.74	-0.02	1	
9	OB⁻		11.42	0.61	0.02	1	
10	OB⁻	B8II?	10.76	0.67	0.08	1	1
11	OB		11.04	0.45	-0.52	2	
12	OB⁻		11.58	0.50	0.02	1	
13	OB⁻	B5	9.08	0.43	-0.29	1	3
14	OB⁻	B8	8.58	0.29	-0.39	1	3
+ 1° 2	OB		11.55	0.72	0.06	1	
3	OB		11.28	0.75	-0.06	1	
4	OB		11.85	0.68	0.63	1	
5	OB		11.06	0.73	0.00	1	
6	OB⁻	B8	10.03	0.40	-0.14	1	3
7	OB⁻		10.68	1.30	1.01	1	

Table 3.1 (continued)

OB No.	OB Class	SpT	V	(B-V)	(U-B)	N	R
+ 1° 8	OB		9.90	0.41	-0.41	1	
9.1			8.94	1.18	0.83	1	
+ 2° 1.1			7.12	1.74	1.99	1	
2	OB		10.32	0.52	-0.48	1	
3	OB		11.43	0.72	-0.00	1	
4	OB		10.86	0.94	-0.06	1	
5	OB		10.85	0.62	-0.23	1	
6	OB		11.59	0.45	-0.15	1	
7	OBh		12.03	0.75	0.39	1	
8	OB		10.52	0.77	-0.16	1	
9	OB		10.34	0.72	-0.34	1	
10.1			10.90	1.70	1.88	1	
+ 3° 2	OB	B0III	9.20	0.58	-0.42	2	1
3	OB		9.32	1.00	0.08	3	
4	OB		11.67	0.61	0.13	1	
4.1			10.34	0.43	0.26	1	
5	OB		10.98	0.51	-0.34	2	R
5.1			9.10	0.13	-0.06	1	
6	OBr	B1Ib	8.60	0.59	-0.37	2	1
7	$OB^{+}h$		11.21	0.63	-0.32	2	
8	OB		11.49	0.37	-0.35	2	
9	OB		11.55	0.57	0.01	2	
9.1			9.19	0.26	0.12	1	R
10.1			12.30	0.84	0.41	2	
11	OB^{+}	B3Ia	7.42	0.45	-0.31	2	1
12	OB		12.00	0.68	0.36	1	
12.1			9.19	0.24	0.13	1	R
13	OB		11.54	0.55	-0.23	2	
14	OB	B0.5Vp	10.86	0.57	-0.23	2	6
15	OB		10.77	0.59	-0.21	3	
16	OB^{-}	B8	8.70	0.36	-0.40	2	3
17		A2II	11.24	0.44	0.32	1	
17.1			11.01	1.52	1.63	1	
18		B7II	10.22	0.94	0.78	2	
+ 4° 4	OB		10.89	0.57	-0.03	3	

Table 3.1 (continued)

OB No.	OB Class	SpT	V	(B-V)	(U-B)	N	R
+ 4° 5	OB		11.59	0.79	0.04	5	
6	OB	B2III	10.31	0.61	-0.18	20	7
7	OB		11.72	0.60	-0.33	4	
8	OB		10.59	0.68	0.02	4	
9	OB		11.74	0.83	-0.01	3	
9.1			12.06	0.79	0.31	1	
10	OB⁻		11.85	0.51	0.02	2	
11	OBh	B0	10.84	0.68	-0.31	2	3
+ 5° 6.1			12.10	0.46	0.28	3	
6.2			12.75	0.64	0.10	3	
7		B9II	10.58	0.54	0.14	2	1
7.1			11.14	1.29	1.20	1	
8	OBr	G	9.69	1.20	0.17	4	3
9	OB⁻		10.84	0.68	0.36	1	
10.1			10.36	0.95	0.53	3	
10	OB		11.14	0.58	-0.27	2	
11		F6I-II	6.91	0.81	0.58	1	1
12	OB		10.54	1.86	2.14	1	
13	OB		9.75	0.54	-0.46	2	
+ 6° 5.1			9.65	0.73	0.24	2	
6	OB		10.72	1.18	0.25	2	
7.1			8.46	1.10	0.83	1	
8		A8Ib	10.70	0.73	0.75	2	1
+ 7° 6		F5I	9.84	1.00	0.76	3	1 R
7		F8I	8.57	1.30	0.99	2	1
8	OB		10.17	0.18	-0.19	2	
+ 8° 2	OB	A0Ia	10.62	0.60	0.01	2	6
3	OB⁻		10.11	0.60	0.10	2	
4	OB		11.09	0.60	-0.32	2	
5	OB⁺	B1Ia	9.81	0.22	-0.69	2	6
+ 9° 5	OB⁺	08:Vnn	8.59	0.54	-0.47	3	1
6	OB⁻		11.29	0.71	-0.05	2	
6.1			11.14	0.75	0.25	2	
+10° 2	OB⁺		10.61	0.22	-0.68	3	
3	OB	B2V	6.73	0.23	-0.42	3	8

Table 3.1 (continued)

OB No.	OB Class	SpT	V	(B-V)	(U-B)	N	R
+10° 4	OB⁻		10.58	0.61	-0.09	3	
5	OB		10.60	1.04	-0.08	2	
+11° 4	OB⁻		11.11	0.54	0.22	2	
5	OB⁺	B1Ia	10.59	0.95	-0.12	3	5
6	OB	B1.5:IV:ne	8.95	0.46	-0.32	2	5
7	OB⁻	B1Vnn	9.43	0.38	-0.36	3	5
8	OBh	F8	10.05	0.57	-0.28	3	3

Notes on Table 3.1 :

In the first column, stars whose numbers have a decimal are near OB stars.

The numbers in the last column indicate the reference sources for the spectral types in the third column; R indicates a note.

1 Luminous Stars in the Northern Milky Way IV, 1963.

2 Henry Draper Catalogue.

3 Zweiter Katalog der Astronomischen Gesellschaft, Bonn, 1958.

4 Bergedorfer Spektral Durchmusterung, 1953.

5 Hiltner, W.A. ApJ Suppl 2, 389, 1956.

6 Blanco, V.M., Demers S., Douglass G.G., and Fitzgerald M.P. Publ US Naval Obs., 2nd Series, XXI, 1968.

7 Svolopolous, S.N. ZfA 61, 107, 1965.

8 Andrews, P.J. Mem RAS 72, 35, 1968.

9 Roberts, M.S. AJ 67, 79, 1962. (-4°33=MR 91)

-2°24 Variable?

+0° 3 Variable (reference no. 4)

+3° 5 Coordinates given for +3°5.1, finder chart for +3°5 in reference 1 above.

+3° 9.1 Same as +3°12.1.

+3°12.1 Same as +3° 9.1.

+7° 6 Variable. RZ Oph.

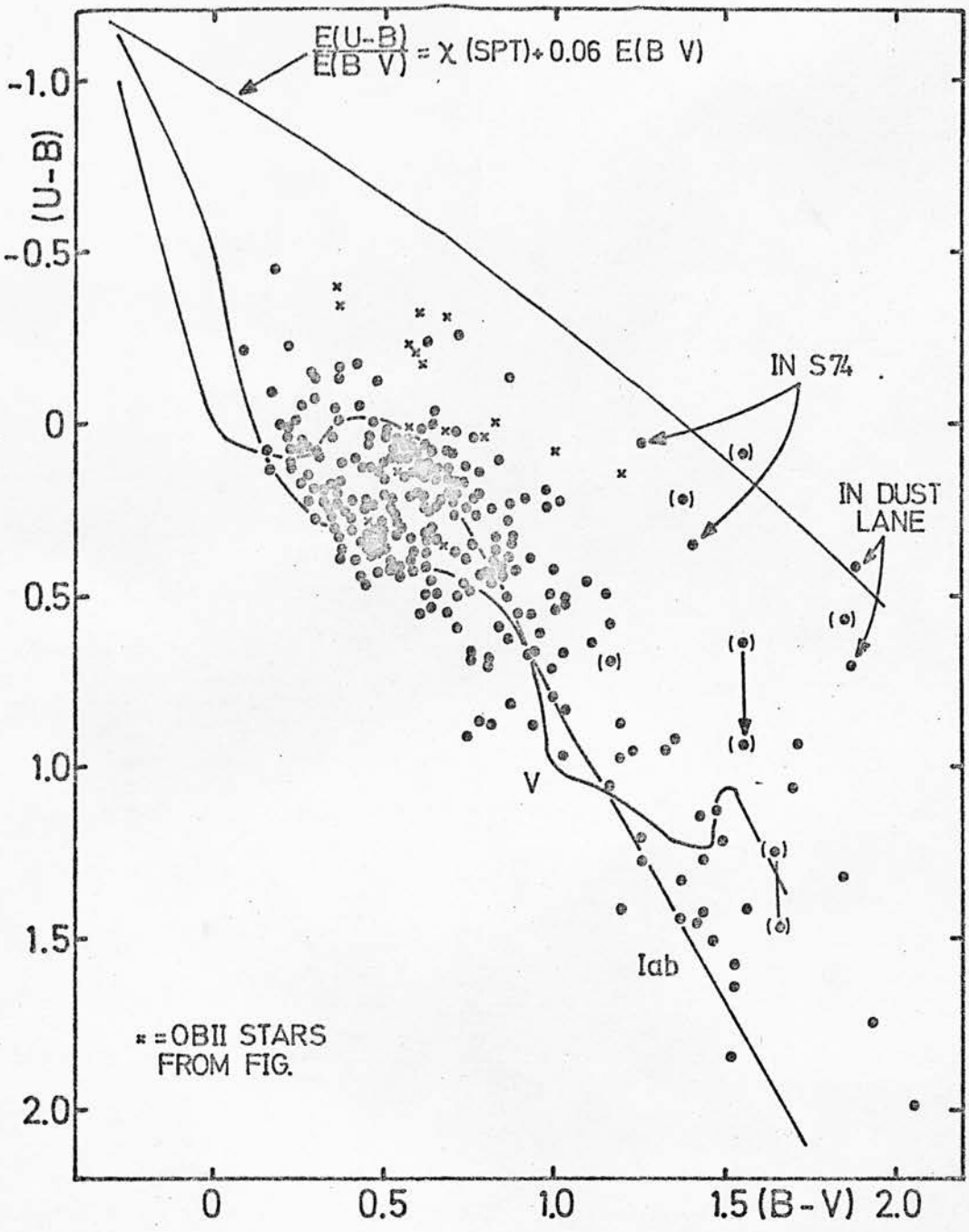

FIG. 3.2

OBAF STARS IN THE SCHMIDT FIELD ABOUT

l^{II} = 40 (PHOTOELECTRIC OBSERVATIONS BY SHERWOOD)

and a "+" respectively. The intrinsic colour relationships indicated for luminosity classes V and Iab are taken from FitzGerald (1967); the reddening line is that used by FARBE (see Appendix A2) for an O star.

In order to study the region about $l^{II}=40^{o}$ in detail and to calibrate the Schmidt plates, several hundred stars with O, B, A, and F spectral types were selected for an observing programme. The F-type stars were included in case there should be some pre-main sequence stars in the region. The stars were taken from the Second Catalogue of the Astronomische Gesellschaft (AGK_2) Bonn (1958), Apriamashvili (1966), and from a study of the objective prism plates (Table 2.9) taken with the Curtis Schmidt on Cerro Tololo. The 262 stars observed are listed in Table 3.2 in order of increasing right ascension (1950.0). The second last column contains the number of nights, N, on which a star was observed; in the last column, a "c" means that the star was used in calibrating the photographic photometry. The stars 13, 180, and 181 (-1 and -2) are close visual doubles. Stars 180 and 181 are both F spectral types and visually have a reddish colour. The (U-B) for 181-2 is probably not affected by scattered light since the effect is not seen in the other fainter two stars. The data are shown in the two-colour diagram of Figure 3.2. A few stars from Table 3.1 which are in the Schmidt field are also shown in this figure - they are denoted by "x" as before. The stars

Table 3.2

Photoelectric Observations of OBAF Stars in the Field Photographed with the Schmidt Telescope.

Star No.	RA (1950.0)	DEC	V	(B-V)	(U-B)	N	R
108	$18^h57^m43^s.2$	$+5^\circ16'.4$	12.47	0.63	0.49	1	
107	49.8	5 12.5	12.16	0.62	0.06	1	
106	51.5	5 9.8	11.76	0.72	0.22	1	
111	58 25.8	4 57.5	11.34	0.63	0.13	1	c
115-1	49.4	4 37.9	11.75	0.86	0.33	1	c
35	59 14.4	6 18.8	11.37	0.40	0.24	1	
38	14.5	6 17.0	12.11	0.51	0.16	1	
37	14.5	6 17.1	10.17	0.23	0.07	1	
101-1	18.9	5 8.6	12.85	0.89	0.42	4	c
36	22.2	6 18.7	10.69	0.28	0.15	1	
65	23.4	5 25.2	10.85	0.84	0.10	1	c
39	32.0	5 57.0	11.51	0.61	0.11	1	
34	44.5	6 22.7	11.84	0.56	0.30	1	
66	57.2	5 20.9	9.28	0.31	0.28	1	c
130	19 0 0.0	4 19.7	9.77	0.59	0.14	1	
67	26.4	5 16.3	7.71	0.23	0.13	1	
135	35.7	4 8.1	11.94	0.87	0.27	1	
42	37.5	5 48.4	11.14	0.49	0.15	1	
136	38.3	4 5.0	11.99	0.74	0.17	1	
41	46.2	5 52.2	9.56	0.33	0.23	1	
73	50.7	5 29.0	11.09	1.94	1.74	1	c
74	51.2	5 29.0	12.78	0.71	0.22	1	c
75-4	51.9	4 42.0	13.72	1.56	0.63	1	c
75-6	52.9	4 42.0	15.69	2.31		1	
40	58.2	5 55.1	7.81	0.31	0.08	1	
29	1 9.6	6 19.5	12.00	0.60	0.43	1	
75-2	16.9	4 42.1	13.51	0.87	0.23	1	c
75-3	16.9	4 42.1	14.58	0.86	0.50	1	c
126	21.6	4 32.6	10.91	0.55	0.42	1	c
28	27.4	6 48.1	11.05	0.60	0.19	1	
95	27.7	4 49.1	11.81	0.84	0.59	1	c
30	28.8	6 19.1	10.24	0.56	0.11	1	

Table 3.2 (continued)

Star No.	RA (1950.0)	DEC	V	(B-V)	(U-B)	N	R
32	$19^h\ 1^m32^s.3$	$+6^\circ11'.1$	12.06	0.46	0.32	1	
27	35.7	6 38.6	11.33	0.46	0.12	1	
33	38.8	6 9.5	11.26	0.40	0.32	1	
31	40.2	6 14.5	11.64	0.70	0.24	1	
75	40.9	5 9.9	8.16	0.48	-0.13	2	
26	42.8	6 22.3	11.15	0.58	0.06	1	
79	48.9	4 56.1	11.10	0.52	0.06	1	c
77-3	49.0	4 55.3	14.51	1.12		1	c
80	49.1	4 54.2	9.55	0.39	0.25	1	c
77-1	50.6	4 55.3	12.42	1.02	0.22	1	c
75-1	51.1	5 4.2	12.60	0.74	0.12	2	c
77-2	56.9	4 56.2	12.55	0.76	0.66	1	c
76	2 9.7	5 11.7	11.45	0.50	0.11	1	c
24	11.6	6 23.1	10.54	0.56	0.06	1	
25	11.7	6 20.1	9.54	0.20	-0.00	1	
78	12.6	4 55.5	11.17	0.46	0.37	2	c
89-1	17.8	4 26.4	12.69	0.82	0.87	1	c
141-1	22.6	3 56.2	10.63	2.45	2.03	1	
88	23.5	4 33.2	10.89	0.44	0.33	1	c
89	24.1	4 28.4	8.70	0.26	0.05	1	c
89-2	32.2	4 25.3	12.58	0.81	0.70	1	c
23	34.0	6 11.0	10.39	0.59	0.41	1	c
77	37.5	4 56.7	11.61	0.98	0.19	2	c
1	40.0	6 51.4	10.60	0.41	0.31	1	
43	52.9	5 48.8	8.90	0.51	0.03	1	c
86	57.3	4 37.3	12.24	0.76	0.68	1	c
14	3 10.2	6 25.7	11.47	0.71	0.17	1	c
15	10.3	6 22.7	11.59	0.64	0.13	1	c
2	15.4	6 42.4	11.83	0.55	0.31	1	
13-1	21.2	6 28.4	6.88	0.46	0.05	1	
13-2	21.2	6 28.4	8.80	0.63	0.12	1	
22	22.2	6 2.1	11.98	0.65	0.10	1	c
20	22.9	6 9.9	10.57	0.45	0.30	1	c
84	27.9	4 32.2	10.87	0.50	0.37	1	c
19	31.7	6 9.2	11.11	0.66	0.24	1	c

Table 3.2 (continued)

Star No.	RA (1950.0)	DEC	V	(B-V)	(U-B)	N	R
349	$19^h\ 3^m34^s.1$	$+3^\circ57'.0$	11.26	0.70	0.08	2	c
12	43.5	6 23.3	10.03	0.53	0.41	1	c
21	44.2	6 4.0	11.87	0.82	0.41	1	c
17	44.3	6 10.7	11.28	0.72	0.20	1	c
85	47.5	4 26.8	11.45	0.58	0.33	1	c
3	50.4	6 45.7	10.15	0.58	0.10	1	
148	50.9	4 14.8	12.47	0.69	0.16	1	
350	51.1	3 56.2	9.87	0.50	0.31	2	c
9	52.0	6 33.5	8.89	0.30	0.19	1	
149	54.9	4 14.8	11.52	0.47	0.39	1	c
18	57.9	6 6.0	10.67	0.38	0.17	1	c
11	58.2	6 25.8	11.23	0.63	0.25	1	c
348	4 0.1	4 1.8	11.95	0.72	-0.26	2	c
4	7.7	6 48.5	7.27	0.17	0.13	1	
10	8.6	6 23.4	11.05	0.51	0.28	1	c
85-1	9.9	4 26.1	11.98	0.61	0.55	1	c
354	20.7	3 39.5	11.48	0.60	0.08	1	
82-1	21.1	4 27.7	12.31	0.92	0.69	1	c
8	22.2	6 32.2	9.21	0.34	0.24	1	c
16	23.0	6 10.8	11.30	0.62	0.34	1	c
351	24.0	3 53.4	11.68	0.52	0.21	2	c
355	24.6	3 37.4	10.34	0.51	0.36	1	
50	24.7	5 9.9	8.28	0.47	0.23	1	
347	26.0	3 59.9	10.80	0.65	0.15	2	c
150	30.2	4 41.2	9.77	0.87	-0.14	1	
150-1	30.2	4 41.2	13.96	0.98	0.24	1	
150-2	30.2	4 41.2	14.25	2.69		1	
150-3	30.2	4 41.2	13.34	2.57	1.72	1	
150-4	30.2	4 41.2	14.22	0.96	0.61	1	
150-5	30.2	4 41.2	13.46	0.78	0.20	1	
150-6	30.2	4 41.2	12.73	0.85	0.43	1	
150-7	30.2	4 41.2	14.36	1.86	0.56	1	
150-8	30.2	4 41.2	15.16	1.17	0.69	1	
150-9	30.2	4 41.2	9.32	1.20	0.97	1	
352	34.7	3 53.4	11.91	0.63	-0.24	2	

Table 3.2 (continued)

Star No.	RA (1950.0)	DEC	V	(B-V)	(U-B)	N	R
7	$19^h\ 4^m 37^s.8$	$+6^\circ 37'.8$	11.79	0.77	0.26	1	c
346	41.9	4 2.6	11.80	0.82	0.26	3	c
344	45.0	4 11.9	12.44	0.63	0.37	3	c
353	48.5	3 49.8	8.15	0.28	0.22	3	
360	48.7	3 36.3	8.68	0.35	0.27	1	
5	51.9	6 50.6	11.79	0.64	0.53	1	
6	57.5	6 45.6	11.72	0.89	0.54	1	
329	5 3.5	4 29.0	10.28	0.58	0.09	1	c
360-1	5.2	3 21.9	11.09	0.30	-0.08	2	
360-2	5.2	3 21.9	10.33	0.26	-0.06	2	
330	11.6	4 31.7	11.89	0.67	0.22	1	c
190	13.0	5 17.6	11.96	0.72	0.16	3	c
376	21.1	3 54.7	11.34	0.51	0.43	2	c
375	23.0	3 46.8	10.78	0.66	0.15	2	
327	23.8	4 31.9	11.73	1.52	1.84	1	c
328	23.9	4 29.8	8.92	1.17	1.05	1	
377	27.7	3 58.2	11.29	0.52	0.41	2	c
190-10	30.5	5 18.7	13.92	0.82	0.40	3	c
335	30.6	4 20.9	10.86	0.55	0.10	1	c
177	31.8	5 48.3	11.47	0.52	0.40	1	c
178	32.2	5 37.7	12.09	0.53	0.39	1	c
374	34.4	3 43.8	11.38	0.69	0.10	2	
323	34.7	4 44.7	12.01	0.53	0.42	1	
324	34.7	4 44.7	10.65	0.46	0.34	1	
362	36.7	3 32.4	11.48	0.61	0.20	1	
326	38.3	4 32.0	10.04	0.44	0.12	1	c
324-1	39.8	4 46.2	12.40	0.66	0.49	1	
324-2	41.8	4 47.5	12.48	0.76	0.22	1	
179	42.2	5 30.8	11.34	0.66	0.34	1	c
381	44.8	3 52.3	11.00	0.63	0.40	2	c
151	45.0	6 59.6	10.19	0.49	0.29	1	
152	45.0	6 59.6	11.66	0.70	0.19	1	
173	46.0	5 54.4	11.28	0.72	0.59	1	c
380	48.2	3 56.2	11.75	0.75	0.38	2	c
190-1	48.9	5 20.5	10.01	1.19	0.87	6	c

Table 3.2 (continued)

Star No.	RA (1950.0)	DEC	V	(B-V)	(U-B)	N	R
190-12	$19^h\ 5^m48^s.9$	$+5^\circ20'.7$	15.01	0.75	0.91	4	c
190-8	49.2	5 11.4	14.31	0.83	0.32	4	c
180-1	49.8	5 29.2	12.06	0.57	0.03	1	
180-2	49.8	5 29.2	12.65	0.80	0.43	1	
324-3	51.4	4 46.8	12.24	0.71	0.02	1	
172	51.4	5 53.4	10.99	0.53	0.26	1	c
190-2	52.1	5 16.23	11.09	0.47	0.36	6	c
190-7	52.2	5 13.8	13.95	1.89	0.41	4	c
334	54.6	4 26.4	11.62	0.48	0.43	1	c
190-11	56.4	5 21.0	13.86	0.99	0.49	4	
190-4	57.1	5 14.3	11.66	1.88	0.70	4	
379	57.7	4 0.4	11.70	0.43	0.15	1	c
363	58.4	3 27.9	10.93	0.45	0.24	1	
190-54	59.8	5 14.3	12.04	1.46	0.62	1	
190-5	6 0.1	5 14.3	14.06	1.03	0.96	4	c
342	1.9	4 7.8	10.44	0.71	0.23	2	c
331	6.7	4 31.4	11.72	0.64	0.00	1	c
341	7.2	4 11.9	12.16	0.75	0.48	2	
181-3	9.6	5 29.1	12.82	0.82	0.24	3	c
333	12.1	4 25.7	11.84	0.64	0.08	1	c
369	15.9	3 36.0	11.40	0.71	0.27	1	
181-1	17.7	5 26.0	11.02	0.56	0.15	3	
181-2	17.7	5 26.0	11.91	0.18	-0.45	3	
382	18.0	3 56.5	12.03	0.56	0.10	1	c
171	18.1	5 51.7	11.69	0.55	0.42	1	c
157	18.1	6 17.2	11.24	0.75	0.24	1	c
157-2	18.1	6 17.5	13.92	1.00	0.71	1	c
157-3	18.1	6 17.5	13.58	1.04	0.83	1	c
182-6	19.0	5 35.3	12.40	0.88	0.34	5	c
182-5	19.5	5 33.3	13.85	1.00	0.79	5	c
182-7	20.6	5 31.1	14.15	0.96	0.60	6	c
183	20.6	5 36.6	12.13	0.83	0.36	3	c
367	21.6	3 27.9	10.20	0.42	-0.18	1	
191-1	26.0	5 19.2	11.95	0.78	0.14	4	
368	28.6	3 29.2	11.48	0.59	0.42	1	
191-2	29.0	5 18.4	11.70	1.57	1.41	4	

Table 3.2 (continued)

Star No.	RA (1950.0)	DEC	V	(B-V)	(U-B)	N	R
364	$19^h\ 6^m 29^s.2$	$+3^\circ 20'.4$	11.08	0.53	0.09	1	
182	30.3	5 31.1	12.42	1.26	0.05	6	c
182-8	30.3	5 34.6	14.30	0.90	0.42	4	c
182-1	31.9	5 32.3	13.57	1.41	0.35	6	c
157-1	31.9	6 23.5	11.80	0.94	0.66	1	
383	34.2	3 58.3	12.64	1.85	1.32	1	
373	36.6	3 39.4	12.07	0.49	0.14	1	
371	37.0	3 30.2	9.68	0.43	-0.06	1	
182-3	44.6	5 34.6	12.27	0.64	0.45	5	c
372	44.7	3 38.6	11.91	0.45	0.22	1	
192	45.1	5 16.9	9.93	0.46	0.03	1	
365	45.3	3 19.4	10.61	0.37	0.20	1	
182-4	47.4	5 36.2	12.90	1.00	0.42	5	c
366	50.1	3 17.3	11.89	0.44	0.35	1	
387	55.0	4 13.8	11.65	0.78	0.03	1	c
384	57.0	3 57.5	11.81	0.47	-0.01	1	c
195	7 5.3	5 3.5	9.25	0.26	0.17	1	
385	5.4	3 57.9	10.35	0.41	0.27	1	c
195-1	6.2	5 1.0	9.76	1.37	1.44	1	
386	9.9	4 5.4	11.84	0.76	0.35	1	
186	10.2	5 28.8	8.62	0.16	0.08	1	
184	18.3	5 35.8	8.06	0.30	-0.14	2	
393	21.9	3 50.3	12.04	0.63	0.33	1	
184-2	27.3	5 35.8	12.71	0.71	0.37	2	
184-1	28.8	5 33.5	12.20	0.81	0.68	2	
196	28.9	5 7.2	9.66	0.38	0.37	1	
395	34.1	3 44.8	9.67	0.38	0.11	1	
391	37.1	4 1.5	9.97	0.51	0.20	1	
396	37.8	3 38.5	10.70	0.47	0.24	1	
199	41.4	5 13.9	10.75	0.58	0.21	2	
392	42.0	3 56.8	12.16	0.65	-0.04	1	
394	46.4	3 45.7	11.64	0.50	0.28	1	
185	48.9	5 29.0	10.85	0.62	0.14	2	
184-3	50.8	5 36.6	12.07	1.49	1.21	2	
184-4	55.3	5 36.6	12.97	0.94	0.87	2	

Table 3.2 (continued)

Star No.	RA (1950.0)	DEC	V	(B-V)	(U-B)	N	R
184-5	$19^h\ 7^m57^s.8$	$+5^\circ36'.9$	12.86	0.75	0.38	2	
184-6	59.4	5 38.7	12.72	0.74	0.39	2	
255	8 25.4	5 59.8	9.05	0.35	-0.17	1	
284	38.1	5 11.5	7.05	0.09	-0.22	1	
293	9 0.3	4 56.4	10.92	0.33	0.19	1	
283	13.8	5 12.7	10.20	0.37	-0.14	1	
261	14.2	5 31.1	11.52	0.50	0.33	1	
251	36.7	5 49.8	12.47	1.43	1.14	1	
252-7	43.0	5 53.9	13.09	1.26	1.27	2	
252-6	43.5	5 52.4	13.47	1.95		1	
250	44.4	5 47.5	12.53	1.70	1.06	1	
252	47.4	5 52.4	11.44	0.44	0.44	2	
296	47.5	4 53.0	11.44	0.79	0.44	1	
252-9	47.7	5 55.5	12.66	0.88	0.81	1	
252-8	47.8	5 53.7	12.13	0.36	0.30	1	
252-10	49.3	5 55.5	13.09	1.20	1.41	1	
252-1	49.5	5 51.0	12.96	1.33	0.95	2	
252-11	50.9	5 56.3	12.54	1.04	0.51	1	
249	51.0	5 42.9	10.21	0.38	0.36	1	
252-2	53.9	5 50.5	11.91	0.54	0.28	1	
253	54.5	5 56.2	11.20	0.37	0.32	1	
252-5	55.5	5 51.2	11.72	1.23	0.95	1	
252-3	57.1	5 50.1	12.10	0.62	0.24	1	
252-4	58.7	5 50.5	12.57	1.44	1.42	1	
254	10 10.0	5 57.2	7.46	0.63	0.40	1	
300	17.3	4 40.3	8.74	0.17	-0.10	1	
265	19.9	5 24.4	10.63	0.22	0.01	1	
248	21.8	5 42.0	11.43	0.37	0.23	1	
247	26.2	5 42.3	10.51	0.54	0.04	1	
240	28.8	5 55.4	12.75	0.42	0.39	1	
278	30.4	5 10.5	10.76	0.36	-0.02	1	
246	39.3	5 38.8	11.57	0.48	0.34	1	
239	45.8	5 58.7	10.29	0.22	0.03	1	
299	53.9	4 44.7	9.52	0.26	0.05	1	
245	11 3.6	5 41.8	9.86	0.31	0.26	1	
275	17.1	4 54.1	8.61	0.24	-0.01	1	

Table 3.2 (continued)

Star No.	RA (1950.0)	DEC	V	(B-V)	(U-B)	N	R
437	$19^h11^m19^s.0$	$+4^\circ43'.7$	9.34	0.46	0.12	1	
241	21.2	5 54.7	10.93	0.26	0.06	1	
244	23.1	5 42.6	11.09	0.52	0.25	1	
243	28.1	5 40.4	11.57	0.55	0.44	1	
242	37.3	5 40.5	11.44	0.72	0.50	1	
274	38.5	4 58.1	9.64	0.42	0.10	1	
273-3	38.6	5 10.2	9.70	1.38	1.33	1	
274-2	40.5	4 59.1	14.22	0.69	0.55	1	
274-1	43.3	4 59.6	11.47	1.87	2.20	1	
273-2	46.9	5 8.8	10.38	1.53	1.57	1	
273-1	48.3	5 6.1	11.74	1.44	1.27	1	
273	52.4	5 3.8	11.05	0.36	-0.05	1	
435	12 0.0	4 33.9	10.80	0.29	-0.15	1	
272	10.1	5 2.6	11.02	0.37	-0.02	1	
271	12.1	4 58.8	9.83	0.27	0.06	1	
268	49.8	5 8.9	11.90	0.47	0.36	1	
356	$19^h\ 4^m16^s.0$	$+3^\circ31'.2$	10.89	0.33	0.22	1	

Notes on Table 3.2

In the last column, c denotes stars used to calibrate the photographic photometry. Stars 180-1 and -2, 181-1 and -2, and 13-1 and -2 are visual double stars. Star 157-7 is double on the Schmidt plates. Star 356 was inadvertently omitted from the table and appears at the end.

labelled "in S74" in the figure are projected on the HII region S74 (Sharpless, 1959) and are numbers 182, at the centre, and 182-1, at the edge. Other "182" stars are located nearby. The stars "in a dust lane" are 190-4 and 190-7. The "190" stars were chosen because they lie in a region of lowest number of stars per unit area on the Palomar red charts (the area is at the edge of two charts); some of the stars had nearly equal P and r magnitudes, possible for late type dwarfs or highly reddened OB stars. Points bracketed in Figure 3.2 have a large uncertainty mainly in the (U-B) value as illustrated by the range in values, (B-V) and (U-B), for two stars.

The stars are identified on the negative prints of Plates 2 (west half) and 3 (east half), copied from the yellow plate, V1060 (see Table 2.4). The numbers are grouped so that the observer could use the finder telescope to locate the stars rather than use the coordinates to set the telescope. In a few crowded regions, the whole number is sometimes omitted and only the hyphenated portion identifies the star. About half of the stars originally selected were not observed for the following reasons: i) there was insufficient time to observe all the stars and ii) the study of the objective prism plates taken at Cerro Tololo enabled a better selection to be made in the limited time available. That is why there are omissions in the numbering of stars. The large black circles at the

PLATE 2. FINDER CHART FOR STARS IN TABLE 3.2.

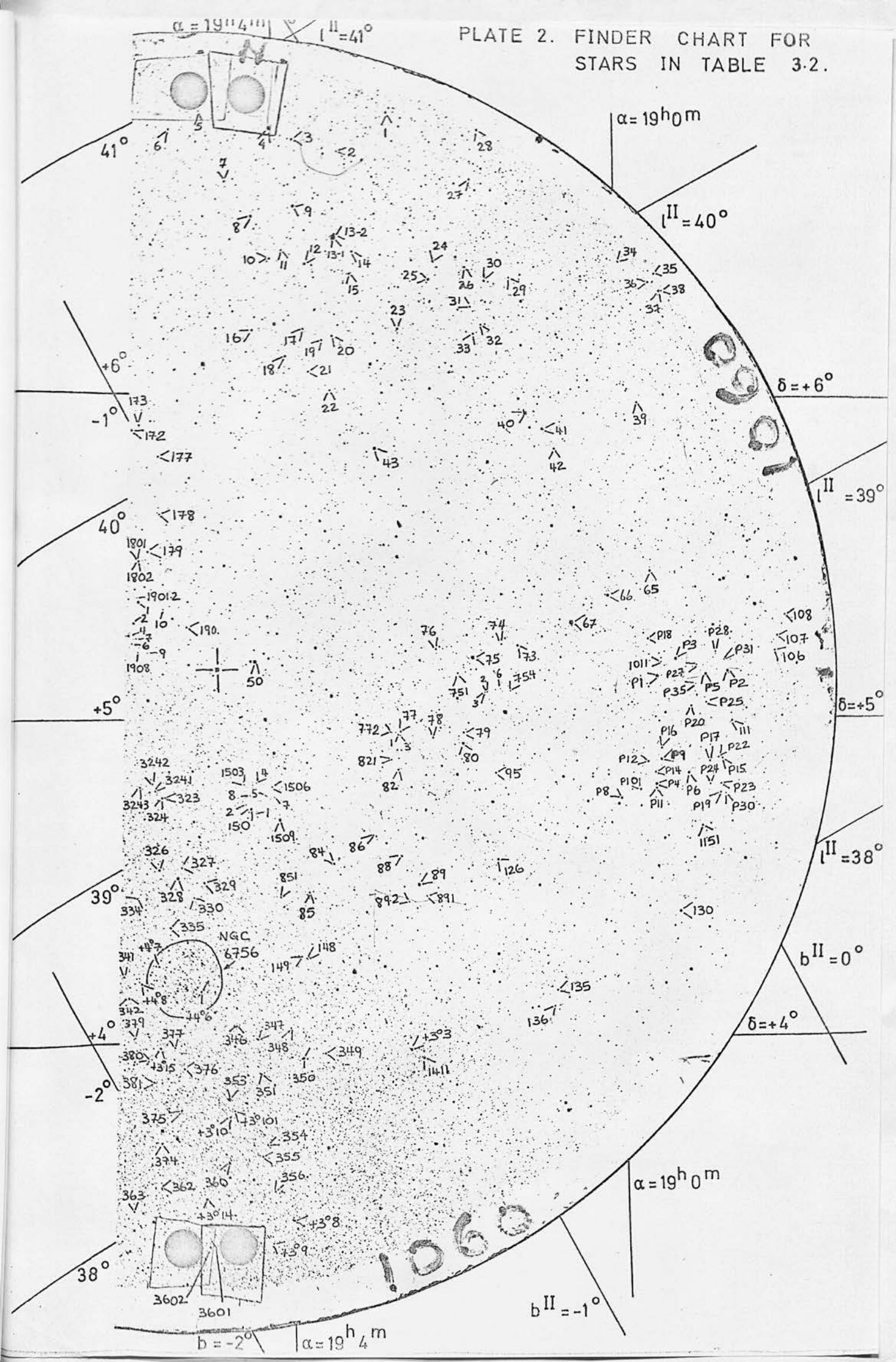

PLATE 3. FINDER CHART FOR STARS IN TABLE 3.2.

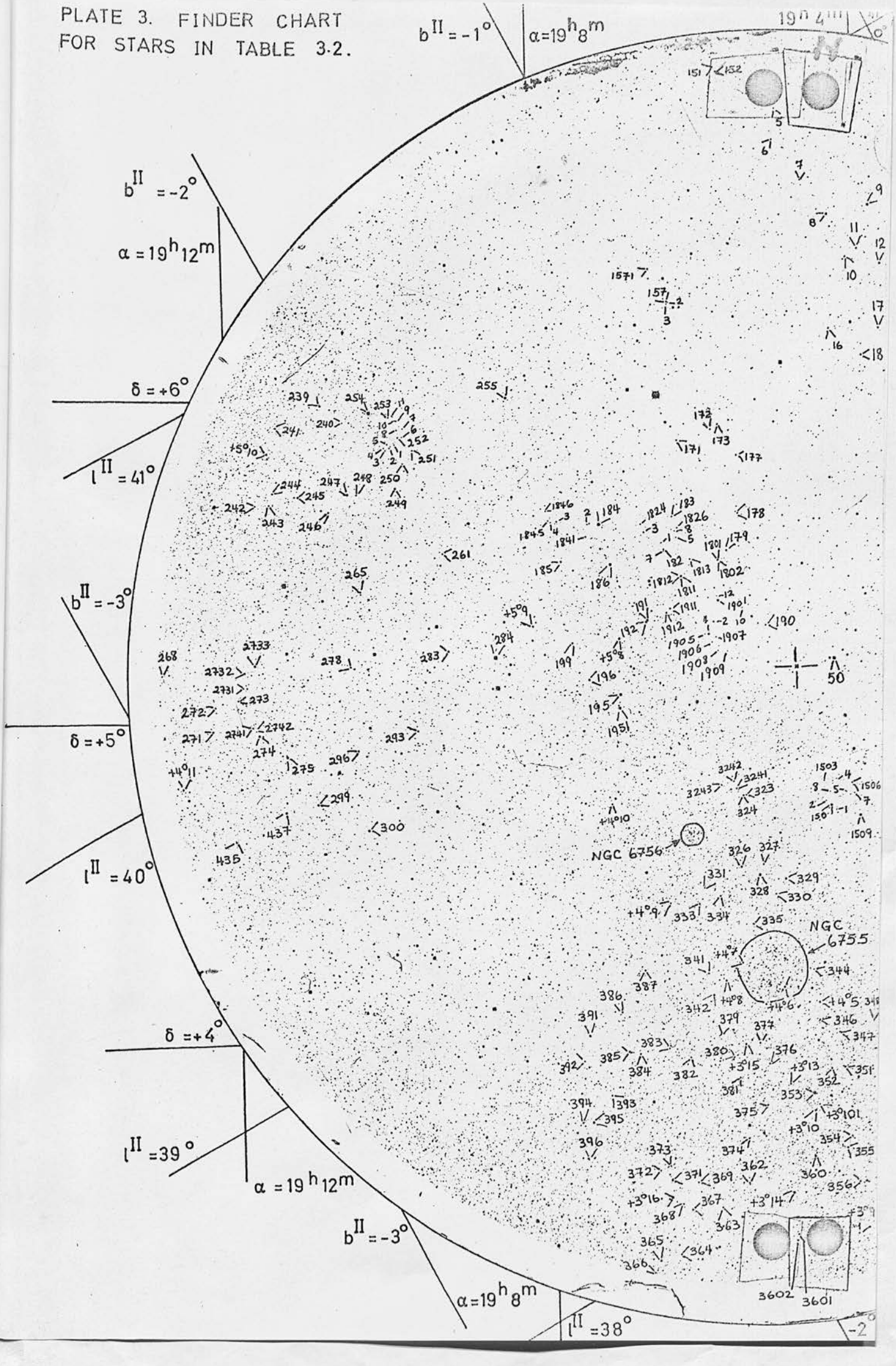

north and south edges of Plates 2 and 3 are the special datum plates used by GALAXY for the purpose of relating the coordinates in the search mode to those in the measurement mode (Pratt, 1971). Equatorial (1950.0) and galactic coordinates and the field centre are marked on these plates.

Table 3.3 contains the photometric data for the field stars first observed by Purgathofer (1969) and the stars of NGC 6755 observed by Hoag et al. (1961). These references contain finder charts but the Purgathofer stars(P-numbers on Plate 2) are marked to show their location relative to the cluster (also marked). The data have been set out in their own table to enable an easy comparison to be made between observers but will be analyzed with the other data in Table 3.2 without further distinction.

The observations of the thousands of stars measured by GALAXY are too extensive to be presented individually. Instead, the collective information will be presented in several different forms throughout this chapter (see also Appendices A1 and B).

Figures 3.1 and 3.2 are based on data selected by luminosity and spectral type respectively. Figure 3.3 is based on all the stars with three-colour photometry measured by GALAXY within the regions marked in Figure 2.2. The stars were summed in 0.1 magnitude intervals in (B-V) and (U-B) and then smoothed contours were drawn by hand.

Table 3.3a

Photoelectric Observations of Purgathofer's Stars.

No.	RA (1950.0)	DEC	V	(B-V)	(U-B)	N	R
1	$18^h59^m22^s.2$	$+5^\circ\ 5'.9$	8.22	0.46	0.25	24	R
2	58 27.6	5 6.7	8.76	0.23	0.14	3	
3	59 8.8	5 9.2	9.04	0.53	0.07	4	
4	59 23.6	4 45.6	9.18	0.30	0.08	3	
5	58 46.0	5 5.7	9.80	0.22	-0.20	3	
6	58 59.1	4 48.2	9.64	0.61	0.14	18	
8	59 51.1	4 42.9	10.38	0.87	0.35	1	
9	58 16.9	4 50.5	10.30	1.67	1.46	1	VAR.
10	59 37.2	4 45.0	10.73	0.56	0.32	1	
11	59 23.6	4 44.8	11.03	0.63	-0.01	1	
12	59 31.0	4 50.1	11.12	0.42	0.20	3	
14	59 24.4	4 48.2	11.42	0.67	0.08	1	
15	58 32.0	4 50.8	11.38	0.53	0.10	2	
16	58 16.9	4 52.6	11.49	0.70	0.10	1	
17	58 43.0	4 50.4	11.50	0.53	0.04	3	
18	59 28.8	5 13.8	11.56	0.63	0.13	4	
19	58 35.2	4 44.3	11.62	0.73	0.22	3	
20	58 57.7	5 0.0	11.64	1.17	0.60	3	
22	58 36.6	4 50.8	11.97	0.60	0.20	2	
23	58 35.1	4 46.2	12.08	0.61	0.05	1	
24	58 26.9	4 46.2	12.14	0.94	0.33	1	
25	58 46.2	5 0.5	12.42	0.61	0.21	3	
27	58 53.4	5 7.8	12.97	0.93	0.40	3	
28	58 38.6	5 9.8	13.13	0.64	0.09	2	
30	58 31.1	4 44.1	13.56	0.89	0.27	3	
31	58 49.2	5 8.6	13.60	1.03	0.51	3	
35	58 53.4	5 3.8	14.58	1.32	0.13	1	
36	58 55.9	4 48.9	14.99	0.97	0.32	1	
37	58 54.3	4 49.1	15.42	1.25	0.49	1	

Note on Table 3.3a:

1 Too bright for GALAXY to measure.

Table 3.3b

Photoelectric Observations of Stars in NGC 6755.

No.	RA (1950.0)	DEC	V	(B-V)	(U-B)	N	R
1	$19^h\ 5^m 22^s.4$	$+4^\circ\ 8'.8$	10.31	0.61	-0.18	20	$+4^\circ 6$
2	5 17.9	4 17.9	10.89	1.50	1.12	2	
3	5 18.0	4 9.0	11.38	1.33	1.18	4	
4	5 32.3	4 14.5	11.53	0.71	0.18	3	
5	5 7.7	4 14.3	11.44	0.53	0.22	3	VAR?
6	5 18.0	4 9.0	12.53	0.79	0.48	2	
7	5 18.0	4 9.0	12.73	2.01	1.42:	1	
8	5 18.0	4 9.0	12.91	0.60	0.19	4	

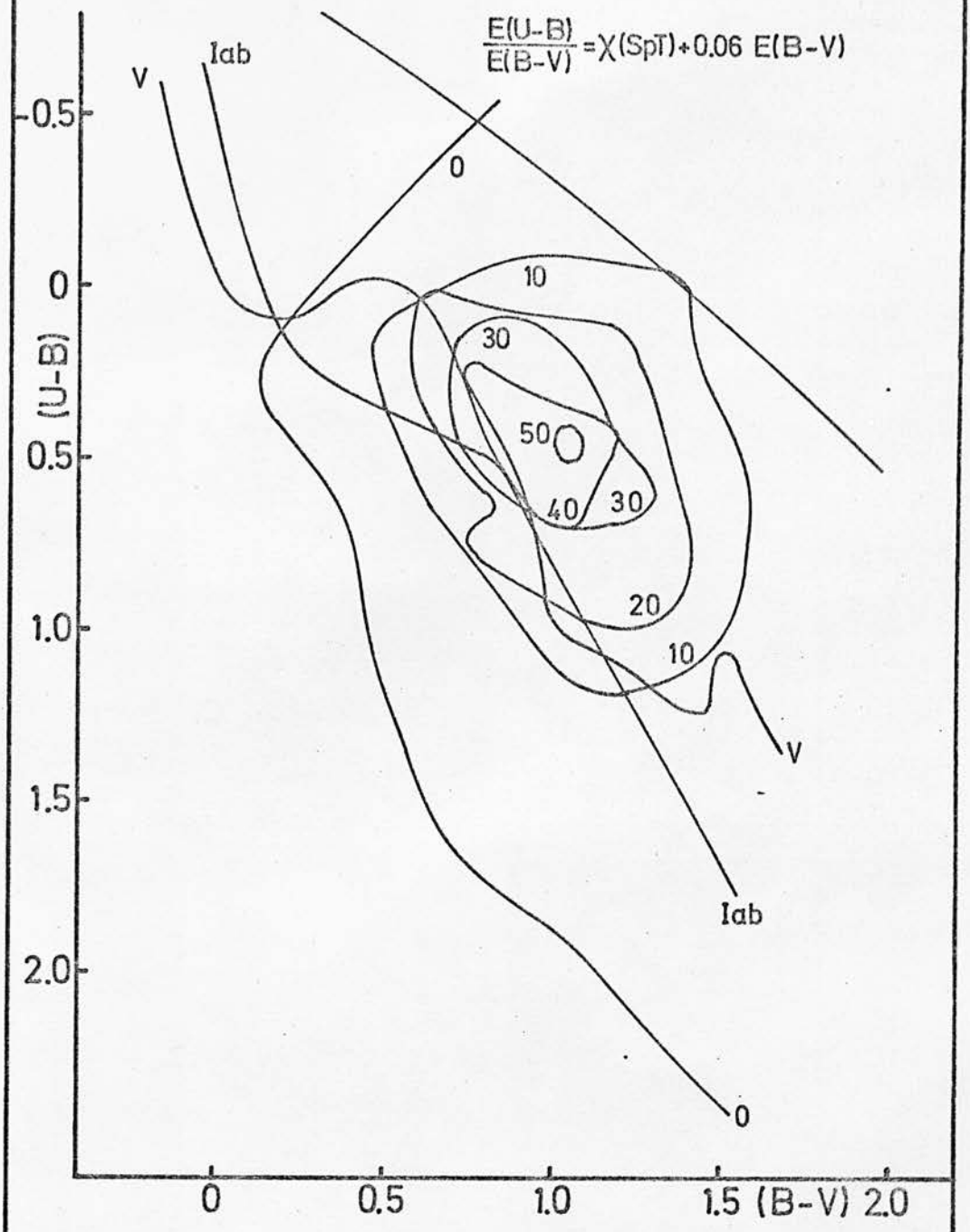

FIG. 3.3
TWO-COLOUR DIAGRAM OF 3279 STARS
(GALAXY PHOTOGRAPHIC PHOTOMETRY)
CONTOUR UNIT EQUALS NUMBER OF STARS
PER 0.1 MAG. COLOUR INTERVAL.

Figure 3.2 shows two groupings of stars: F dwarfs reddened about $0^m.14$ and B8-A3 dwarfs reddened about $0^m.36$. In Figure 3.3, the F grouping may still be recognized with a reddening of $0^m.5$ to $0^m.6$; it shows the effect of the limiting magnitude in U. The effect is not so pronounced for later type dwarfs because they are still relatively nearby and little affected by reddening. Nevertheless, the distribution is asymmetrical about the dwarf intrinsic colour line suggesting perhaps that at least some stars may have ultraviolet excesses or that nearly all the stars in the area are far enough away (or that the clouds are so near) that they are affected by interstellar reddening.

The B8-A3 grouping will merge into the unreddened dwarfs when $E_{(B-V)} \approx 1^m.0$ and may be responsible for the lower extension of the "20" contour line. The upper extension of the "20" and "10" lines are due to the admission of luminous, more reddened stars of early B spectral types. The incorporation into the figure of faint stars with photometry of lower accuracy results in the large outer envelope of the zero contour line (essentially no stars outside it). The error of the mean for the "50" contour is $\pm 0^m.02$ and $0^m.03$ in (B-V) and (U-B) respectively.

In Figure 3.1, two main distributions of stars may be seen reflecting the nature of the selection of luminous stars. The first group consists mostly of stars within $0^m.4$ (U-B) of the reddening line. This

corresponds to a cut-off in $(U-B)_o$ equivalent to a B3V star.

The second group consists of highly luminous stars of later spectral type judging by their distribution parallel to the Iab line to $(U-B)=0^m.4$ although they are displaced $0^m.3$-$0^m.4$ or more in (B-V). An admixture of dwarfs is also present from about (U-B)=0 and later.

In order to study the dust cloud and to locate it relative to spiral and galactic structure, we must determine the distances to these stars. For those stars with spectral types, this presents little difficulty. Figure 3.4 compares spectral types determined from spectrograms (slit as well as slitless) with those determined from photoelectric photometry using the procedure FARBE (see Appendix A2) to unredden the observations. Given a spectral type, it is possible to choose a solution for the photometry to within two subclasses for 90% of the early type stars. It is not clear why FARBE classifies F stars too early. There are at least three possibilities:

i) The ratio $X=E_{(U-B)}/E_{(B-V)}$ is too large by a few per cent (X=0.78 for F5V).

ii) The F stars have been systematically classified too late or the (U-B) values are too small.

iii) Some F stars may have ultraviolet excesses.

On underexposed objective prism spectra of A-F stars, the strength of the K-line is often difficult to judge.

For most of the stars in LS II and LS IV, only

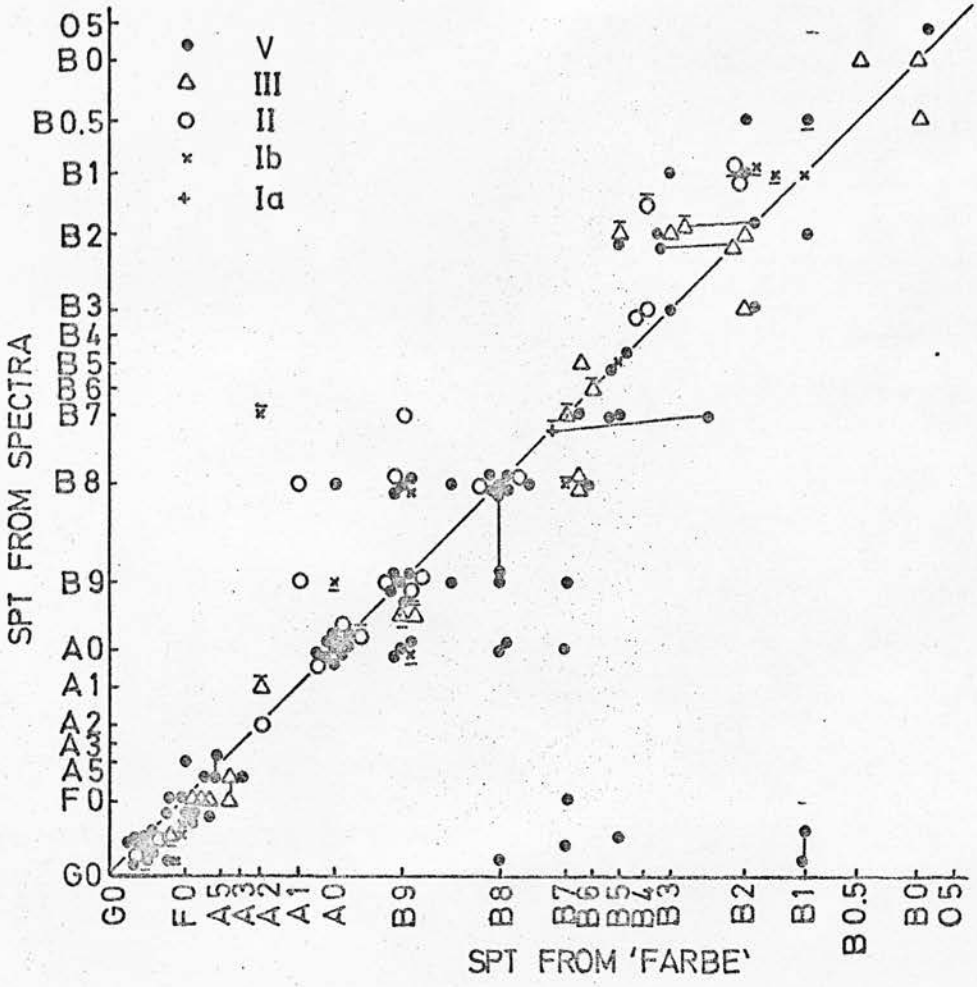

FIG. 3.4

COMPARISON OF SPECTRAL TYPES FOUND FROM SPECTROGRAMS WITH THOSE FROM 'FARBE'. A BAR OVER/UNDER SYMBOL INDICATES THAT 'FARBE' CLASSIFICATION IS OVER/UNDER LUMINOUS.

general notice is given to the spectral type and luminosity of a star: whether it is OB^+, OB, or OB^-. Bidelman (1972) has located these domains for stars observed from the southern hemisphere. Because the seeing is so much better at Cerro Tololo than at Cleveland, this scheme will not in general be valid for the stars in LS II and IV. To learn how the OB classification depends on absolute magnitude and intrinsic colour, those stars which had both MK and OB classifications were plotted in a modified HR diagram, Figure 3.5. The result is nearly a scatter diagram; at B2, OB^+ and OB classifications are found together over a range of three magnitudes in M_V while in $(B-V)_o$, the range for the OB class covers virtually all that is worthwhile to distinguish. It is obvious that in LS II and IV, the OB classification plus photoelectric photometry will not solve the question of which luminosity class reddening solution should be chosen.

It is likely that the confusion in Figure 3.5 results from the effects on classification of variable seeing conditions. The mean values for OB^+, OB, and OB^- obtained by Schmidt-Kaler (1971) are systematically bluer and brighter than for the means of Figure 3.5.

Most stars brighter than $B=13^m$ in Tables 3.2 and 3.3 have been classified on one or more objective prism plates. For the fainter stars and OB stars without spectral classification, a likely reddening solution may be chosen in one of the following ways:

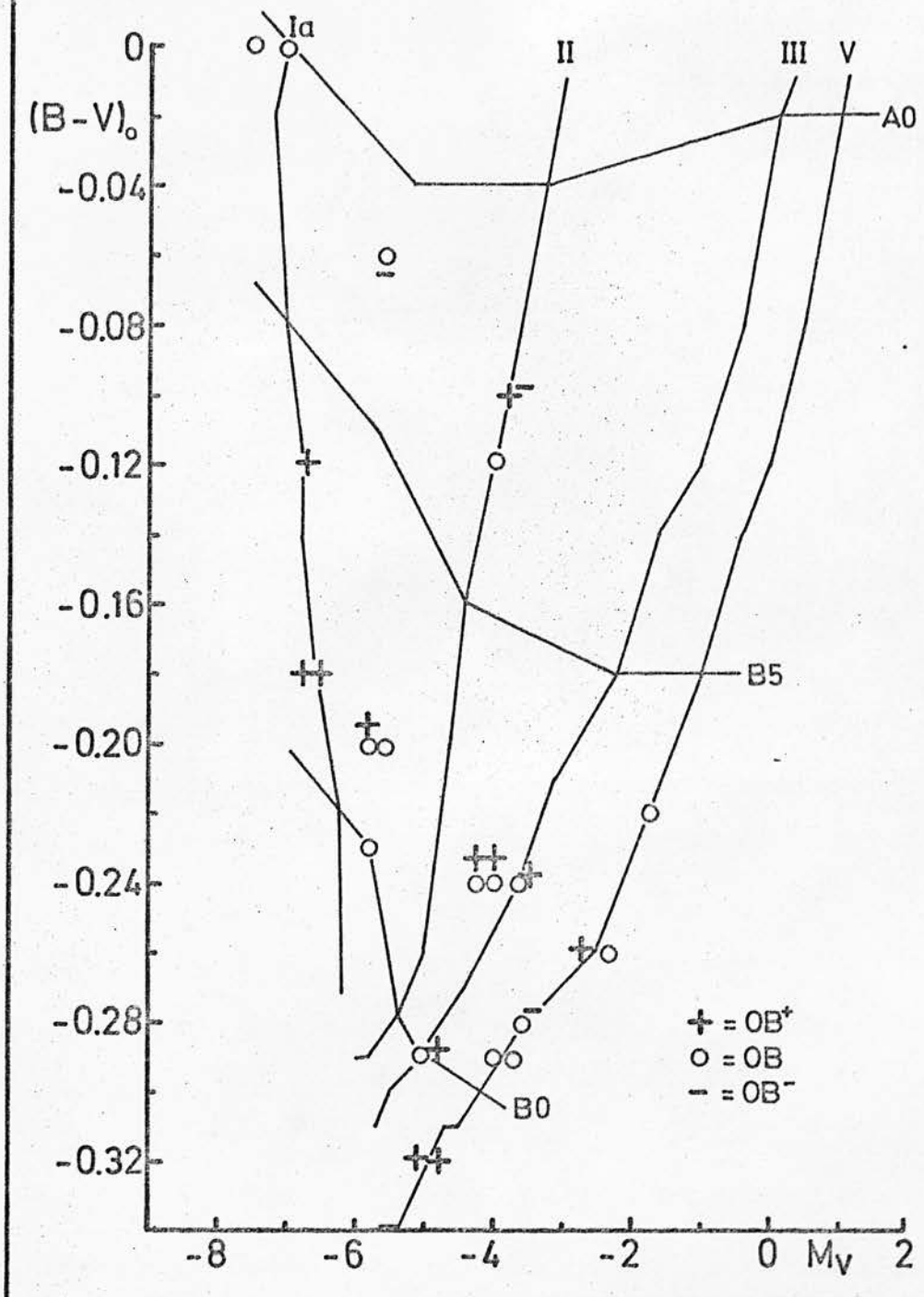

FIG. 3.5
DOMAINS OF THE OB STARS FROM THE WARNER & SWASEY/HAMBURG CATALOGUE
M_V AND $(B-V)_o$ FROM SCHMIDT-KALER (1965)

i) Assume the star to be a dwarf, statistically the most likely luminosity class if all stars to some limiting magnitude are measured. This assumption can be applied with certainty to the GALAXY data as will be shown later and with less certainty to the data in Tables 3.2 and 3.3. The assumption breaks down in the case of stars admittedly chosen for their high luminosity (Table 3.1).

ii) Adopt a reddening $E_{(B-V)}$ with $(V-M_V)$ relation and choose a luminosity class which satisfies it.

iii) Study all possible reddening with $(V-M_V)$ relations for as large a number of stars as possible in the smallest possible area of the sky. If there is a good range of true distances, then the fact that $E_{(B-V)}$ is at least a step-wise monotonically increasing function of distance over a small area will allow an appropriate reddening solution and hence spectral type and luminosity class to be chosen.

Techniques ii) and iii) result usually in reducing the actual dispersion in the observations if not applied iteratively. In practice, there are usually some stars with spectral types or unique reddening solutions which allow one to test the validity of the results obtained by the other techniques.

These spectroscopic and statistical methods have been applied to all the photoelectric data including 47 B stars between $30^\circ \leq l^{II} \leq 50^\circ$ listed in the catalogue by Blanco et al. (1968). The results for about 450

stars are presented in Table 3.4. The stars from Blanco et al. (1968) have HD or BD numbers. Do not confuse the stars from Table 3.1 with the similarly formated but larger BD numbers. The first column of spectral types are from spectrograms (references in Blanco et al. or to be found in this thesis). Spectral types without luminosities have been classified in this work or have been taken from the HD or AGK_2 catalogues. The next column contains the values adopted from the photoelectric observations using the procedure FARBE (see Appendix A2). Occasionally a second possibility is also given on the next line. Colour excess $E_{(B-V)}$ and the distance to the star in parsecs are given in columns 6 and 7. In the last column an "R" denotes a remark given at the end of the table.

Some stars were marked with an "X" (for ultraviolet excess); they have a much earlier implied spectral type from the photometry than from the spectroscopy. There can be no doubt that these stars are F or G rather than B and the distances and reddening when given are for the late-type dwarf spectral type. This problem will be discussed in Chapter 4 after the study of other features in this region.

Table 3.4

Reddening with Distance for Stars between $30^{\circ} \leq l^{II} \leq 50^{\circ}$ with Spectrographically and/or Photoelectrically Determined Spectral Types

Star No.	l^{II}	b^{II}	Sp SpT	Pe SpT	E_{B-V}	Dist.	R
164353	29°.72	12°.64	B5Ib	B5Ib	0.12	690	
-4°32	30.12	- 3.28	A7Ib				
-2°13	30.21	0.66	OB⁻	B5III	0.72	1249	
-3°16	30.27	- 2.65	OB	B7III	0.63	2061	
-2°14	30.30	0.62	OB	B2V	0.92	1722	
-2°14.1	30.30	0.62		B7V	0.76	1132	
-3°17	30.39	- 2.84	OB⁻	B6.5II	0.70	2540	
-2°16	30.46	0.39	OB	B6II	1.01	2801	
				B3V	1.08	856	
-4°33	30.51	- 4.75	WN8		0.71	9818	
-1° 9	30.62	- 0.96	OB	B7V	0.59	1154	R
				B8II	0.54	5154	
-1° 8	30.64	0.76	OB,B2,B8	B3III	0.78	1560	
-1° 4	30.71	1.48	B8II	B7Ib	1.49	1032	
-1° 7	30.72	- 0.73	B1V	B2V	0.55	640	
-2°17	30.93	- 2.28	OB	B0.5III	1.22	2058	R
-1° 6	30.94	1.06	OB⁻,B5	B2III	0.67	786	
-1° 5	30.98	1.32	OB	B2V	1.12	881	
164284	31.00	13.38	B2Ve	B1V	0.24	301	
166917	31.01	9.89	B7V	B2.5V	0.29	406	
				B7Ia	0.09	5048	
172028	31.04	2.82	B3II	B4II	0.73	1018	
-3°18	31.09	- 3.36	OB				
+0° 2	31.11	3.65	OB⁻,B5	B5II	0.83	899	
-2°18	31.12	- 2.22	OBh	B0.5V	1.09	1922	
-2°19	31.17	- 2.46		B3III	1.06	1432	
-0° 4	31.60	0.81	OB	B1.5V	1.33	1106	
-2°20	31.74	- 2.56	OB	B7.5III	0.83	914	R
184915	31.77	-13.29	B0.5III	B0III	0.28	724	
-2°25	32.00	- 4.45	OB	B2III	0.81	1992	
-2°22	32.02	- 3.79	B9Ib	B9II	0.84	1316	

Table 3.4 (continued)

Star No.	l^{II}	b^{II}	Sp SpT	Pe SpT	E_{B-V}	Dist.	R
-1°10	32°.02	- 0°.72	OB	O8V	0.80	4036	
-0° 5	32.14	0.26	B7II?	A2Ib	1.41	1622	R
-2°23	32.28	- 3.71	OB	B3V	0.61	1826	
-1°11	32.33	- 2.35	B8II	A1II	0.67	1144	
-0° 6	32.34	0.29	OB^-,B5	B3III	0.71	955	
-2°26	32.36	- 4.31	OB	B2.5V	0.69	1491	
-2°21.1	32.36	- 3.47		G7II	0.78	1013	
-0° 8	32.54	- 0.96	OB^-	B8III	0.74	978	
-2°24	32.57	- 3.76	B0.5p	B0V	0.74	1226	
-1°12	32.68	- 2.34	OB	B4V	0.68	1631	
-0° 7	32.68	- 0.73	O8		0.90	2742	
-1°13	32.69	- 3.60	B7II	B9II	0.53	1668	
164432	32.81	14.08	B3III	B2III	0.16	1039	
-0°11	32.94	- 1.51	OB^-	B3V	0.69	1485	
-0°12	32.96	- 1.70	OB^-	B6V	0.64	1108	
-0°10	33.06	- 1.03	OB^-	B3V	1.01	1083	
-0° 9	33.13	- 0.96	OB^-	B6V	0.87	736	R
+0° 3	33.16	0.83	OB^+(h),B0				
-1°15.1	33.32	- 4.84		G2II	0.73	2035	
177880	33.46	- 3.98	B8	B7II	0.22	1024	R
-1°14	33.50	- 3.23	OB^-	B2.5V	0.46	1732	
-1°17	33.55	- 4.92	OB^-	B2V	0.55	1650	
+0° 7	33.58	- 0.90	OBr	B8Ib	1.51	1566	R
-1°18	33.60	- 4.92	OB^-	B9III	0.49	987	
+0° 6	33.66	- 0.84	B3V	B2V	0.34	543	
-0°15.1	33.85	- 3.63		B8II	0.63	2440	
+0° 4	33.86	0.50	OB^-	B8III	0.93	807	
+0° 5.1	33.88	0.26					
170973	33.99	5.97	B9	B9V	0.04	171	
173370	34.01	2.40	B9V	B8.5V	0.05	95	
-1°16	34.01	- 4.68	OB	B3V	0.68	2155	
170580	34.13	6.60	B2V	B3.5V	0.31	311	
-0°13	34.28	- 2.76	OB	B0.5V	0.58	4125	R
-0°14	34.33	- 2.97	OB	B2.5V	0.49	2790	
+0° 8	34.35	- 1.90	OB	B5III	0.93	950	

Table 3.4 (continued)

Star No.	l^{II}	b^{II}	Sp SpT	Pe SpT	E_{B-V}	Dist.	R
168797	34°.39	9°.15	B2e-B5ne	B3V	0.18	309	
				B3.5III	0.15	549	
169578	34.49	8.16	B9	B8.5V	0.12	187	
+0° 9	34.53	- 1.99	OB⁻	B6.5V	0.77	937	
+0°11	34.62	- 2.84	OB	B0.5III	0.73	5723	
178744	34.64	- 4.30	B8	B5.5V	0.13	261	
+1° 3	35.00	- 1.64	OB	B3V	0.98	1100	
+0°10	35.12	- 2.02	OB⁻,B8II?	B6.5III	0.81	957	
+1° 2	35.24	- 1.05	OB	B5.5V	0.89	935	
178065	35.31	- 3.21	B9	B8II	0.15	928	
181440	35.48	- 6.88	B9V	B9V	0.04	107	
184790	35.56	-11.24	B8	B7.5II	0.28	1700	
+0°12	35.77	- 3.59	OB⁻	B7.5V	0.62	1018	
170200	35.81	8.02	B8	B7.5V	0.09	155	
+0°13	35.83	- 3.62	OB⁻,B5	B3III	0.64	1141	
+1° 6	35.84	- 3.10	OB⁻,B8	B6.5III	0.55	1085	
+1° 4	35.85	- 1.54	OB				
175869	35.86	- 0.16	B9n	B8V	0.11	118	
				B9II	0.08	629	
+1° 5	35.98	- 2.35	OB	B7II	0.86	2996	
+0°14	36.10	- 4.17	OB⁻,B8	B3III	0.50	1109	
+4° 4	36.23	3.72	OB	B8II	0.67	3370	
+2° 2	36.30	- 1.44	OB	B0V	0.82	2492	
+5° 6.1	36.33	4.52		A5V	0.31	601	R
+5° 6.2	36.33	4.52		B7.5V	0.77	1488	
+2° 1.1	36.40	- 1.03	K2-5V				
+2° 6	36.57	- 2.01	OB	B5V	0.62	1461	
186660	36.61	-13.41	B3Si	B3V	0.27	317	
+1° 7	36.63	- 3.34	OB⁻				R
+1° 8	36.81	- 3.39	OB	B2III	0.65	2336	
+2° 4	36.91	- 1.71		B3Ib	1.08	4198	
+2° 3	36.98	- 1.35	B5III	B5III	0.90	1743	
184930	36.99	-10.67	B5III	B6.5III	0.07	158	
+2°10.1	37.00	- 3.26		K2III	0.53	428	
+1° 9.1	37.03	- 4.53					

Table 3.4 (continued)

Star No.	l^{II}	b^{II}	Sp SpT	Pe SpT	E_{B-V}	Dist.	R
$+2^{\circ}$ 5	$37^{\circ}.06$	$-1^{\circ}.74$	OB,overlap	B2V:	0.87	1271	R
$+2^{\circ}$ 7	37.12	- 1.92	OBh				
$+3^{\circ}$ 2	37.14	- 1.41	BOIII	BO.5III	0.86	2013	
$+5^{\circ}$ 7	37.29	3.98	B9II	B9II	0.61	2818	
$+5^{\circ}$ 7.1	37.29	3.98					
$+2^{\circ}$ 8	37.38	- 2.38	cf $+2^{\circ}4$	B2III	1.02	1980	
$+3^{\circ}$ 6	37.51	- 1.76	B1Ib	B2II	0.83	1596	
179761	37.52	- 3.91	B8p-Ap		0.07	129	
$+3^{\circ}$ 7	37.55	- 1.79	$OB^{+}h$	B1V	0.91	2306	
				B2II	0.86	4913	
$+3^{\circ}$ 7.1	37.55	- 1.79					
$+3^{\circ}$ 4	37.58	- 1.66	OB,B8	B9II	0.69	4284	
				B8III?	0.73	1173	
$+3^{\circ}$ 4.1	37.58	- 1.66					
$+3^{\circ}$ 5	37.63	- 1.66	OB,overlap	B2V	0.76	1771	R
$+3^{\circ}$ 5.1	37.63	- 1.66		B9V	0.20	391	
$+2^{\circ}$ 9	37.68	- 2.88	OB	09-9.5V	1.03	2322	
$+3^{\circ}$ 9	37.74	- 1.89	OB,overlap	B7III	0.72	1570	R
$+3^{\circ}$ 9.1	37.74	- 1.89	(GO)				R
$+3^{\circ}12$	37.77	- 2.00	cAO	AOIII	0.72	901	
$+3^{\circ}12.1$	37.77	- 2.00					
$+3^{\circ}$ 8	37.78	- 1.75	OB,B5	B3V	0.59	2140	
$+3^{\circ}11$	37.81	- 1.95	B3Ia	B4II	0.62	952	
357	37.82	- 1.58	FOIII	A9III	0.51	319	
360-1	37.84	- 2.01	B8V	B8V	0.42	994	
360-2	37.84	- 2.01	B8V	B8.5V	0.36	685	
157741	37.86	26.11	B9.5IV	B9V	0.04	137	
				B9III	0.04	197	
356	37.88	- 1.76	F0-A7III	A4III	0.20	690	R
$+3^{\circ}17$	37.94	- 2.59	A2II	A2II	0.41	3628	R
$+3^{\circ}17.1$	37.94	- 2.59	G-K	K2III	0.40	524	
136	37.96	- 0.70	F5:	B7.5			X
$+3^{\circ}14$	37.97	- 1.95	BO.5Vp	B2V	0.80	1259	
364	37.98	- 2.34	F5V	F5V	0.13	280	

Table 3.4 (continued)

Star No.	l^{II}	b^{II}	Sp SpT	Pe SpT	E_{B-V}	Dist.	R
366	37°.98	- 2°.44	AOV		0.46	766	
355	37.99	- 1.74	AOV		0.53	340	
135	38.00	- 0.66	F8:	B7.5V			X
365	38.00	- 2.47	AOV	AOV	0.40	473	
354	38.01	- 1.71	F8-GO	B7.5	0.02	232	X
360	38.02	- 1.84	A3V-III?		0.27	242	R
130	38.03	- 0.23	F8-GO	F4V	0.20	144	
141-1	38.03	- 1.15					R
363	38.03	- 2.16	A7V	A7V	0.25	350	
362	38.06	- 2.05	FOV	F2V	0.26	323	
+3° 3	38.07	- 1.17	cB2-5	B4II	1.18	1049	
				B6.5Ib	1.09	1978	
367	38.08	- 2.25	B7V	B5V	0.60	816	
368	38.11	- 2.27	A4-7		0.42	389	
+3°16	38.14	- 2.28	overlap	B2.5V	0.60	654	
371	38.14	- 2.29	overlap	B7V	0.57	503	
+3°10.1	38.16	- 1.77					
349	38.18	- 1.48	F7	B6V			X
369	38.19	- 2.17	F5	F2	0.36	265	
350	38.20	- 1.48	FOIII	A8III	0.30	333	
353	38.22	- 1.74	A5-7				
374	38.22	- 1.95	overlap	B6.5V	0.84	793	
351	38.23	- 1.62	B8V	B9V	0.58	707	
115-1	38.24	- 0.04	B-A	B8V	0.99	582	
375	38.24	- 1.89	G2V	G2V	0.05	146	
352	38.25	- 1.66	OB	B2V	0.89	2181	
+3°13	38.27	- 1.79	OB,B2	B3V	0.78	1708	
373	38.28	- 2.22	GO	FO			
372	38.28	- 2.25	AOV	AOV	0.49	782	
171247	38.29	7.75	B8	B8V	0.08	202	
P-30	38.30	0.07		B7.5V	1.00	1526	
P-19	38.31	0.06	F	F5V	0.27	259	
348	38.31	- 1.47	OB	B1V	1.00	2932	
347	38.33	- 1.58	F7V	F6V	0.20	190	
P-23	38.34	0.07	F	F6V	0.17	344	

Table 3.4 (continued)

Star No.	l^{II}	b^{II}	Sp SpT	Pe SpT	E_{B-V}	Dist.	R
376	38°.36	- 1°.82	A0V		0.53	537	
381	38.37	- 1.93	A5mp	A8III	0.43	461	R
396	38.38	- 2.45	B8V:	A0V	0.50	437	
P-15	38.40	0.12	F7V	F4V	0.13	332	
346	38.40	- 1.61	overlap	B7.5III	0.95	1011	
P-22	38.41	0.10	F8-G0	F4V	0.21	369	
P-17	38.41	0.08	F3	F5V	0.10	325	
P-37	38.41	0.02		B7.5V	1.23	2568	
P- 6	38.41	0.00	F8IV	F5V	0.19	125	
P-11	38.41	- 0.12	overlap	B6V	0.77	812	
P-33	38.41	- 0.23		B5.5V	1.09	3005	
P-36	38.42	0.02		B7.5V	1.29	1839	
P- 4	38.42	- 0.11	F2V	A9V	0.04	191	
377	38.42	- 1.82	A2V		0.47	436	
P- 8	38.43	- 0.23	G0	G5V	0.18	82	
380	38.43	- 1.91	overlap	B8V	0.90	691	
P-10	38.44	- 0.17	A7-F0	A7V	0.37	281	
P- 7	38.44	- 0.25	G2-K0	G0V	0.07	110	
+4° 5	38.44	- 1.59	OB	B5III	0.97	1754	
126	38.45	- 0.64	B8V		0.67	568	
+3°15	38.45	- 1.85	OB,B2V	B3V	0.83	1162	R
P-14	38.47	- 0.09	overlap	B6.5V	0.80	833	
89-1	38.47	- 0.90	A2:		0.76	534	
395	38.47	- 2.39	A0V	B9V	0.44	350	
148	38.48	- 1.33	A0:V	B8V	0.82	1126	
89-2	38.48	- 0.96	A2:		0.76	510	
111	38.49	0.19	F7V	F6V	0.17	247	
P- 9	38.49	- 0.05	M				
149	38.49	- 1.35	B9V		0.55	875	
382	38.49	- 2.01	A0:V	B8V	0.67	1053	
P-12	38.50	- 0.10	A7	A7V	0.22	407	
394	38.50	- 2.42	A0:V:	A0V	0.52	630	
89	38.51	- 0.91	B9V	B9V	0.33	255	
379	38.51	- 1.91	A0V	B9V	0.49	814	
P-16	38.52	- 0.04		F7V	0.26	217	

Table 3.4 (continued)

Star No.	l^{II}	b^{II}	Sp SpT	Pe SpT	E_{B-V}	Dist.	R
393	38°.52	- 2°.30	A7-F0	A8V	0.40	435	
344	38.54	- 1.55	A0V	A0V	0.65	751	
+4° 6	38.54	- 1.66	OB,B2III	B3III	0.82	1634	R
383	38.55	- 2.06					
6755-19	38.56	- 1.70		B8V	1.09	2188	
P-25	38.57	0.14	A-F	F2V	0.28	484	
P-20	38.58	0.10	B8-9	B9II:	1.24	1819	
88	38.58	- 0.87	A7III		0.26	342	
384	38.58	- 2.15	B8V	B7.5V	0.60	1196	
106	38.60	0.42	F7V	F5V	0.30	283	
385	38.61	- 2.18	A0V:		0.43	394	
P- 2	38.62	0.26	A4-7V	A6V	0.06	178	
6755-5	38.62	- 1.62	F5	A8V	0.27	391	R
342	38.63	- 1.87	F7V	F4V	0.31	162	
107	38.64	0.44	F0V	B7V			X
P- 5	38.65	0.18	B7V	B6.5V	0.37	746	R
85	38.65	- 1.23	A0V	A0V	0.61	513	
+4° 8	38.65	- 1.81	B2-5	B5.5III	0.84	1070	
392	38.66	- 2.32	F5V	B5V			X
6755-4	38.67	- 1.71	F8-G	G3-5V	0.05	191	
+4° 7	38.67	- 1.74	OB	B1.5V	0.87	2820	
85-1	38.68	- 1.32	A7:V:		0.42	445	
108	38.68	0.50	A2V		0.58	634	
84	38.69	- 1.11	A0V		0.52	438	
6755-2	38.69	- 1.63					
341	38.70	- 1.86	A0V	A0V	0.81	526	
95	38.71	- 0.54	F8V:		0.32	209	
86	38.71	- 0.96	A0V:		0.77	570	
P- 1	38.72	0.05	F0III	A7III	0.22	165	
386	38.72	- 2.14	F-G	F0V	0.46	310	
391	38.72	- 2.27	F2V	F0V	0.24	193	
+7° 6	38.73	4.54	F5I	F1Ib	0.75	2700	R
82-1	38.73	- 1.34	overlap				
P- 3	38.74	0.13	F7-8V-IV	F6V	0.09	101	
101-1	38.75	0.08		G5V	0.20	243	
335	38.76	- 1.65	F5V	F5V	0.14	244	

Table 3.4 (continued)

Star No.	l^{II}	b^{II}	Sp SpT	Pe SpT	E_{B-V}	Dist.	R
328	38°.80	- 1°.56	K2	KOIII	0.19	234	
80	38.83	- 0.58	A7V	A3V	0.30	228	
329	38.83	- 1.49	F5	F6V	0.12	164	
77-3	38.84	- 0.57					
P-18	38.85	0.09	F5-7	F7V	0.13	770	
77-1	38.85	- 0.58	B-A	B5III	1.21	1833	
79	38.86	- 0.56	overlap	F5V	0.08	276	
77-2	38.87	- 0.59	B-A				
330	38.88	- 1.50	A0	B8V	0.77	764	
75-4	38.89	- 0.46					
75-6	38.89	- 0.47					
78	38.89	- 0.66	A1V		0.45	487	
334	38.89	- 1.70	F5				
327	38.91	- 1.54	A-F				
333	38.91	- 1.77	G0	B7V			X
75-2	38.93	- 0.55		B6.5V	1.01	1607	
75-3	38.93	- 0.55					
150	38.94	- 1.27	F5-8V:	B1V			X
150-1	38.94	- 1.27		B5V			R
150-2	38.94	- 1.27					
150-3	38.94	- 1.27		B8			
150-4	38.94	- 1.27					R
150-5	38.94	- 1.27		B7			
150-6	38.94	- 1.27					
150-7	38.94	- 1.27					
150-8	38.94	- 1.27					
150-9	38.94	- 1.27	G8:	G5III	0.35	203	
326	38.94	- 1.59	F0V	F0V	0.14	216	
+4° 9	38.94	- 1.84	OB	B3III	1.04	2256	
+4° 9.1	38.94	- 1.84					
77	38.96	- 0.74	B2V	B5III	1.17	1331	
67	38.99	- 0.11	A0-A2	A0V	0.24	147	
331	38.99	- 1.70	B7V	B5.5V	0.81	1137	
65	39.01	0.20	B2V:	B5V	1.04	645	
66	39.01	0.04	A7		0.12	200	

Table 3.4 (continued)

Star No.	l^{II}	b^{II}	Sp SpT	Pe SpT	E_{B-V}	Dist.	R
+3°18	39°02	- 3°49	B7II				
75-1	39.03	- 0.51		B6V	0.90	1347	
73	39.03	- 0.10	G:				
74	39.03	- 0.10	G:	G4-F5			
75	39.04	- 0.43	F5	F5V	0.06	77	
76	39.12	- 0.52	F5	F2V	0.15	371	
323	39.12	- 1.48	A4-7		0.38	547	R
324	39.12	- 1.48	A1-2		0.41	352	R
324-1	39.15	- 1.49	A0-1		0.65	640	
324-2	39.18	- 1.49		B8V	0.88	1012	
324-3	39.18	- 1.53	B5V	B5V	0.89	1414	
+4°10	39.30	- 1.85	B9-A0	B7.5V	0.64	1146	
50	39.36	- 1.03	F0	F0III	0.19	167	
39	39.49	0.41	F8-G0III	F7V	0.13	270	R
42	39.49	0.10	B8	B9V	0.57	630	
41	39.56	0.10	A2-3	A2III	0.30	385	
190	39.56	- 1.15	F8V	B8V	0.20	265	X
190-8	39.56	- 1.33		B8V	0.94	1908	
195-1	39.56	- 1.69	K5	K5III	0.23	389	
190-6	39.57	- 1.34		K5	0.07	161	
195	39.57	- 1.67	A0	A1V	0.25	267	
190-7	39.58	- 1.32		B1V	2.13	1369	
190-4	39.60	- 1.34	B	B0V	2.17	611	
				B7.5Ia	1.91	3404	
300	39.60	- 2.56	A0V	B9V	0.26	360	
190-5	39.61	- 1.35					
+6°5.1	39.62	0.66					
190-10	39.62	- 1.20					
190-2	39.62	- 1.30	A3V		0.39	406	
40	39.63	0.08	A4m				
196	39.67	- 1.73	A2:V:				
190-12	39.68	- 1.26					
190-1	39.68	- 1.26	G8	G5III	0.42	250	
190-11	39.70	- 1.28					
191-2	39.72	- 1.42					
191-1	39.73	- 1.40	B8:	B6V	0.93	949	

Table 3.4 (continued)

Star No.	l^{II}	b^{II}	Sp SpT	Pe SpT	E_{B-V}	Dist.	R
192	39°.73	- 1°.49	A0	B8V	0.57	461	
+5° 8	39.73	- 1.58	OBr,G	B5Ib	1.31	1717	
299	39.74	- 2.66	A0	B9V	0.32	376	
38	39.75	0.63	A5:V:	F0V	0.21	508	
37	39.76	0.63	B8	A0V	0.28	490	
43	39.76	- 0.39	F5-6	F7V	0.04	96	
437	39.77	- 2.76	F5V	F1V	0.15	152	
35	39.78	0.64	A7	A5V	0.25	473	
183227	39.78	- 6.87	B9	B6V	0.16	180	
				B7.5II	0.11	757	
36	39.79	0.61	A2	A0V	0.30	560	
293	39.79	- 2.15	A0V	A0V	0.35	579	
199	39.80	- 1.72	B8	B9V	0.66	445	
180-1	39.81	- 1.19	F				
180-2	39.81	- 1.19					
181-1	39.81	- 1.32	F0	F2V	0.20	275	
181-2	39.81	- 1.32		B3V			R
179	39.82	- 1.15	F2p	A8V	0.42	301	
435	39.82	- 2.92	A0V	B7V	0.43	1006	
296	39.83	- 2.35	A0V	A0V:	0.84	388	
				A0II	0.83	2737	R
181-3	39.84	- 1.27	GV	G3V	0.20	268	
284	39.87	- 1.95	B8V	B8V	0.21	212	
34	39.90	0.56	B8-A0	A0V	0.60	641	
178	39.90	- 1.06	A2V		0.48	614	
182	39.91	- 1.33	O	BOIb-09Ia	1.52	5311	
182-7	39.91	- 1.33					
33	39.92	0.04	A0V:		0.42	611	
275	39.92	- 2.67	B8V	B9V	0.32	278	
32	39.93	0.08	A5V		0.31	617	
182-5	39.93	- 1.27		K2V	0.08	266	
182-1	39.93	- 1.32		B1.5V	1.68	1870	
182-6	39.95	- 1.25					
182-8	39.95	- 1.27					
186	39.96	- 1.49	A0	A0V	0.17	253	
283	39.96	- 1.80	B8	B6.5V	0.53	748	

Table 3.4 (continued)

Star No.	l^{II}	b^{II}	Sp SpT	Pe SpT	E_{B-V}	Dist.	R
183	39°.98	- 1°.25	F8V	F2V	0.47	304	
182-3	39.99	- 1.35	A2		0.59	568	
+4°11	39.99	- 3.00	OBh, BO	BO.5V	0.97	2021	
31	40.00	0.07	F8	F3V	0.32	291	
29	40.01	0.22	A2V		0.55	532	
22	40.01	- 0.40	F6V	B7V	0.20	322	X
182-4	40.02	- 1.35		B8V	1.11	824	
274	40.02	- 2.72	A7	F1V	0.12	184	
185	40.03	- 1.63	B8-9V	B8V	0.74	556	
30	40.04	0.15	F8	F5V	0.15	180	
274-2	40.04	- 2.72					
23	40.05	- 0.15	A7		0.40	221	
177	40.05	- 0.98	AO				
274-1	40.05	- 2.72	G-K	K3III	0.55	628	
184-1	40.06	- 1.52	A2V		0.76	430	
184	40.07	- 1.47	Be	B7.5V:	0.44	279	
278	40.07	- 2.37	B8	B8V	0.47	757	
21	40.08	- 0.46	F7	F4III	0.44	564	
184-2	40.09	- 1.50	B9-AO	AOV	0.76	807	
271	40.10	- 2.83	B9V	B9V	0.33	426	
26	40.12	0.12	B8V	B8V	0.71	755	
20	40.12	- 0.34	A1V	A2III	0.42	517	
19	40.13	- 0.38	FO	F2V	0.32	251	
273	40.13	- 2.72	B9V	B8V	0.48	919	
25	40.14	0.00	B8	B9V	0.27	427	
18	40.14	- 0.50	B8	AOV	0.43	494	
172	40.15	- 1.01	A7	A7V	0.30	310	
184-3	40.15	- 1.58	G-K	G5III	0.70	420	
272	40.15	- 2.80	AO	B8V	0.48	851	
184-4	40.16	- 1.60	A				
273-1	40.16	- 2.69	G	G7III	0.56	448	
173	40.17	- 0.99	A2				
184-5	40.17	- 1.60	AO	B9V	0.81	853	
24	40.18	0.02	GO	F7V	0.08	189	
17	40.18	- 0.41	B8	B8V	0.84	613	
171	40.19	- 1.12	A4				

Table 3.4 (continued)

Star No.	l^{II}	b^{II}	Sp SpT	Pe SpT	E_{B-V}	Dist.	R
184-6	40°.20	- 1°.60	A0	A0V	0.80	774	
273-3	40.20	- 2.62	K	K0III	0.38	260	
273-2	40.20	- 2.66	K	K1III	0.47	331	
261	40.23	- 1.93	B8V		0.62	809	
16	40.25	- 0.55	A7	A8V	0.41	316	
265	40.26	- 2.22	A0	B9V	0.29	677	
15	40.29	- 0.19	F5V	F7V	0.16	274	
268	40.32	- 2.89	A0		0.49	731	
14	40.33	- 0.17	A0	B7.5V	0.84	704	
27	40.34	0.28	F2V	F0V	0.15	383	
12	40.36	- 0.31	A3V		0.45	228	
13-1	40.39	- 0.19	F5Ve	F5V	0.07	46	R
13-2	40.39	- 0.19		G2V	0.02	62	
10	40.41	- 0.40	A0	A0V	0.54	479	
11	40.43	- 0.35	F0	F0V	0.33	284	
28	40.47	0.38	F2V	F2V	0.25	269	
249	40.47	- 1.97	A0		0.40	386	
+5°13	40.49	- 3.48	OB	B0V	0.84	1879	
183656	40.50	- 7.08	B6pe		0.12	801	
246	40.51	- 2.18	A0		0.50	622	
248	40.52	- 2.09	A0	A1V	0.36	618	
9	40.53	- 0.26	B8	A1III	0.30	338	
250	40.53	- 1.91					
247	40.53	- 2.11	F5V	F7V	0.06	191	
251	40.55	- 1.87					
255	40.56	- 1.53	B8V	B6V	0.50	469	
8	40.57	- 0.39	A2V		0.29	217	
157	40.57	- 0.93	F7	F5V	0.31	201	
157-2	40.57	- 0.92		K1V	0.15	290	
157-3	40.57	- 0.92		K2V	0.13	220	
2	40.59	- 0.06	F3V	A7V	0.36	455	
252-1	40.59	- 1.90		G0III	0.65	686	
252-2	40.59	- 1.92		A8V	0.32	472	
252-3	40.59	- 1.94		F1V	0.32	424	
252-6	40.60	- 1.87					
252-4	40.60	- 1.94					

Table 3.4 (continued)

Star No.	l^{II}	b^{II}	Sp SpT	Pe SpT	E_{B-V}	Dist.	R
245	40°.60	- 2°.25	A6		0.14	278	
174571	40.61	4.10	B1.5-3Vpe		0.79	1120	
252	40.61	- 1.89	A0				
252-5	40.61	- 1.92		G5III	0.42	553	
252-7	40.62	- 1.86					
252-8	40.63	- 1.88					
243	40.63	- 2.35	B8,A0		0.67	773	
242	40.64	- 2.38	A7,A5		0.57	319	
252-9	40.65	- 1.86					
244	40.65	- 2.31	A7	A8V	0.29	327	
1	40.66	0.14	A0		0.43	443	
252-10	40.66	- 1.87					
252-11	40.67	- 1.87					
7	40.68	- 0.40	G0	G2V	0.14	193	
253	40.68	- 1.88	A5		0.22	479	
157-1	40.69	- 0.93	B8V	K1V	0.09	119	R
3	40.71	- 0.16	F7V	F6V	0.13	155	
254	40.72	- 1.93	A7-F8				
240	40.73	- 2.01	A0		0.44	1175	
+5°10	40.75	- 1.80	overlap	B2V	0.84	1610	
+5°10.1	40.75	- 1.80					
4	40.78	- 0.21	A3-4	A5III	0.05	164	R
239	40.81	- 2.05	B8	B9V	0.28	558	
241	40.82	- 2.21	A0	B9V	0.32	705	
6	40.83	- 0.41	G-K	K0V	0.09	133	
+5°12	40.86	- 2.40	OB				
5	40.90	- 0.35	A0V		0.66	540	
+5°11	40.98	- 2.40	F6I-II	F4II	0.46	355	
152	41.13	- 0.48	F8V	F6V	0.25	259	
151	41.13	- 0.48	A7	A6V	0.32	236	
+3°19	41.15	- 7.62	B0.5IV	B1V	0.30	815	
+6° 7.1	41.18	- 2.69	F8				
185423	41.43	- 8.97	B5	B5II	0.20	1026	
+6° 6	41.50	- 1.77	B2V-B9Ia				
171975	41.56	8.31	B8V	B9V	0.07	157	
168199	41.66	13.53	B5	B3.5V	0.21	286	

Table 3.4 (continued)

Star No.	l^{II}	b^{II}	Sp SpT	Pe SpT	E_{B-V}	Dist.	R
+9° 5	41°.71	3°.38	O8:Vnn	B0V	0.84	1124	
+10° 2	41.92	4.67	OB^+	B0.5V	0.51	3811	
+10° 3	42.85	2.88	B2V	B3III	0.43	487	
				B2V	0.49	340	
+7° 7	42.97	- 2.07	F8I	F1Ib	1.05	963	
+6°8	43.09	- 4.68	A8Ib				R
+8° 3	43.35	- 1.73	OB^-	B8III	0.73	605	
+11° 4	43.49	3.76	OB^-	B9III	0.59	780	R
169820	43.60	12.34	B9V	B7V	0.17	198	
+7° 8	43.67	- 3.31	OB	B8V	0.30	830	R
+8° 2	43.69	- 1.37	AOIa	B9Ib	0.65	6115	
+9° 6	43.86	0.34	OB^-	B3V	0.93	1072	
+9° 6.1	43.86	0.34		G4V	0.09	145	R
+10° 4	44.19	1.12	OB^-	B5V	0.80	816	R
+11° 5	44.21	2.66	B1Ia	B2Ib	1.13	3565	
+11° 6	44.26	2.26	B1.5:IV:ne	B4II	0.64	1927	
+5°4285	44.63	- 9.33	B6e	B5V	0.12	732	
				B7II	0.06	2755	
+10° 5	44.68	0.03	OB	O9-9.5V	1.36	1669	
+11° 8	44.81	1.20	F8	B2V	0.83	1012	R
+11° 7	44.87	1.80	B1Vnn	B3V	0.61	840	
+8° 4	44.96	- 3.60	OB	B1.5V	0.88	2058	
+8° 5	45.04	- 4.82	B1Ia	B1.5Ib	0.41	7160	
164447	45.35	19.72	B7IVne	B7III	0.08	366	
+12° 2	45.35	2.47	B8II	B8II	0.51	2356	
+10° 6	45.58	- 0.55	B9II	B9II	0.30	1485	
174853	45.67	6.20	B8Vn	B8V	0.12	161	
186456	45.82	- 8.12	B2.5e-B6V	B6III	0.18	2252	R
+10° 6	45.94	- 1.71	B8Ib	B9Ib	0.93	3876	R
+12° 1	45.97	3.07	AOII	AOII	0.34	1110	
+14° 4	46.39	5.22	B3	B3III	0.48	1782	
187567	46.84	- 9.29	B2e		0.13	894	
177724	46.86	3.25	AOVnn,B9V	AOV	0.02	23	
180398	47.36	0.63	B6e	B5V	0.24	492	
				Be	0.18	1850	

Table 3.4 (continued)

Star No.	l^{II}	b^{II}	Sp SpT	Pe SpT	E_{B-V}	Dist.	R
171623	47°.55	11°.67	B9.5IVn	B9V	0.06	93	
				B9III	0.05	140	R
+14° 5	47.55	4.13	B1Ib	B1Ib	0.74	6527	
+12° 7	48.38	- 2.53	B1Ib	B2II	0.96	2654	
+15° 4	48.66	2.62	B8II	B8II	0.78	2519	
180555	48.71	1.19	B9V	B9V	0.05	98	
+14° 9	48.71	0.56	B2III	B2III	0.81	3185	
164900	48.90	20.57	B3V	B3V	0.11	341	
+13° 6	49.05	- 1.69	B9II	A1II	0.73	2784	
+17° 3	49.21	6.36	F4Iab	F5II	0.28	207	
+16° 3	49.21	4.59	A0(II)	A0II	0.43	3151	
				A0V	0.44	454	
+10°10	49.32	- 8.73	F8I	F7II	0.41	284	
+11°12	49.39	- 5.29	B0Ibn	B0.5Ib	0.33	6635	
+15° 5	49.44	2.07	B8II	B9II	0.73	3643	
+18° 2	49.49	7.55	F5I-III	F2III	0.33	527	
175744	49.55	7.10	B9Sip		0.12	248	
+14°3887	49.58	0.25	Bpe		1.79	1007	
186122	49.63	- 5.43	B8III	B6.5III	0.11	339	
183144	49.74	- 1.32	B5	B5.5V	0.12	263	
+15° 8	50.01	1.02	B9Iab	A0Ib	0.93	4843	
+15°12	50.01	0.02	B0III	B0III	0.97	2154	
+16° 5	50.05	2.82	F4Iab	F0Ib	0.92	1670	
179588	50.29	3.07	B8V	B8V	0.10	189	

Remarks for Table 3.4

In the final column, "X" indicates ultraviolet excess. For these stars, the spectral type (Sp SpT) is definitely late but there exists no late type reddening solution for the observed colours (see Section 4.3). Where a reddening solution is given, it corresponds to the objective prism spectral type assumed to be dwarf luminosity class.

Star No.	Remarks
-1° 9	M_V low for OB classification.
$-2^{\circ}17$	BOV?
$-2^{\circ}20$	B9II?
-0° 5	Only lower M_V possible.
-0° 9	B6.5III?
177880	B8Ib?
$+0^{\circ}$ 7	B5II?
$-0^{\circ}13$	Only higher M_V possible.
$+5^{\circ}$ 6.1	AOV?
$+1^{\circ}$ 7	Wrong star?
$+2^{\circ}$ 5	B2III?
$+3^{\circ}$ 5	Catalogue coordinates for $+3^{\circ}5$ do not correspond to star in the finder chart. The star given by the coordinates may have a trace of the K-line and is probably more luminous and earlier than A1V. HeI (4026Å, 4471Å) and MgII (4481Å) may be present.
$+3^{\circ}$ 9	M_V is low.
$+3^{\circ}$ 9.1	Same star as $+3^{\circ}12.1$.
356	No dwarf solution.
$+3^{\circ}17$	Star may have been misidentified on finder chart.
360	Sharp lines. A3III adopted.

Star No.	Remarks
141-1	Spectrum faint. A possible emission feature is visible on 40- and 20-minute exposures. Band structure in late-type star might produce a similar spectrum.
381	SrII (4077Å) and G-band present.
+3°15	Second possible reddening solution. Pe SpT=B2III, $E_{(B-V)}=0^m.81$, Distance=2214 pc.
+4° 6	=NGC 6755-1
6755-5	Variable?
P-5	Objective prism classification is in better agreement with the photoelectric photometry in Table 3.3b than with Purgathofer (1969).
+7° 6	RZ Oph.
150-1	Since 150 itself may have an UV excess and the "150" stars were chosen because they were near 150, they too may have an UV excess and no reddening solutions were given unless there is an Sp SpT.
150-4	10 reddening solutions!
323	Uncertainty in Sp SpT.
324	Uncertainty in Sp SpT.
39	F5V?
190	Reddening solution is for F8V.
181-2	Scattered light or UV excess?
296	H_{13} visible.
13-1	Emission is probably spurious - probably due to overlapping images.
157-1	Faint spectrum. AOII solution yields $E_{(B-V)}=0^m.91$, Distance=2234 pc.
4	H_{15} is visible.
+6° 8	Wrong star.
+11° 4	B9V?
+7° 8	Moffat and Sherwood both observed the same star but their $B=10^m.4$ is different from LS IV $m_{pg}=11^m.4$. This may be a typographical error in LS IV or a misidentified star on the LS

Star No.	Remarks
	finder chart.
$+9^{\circ}$ 6.1	Several other reddening solutions possible.
$+10^{\circ}$ 4	B5III?
$+11^{\circ}$ 8	Sp SpT from LS II. Reddening solution is for B2V; no late-type solution possible but higher luminosity solutions exist.
186456	Photometric solutions for both spectral types and luminosity classes.
$+10^{\circ}$ 6	LS IV
171623	Second reddening solution is better than the first.

3.2 Results

3.2.1 Spiral Structure from OB Stars

Becker and Fenkart (1971) suggested that stars with spectral types earlier than B2-3 be used as spiral tracers. There are about 60 of these stars in Table 3.4. These stars are shown in Figure 3.6 projected on the galactic plane. The distances for the two HII regions marked by "*" have been kinematically determined by Georgelin and Georgelin (1970). Star 182 is now identified as the exciting star for S74.

The distribution of stars out to 1000 pc is relatively uniform between $30^{\circ} \leqslant l^{II} \leqslant 50^{\circ}$ but, between 40° and 50° at distances greater than 1000 pc, there are relatively few stars. This is due partly to the cloud complex and partly to the way the spiral structure crosses the line of sight in this cone.

The opacity of the cloud must be very high for only foreground and high latitude stars are visible above the galactic plane as shown in Figure 3.7. Stars in the shadow cone projected by the cloud appear near $l^{II}=30^{\circ}$ or $l^{II}=50^{\circ}$. Plate 1 shows that the brightest part of the Milky Way between Scutum and Cygnus occurs below the galactic plane.

If one allows for the stars not found above the plane by assuming a symmetrical distribution, the spiral arm near the Sun has a thickness between 200 and 300

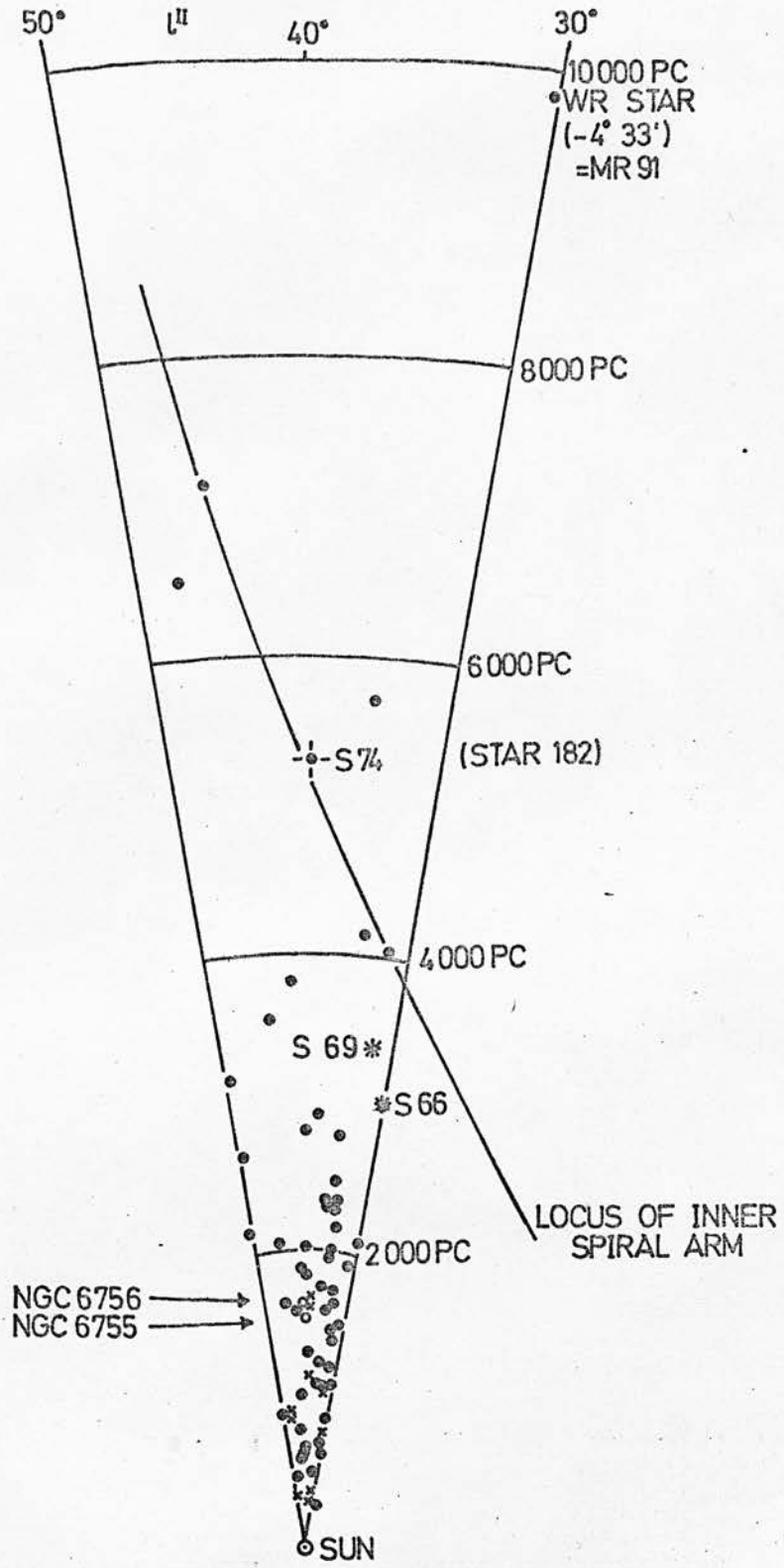

FIG. 3.6
PROJECTION ON THE PLANE OF STARS ≤ B 2/3.

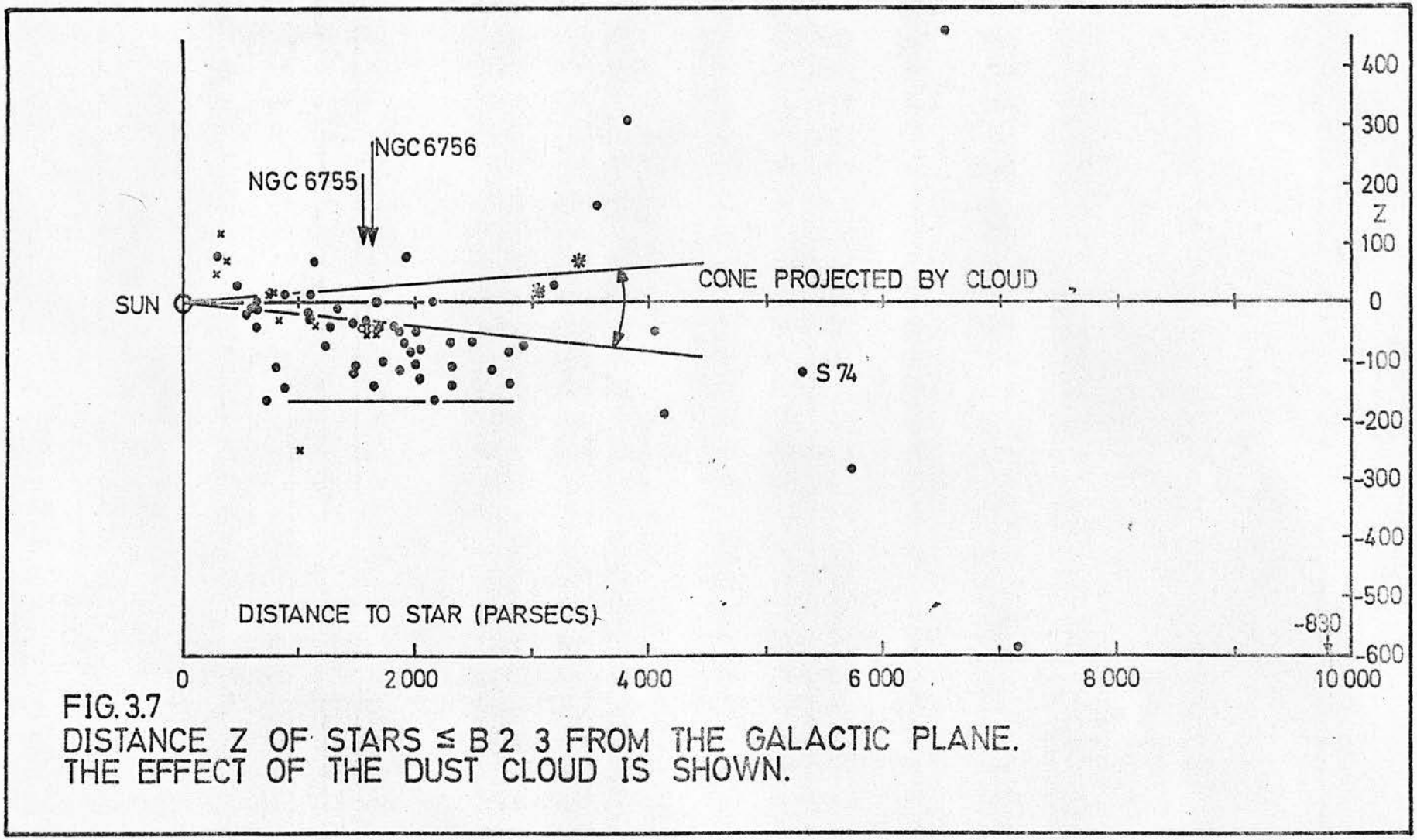

FIG. 3.7
DISTANCE Z OF STARS ≤ B 2 3 FROM THE GALACTIC PLANE.
THE EFFECT OF THE DUST CLOUD IS SHOWN.

parsecs.

The data in Figure 3.6 have been combined with the data in Figure 2 of Moffat and Vogt (1973) to make Figure 3.8. The symbols are defined in Table 3.5.

Table 3.5

Definition of Symbols Used in Figure 3.8.

Symbol	Meaning
•	Stars earlier than B2-3, this work
o	Wolf-Rayet stars, Smith (1968b)
_	δ Cep stars with P 15 days, Tammann (1970)
*	Sun
|	HII regions, Georgelin and Georgelin (1971)
\	Supergiants, Humphreys (1970)
–	Bpe and BO-0.5(III-V)e, Schmidt-Kaler(1964)
/	Young open clusters, Moffat and Vogt (1973)

The new data trace the inner (Sagittarius or -I) spiral arm to more than 6 kpc from the Sun. The arm is now shown to be continuous over more than 12 kpc. The observations also show an increase in space density of O-B2 stars at the outer edge of the arm about 1500 pc from the Sun. This suggests that the Cygnus arm is really a spur which leaves the -I arm near $l^{II}=50^{o}$ at a distance of more than 2 kpc from the Sun. The stars within 1000 pc between $40^{o} \leq l^{II} \leq 50^{o}$ appear to be

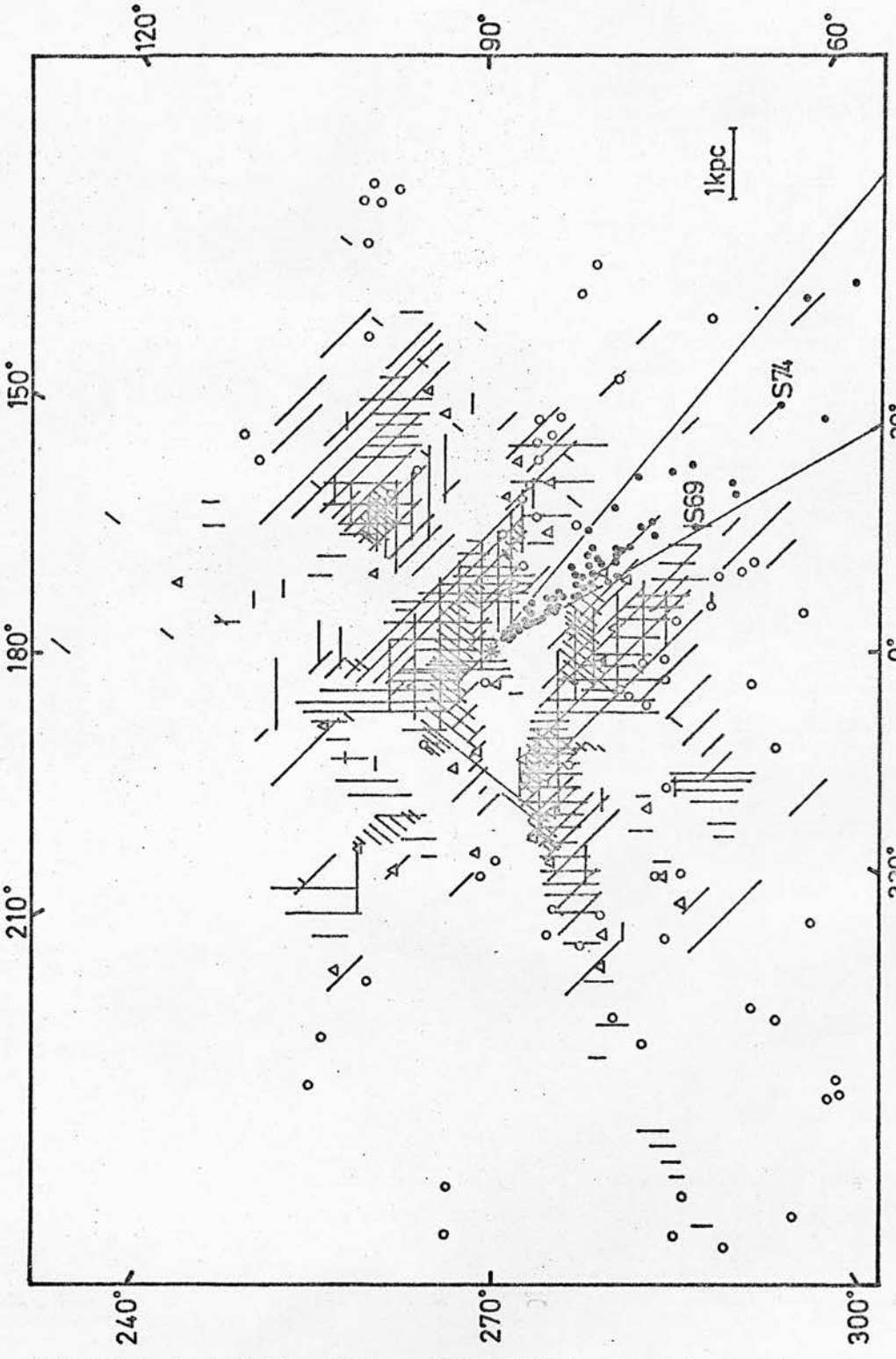

FIG. 3.8 (AFTER FIG. 2, MOFFAT + VOGT, 1973) SPIRAL STRUCTURE BASED ON DIFFERENT TRACERS. SEE TEXT FOR DEFINITIONS.

related to the space distribution of spiral tracers in the Cygnus spur.

The width of the spiral arm is about 1500 pc - approximately equal to the separation between spiral features shown in Figure 3.8. The thickness then is between 15 and 20% of the width of a spiral arm at 8 to 10 kpc from the galactic centre.

3.2.2 Structure of the Dust

The presence of dust is revealed by the non-random fluctuations in the number of stars found per unit area and by the reddening, ie. colour excess, of stars in certain volumes of space. In 3.2.2.1, the total absorption of the dust in the region of the Schmidt plate will be studied by star counts. Next, in 3.2.2.2, the reddening will be studied as a function of the detailed structure revealed from star counts, as well as a function of the general structure of the area from 30° to 50° (l^{II}). Finally, in 3.2.2.3, some characteristics of the dust are summarized and the distribution discussed.

3.2.2.1 Absorption from Star Counts

Stars, counted i) automatically in three colours by means of the programme FIVE-BY-FIVE (Appendix A1) operating on GALAXY measures of stars and ii) visually on the blue POSS prints, have been used to make an estimate of the total absorption. The method is similar to that developed by Bok (1937, 1956) and will be described only briefly here. The stars measured by GALAXY were counted in boxes with an area one-eighth of a GALAXY zone of 4 x 8 mm. On the Monte Porzio Schmidt plates, the boxes had an area of 21.23 square arc minutes. The result for the automatic counts made in the visual (V) colour is shown in Figure 3.9 which has twice the scale of Figure 2.2 and the same orientation as that figure and as Plates 2 and 3.

In order to derive the contours of equal absorption, Bok used van Rhijn's (1929) cumulative stellar distribution table (the logarithm of the number of stars brighter than magnitude $m+\frac{1}{2}$ down to $m_{pg}=18^m$ for the Selected Areas) assumed to be free from the influence of absorption. However, the region at $l^{II}=40^o$ is some distance from the nearest Selected Area and, as was shown in Chapter 1, it has a peculiar star distribution; therefore, interpolation from van Rhijn's table was not used. Instead, a region (0.112 square degrees) at the south edge of the field with counts in V of 80 or more stars per box was adopted as a "clear" region. A "cloud" region was established for comparison where the

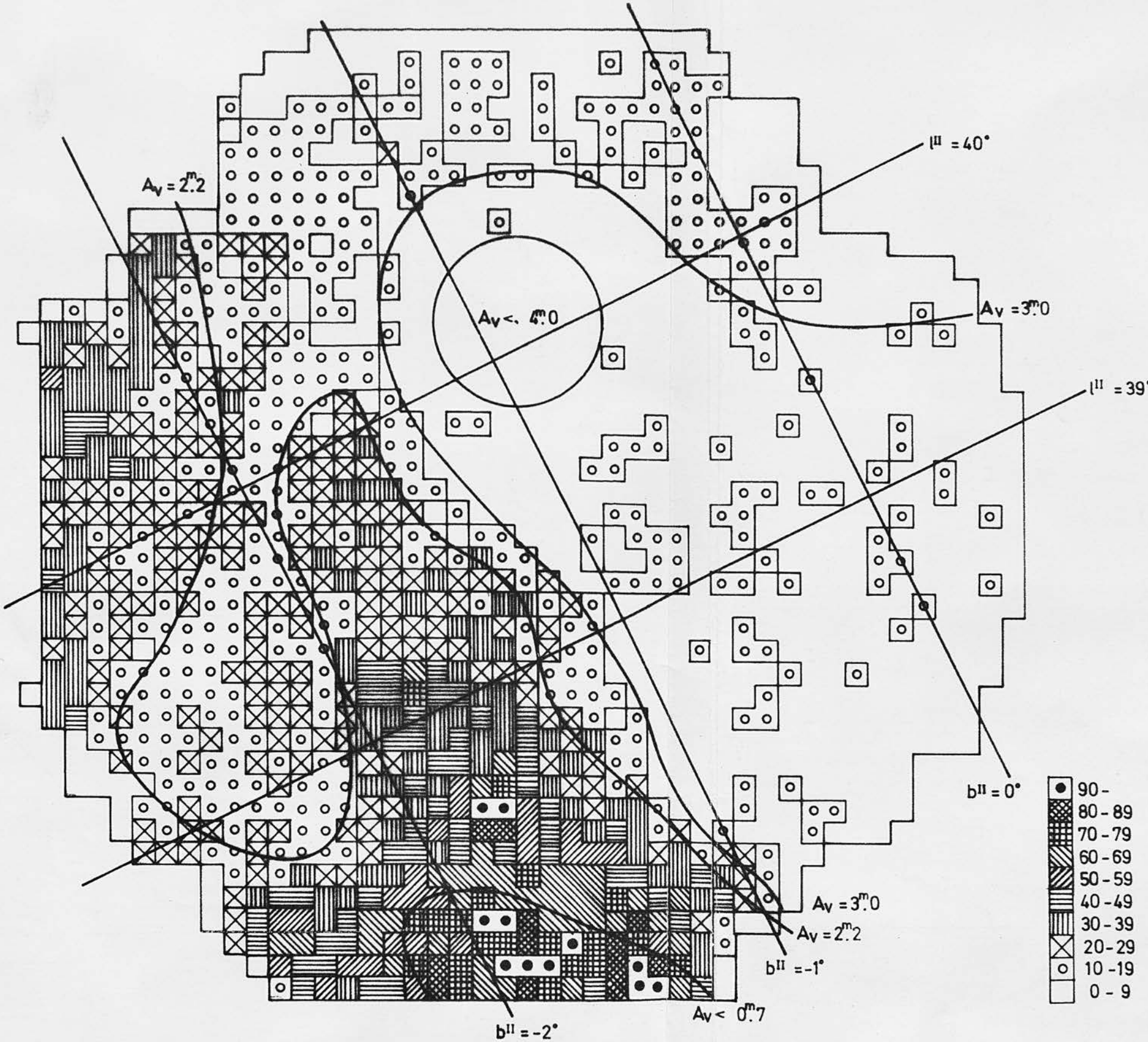

FIG. 3.9 STARS COUNTS (V) PER UNIT AREA MEASURED BY GALAXY.

star counts in V were less than 20 per box. Visual counts on the blue POSS prints were used to extend the distribution in the two regions to a limiting magnitude of $20^{m}.5$ (adopted).

The counts were accumulated by the programme FIVE-BY-FIVE and then converted to N(m) counts per square degree brighter than magnitude $m+\frac{1}{2}$. The yellow (V) and blue (B) cumulative distributions are shown in Figure 3.10. For comparison, van Rhijn's distribution (1929) for these galactic coordinates is also given. The good agreement in blue between the distribution derived by van Rhijn and that derived from GALAXY counts, including the POSS point on the extrapolation, confirms that the GALAXY counts are complete and require no corrections.

In the V distribution for the cloud, one sees that from at least $V=9^{m}$, the star counts are affected by absorption. Even the "clear" region is showing the effects of absorption by $V=11^{m}$. Near the limiting magnitude, the average absorption may have increased to 4^{m} and 2^{m} for the cloud and clear regions respectively.

It is evident that the cloud is nearby and of high opacity. If the distance to the cloud is in the range 300 to 400 pc and the luminosity function for the vicinity of the Sun is used (Allen, 1955), then it may be estimated that fewer than three stars per unit area of 21.2 square arc minutes are foreground stars and the rest are behind the cloud.

If it is assumed that the cloud is so near the Sun

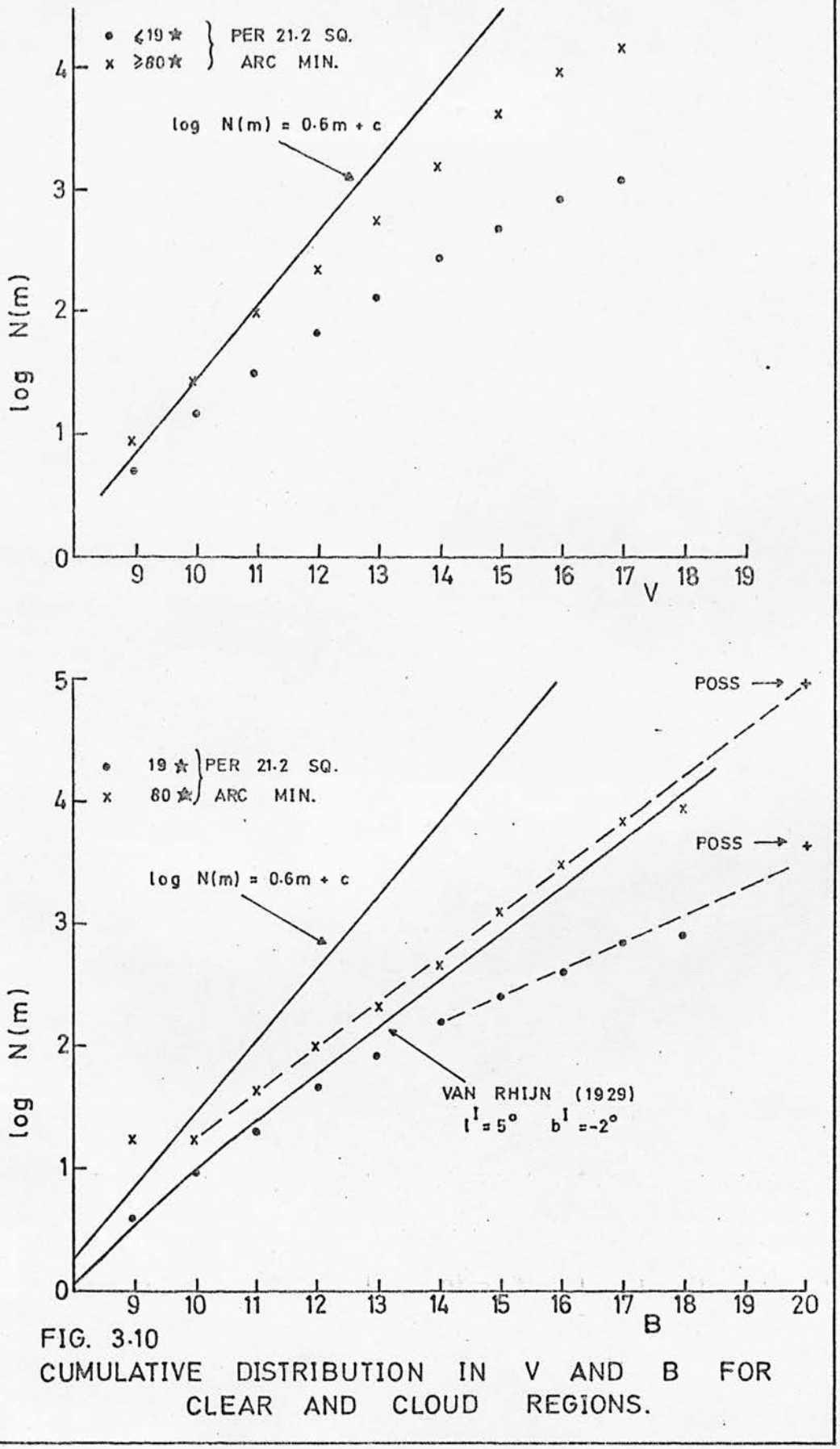

FIG. 3·10
CUMULATIVE DISTRIBUTION IN V AND B FOR CLEAR AND CLOUD REGIONS.

that all the stars are behind it then, following Bok (1937, 1956), we may infer that the rate of decrease in the number of stars per magnitude interval relative to the "clear" region is due to absorbing clouds. The amount of absorption (in magnitudes) as a function of the number of stars per unit area is shown in Figure 3.11.

The contours of equal absorption marked on Figure 3.9 were determined with respect to the clear region assumed to be free from absorption. It is certain from Figure 3.10 that the counts in the clear region are also affected by absorption so that the results are underestimated. The presence of stars associated with the cloud will lead to a further underestimation of the absorption.

The reddening of $2^{m}.0$ for stars 190-4 and 190-7 suggests that 3 magnitudes should be added to the differential absorption in Figure 3.9 to obtain the value of the total absorption. The reddening of NGC 6755 of $0^{m}.9$ at 1800 pc (G. Alter, B. Balazo, and J. Ruprecht, editors of the second edition of the Catalogue of Star Clusters and Associations, Budapest, 1970) suggests a similar addition and may be accepted as confirmation of the zero-point term to be added to Figure 3.9.

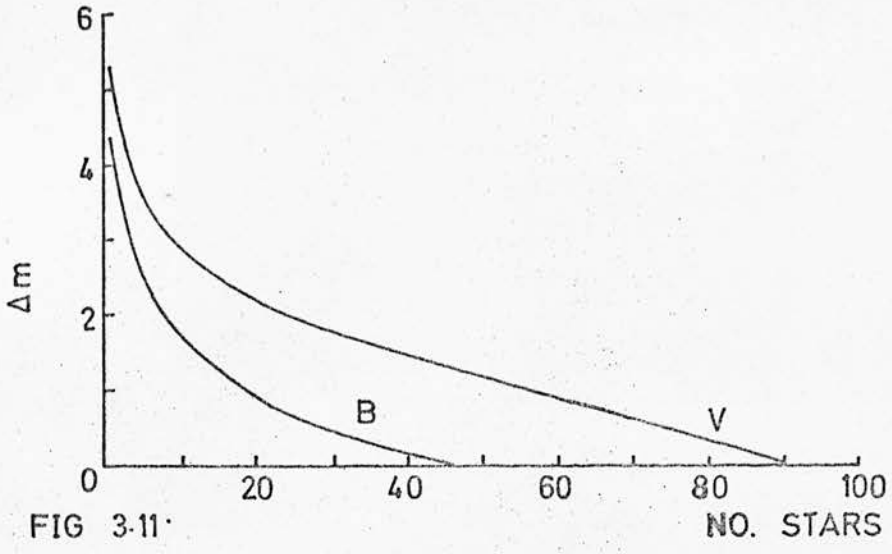

FIG 3·11·

ABSORPTION AS A FUNCTION OF STAR COUNTS.

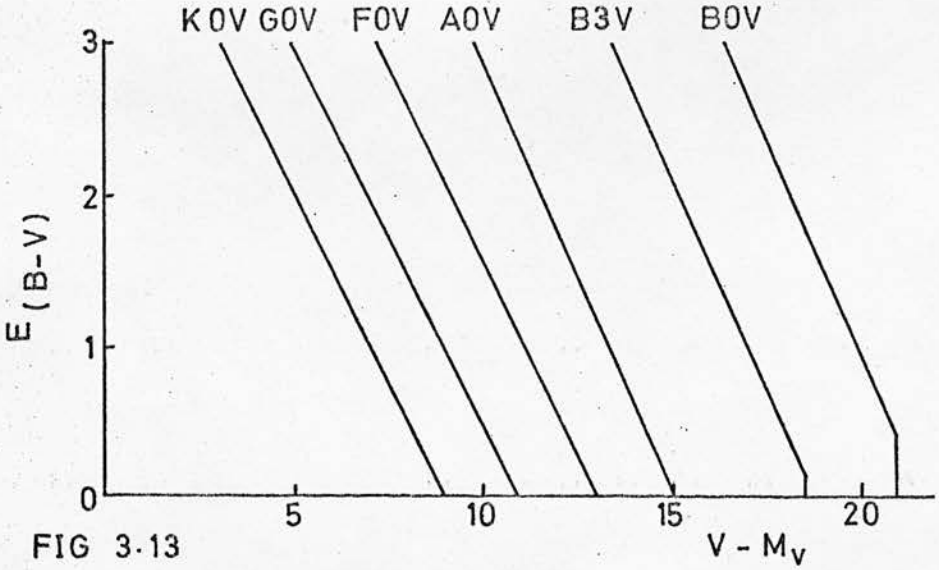

FIG 3·13

THE LIMITS TO WHICH CERTAIN SPECTRAL TYPES MAY BE OBSERVED.

3.2.2.2 Colour Excess as a Function of Position in Space

In Table 3.4, spectral types and luminosities were presented for several hundred stars which enabled their distances to be determined from photoelectric photometry. This is obviously impractical for the vast amount of material produced by GALAXY. One way around the situation is to assume that most of the stars measured will be dwarfs. This can be tested in the following way:

A part of the calibrated north region containing 421 stars was chosen; the data were processed by MODULUS (Appendix A3) for luminosity classes V and Ib. The resulting reddening with distance relation is shown in Figure 3.12.

Approximately 90% of the "dwarf" stars lie within the area marked V; the remaining stars are scattered above as well as to the left of this area. The same stars, now treated as supergiants, also appear in a main group marked Ib with a few stars scattered about - seven stars lying along an obvious extension of the dwarf reddening relation have been enclosed in a smaller area also marked Ib. It may be concluded that

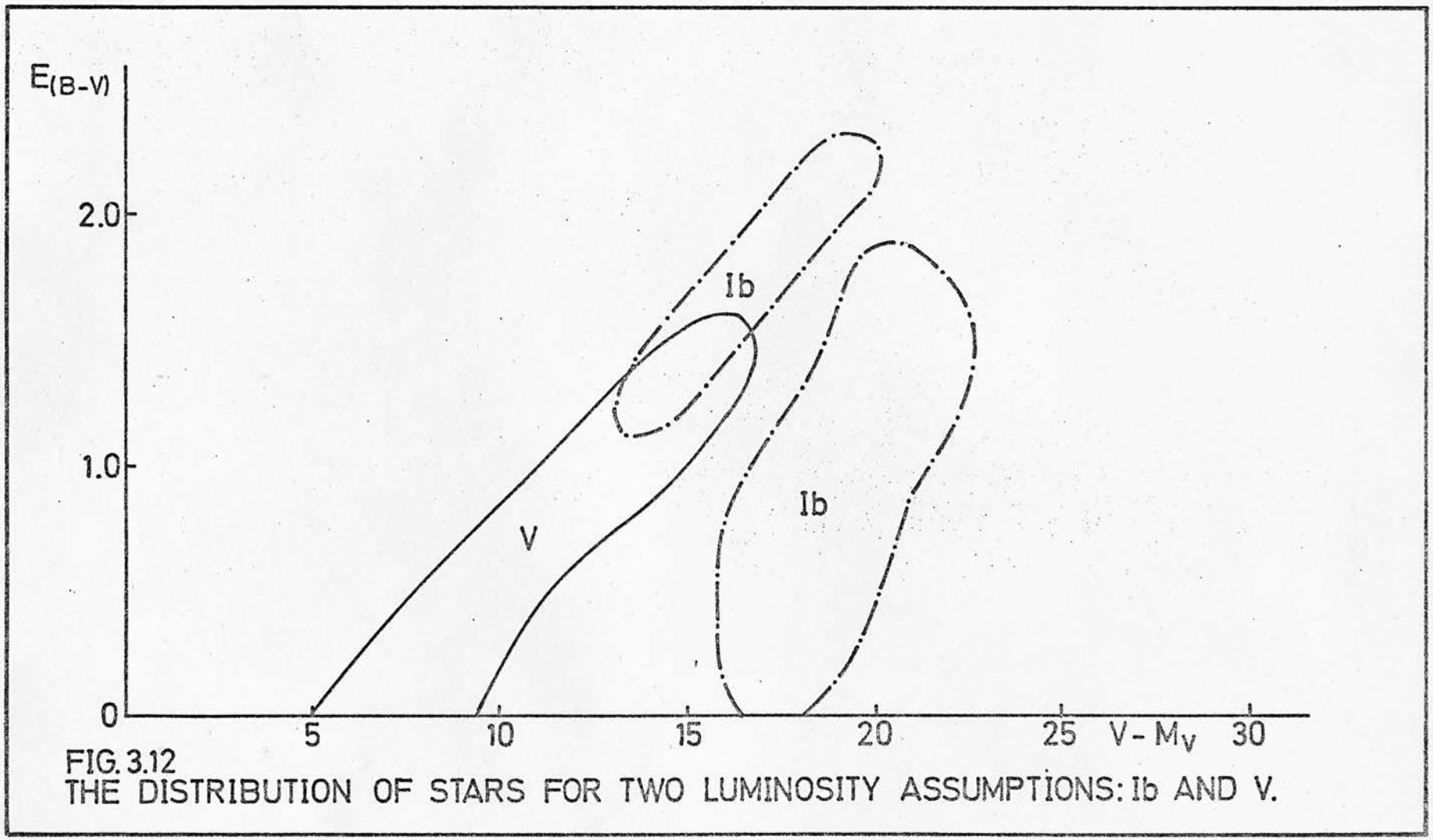

FIG. 3.12
THE DISTRIBUTION OF STARS FOR TWO LUMINOSITY ASSUMPTIONS: Ib AND V.

most of the 400 stars in the sample are reddened dwarfs but a few stars may be of luminosity Ib. Comparison with other luminosity solutions allows the $E_{(B-V)}$ versus $(V-M_V)$ relation to be extended through this overlapping technique to include highly reddened high-luminosity stars. One can also determine which dwarfs have been treated as highly reddened dwarfs when in reality it is only photometric error which gives them such a reddening solution. This is not a serious problem in this region because the reddening sets in so near to the Sun and is very large. Even late type F and G dwarfs are reddened so that they are no longer systematically scattered about the intrinsic two-colour relation but appear as in Figure 3.3.

The affect of the bright limiting magnitude in U must also be considered. Figure 3.13 (on the same page as Figure 3.11) shows the probable limits to which dwarfs of different spectral types can be observed. The reddening with distance relations found in this work (Figure 3.14) cross the cut-offs nearly at right angles. The cut-offs, therefore, have little influence on the determination of reddening with distance.

In Figure 3.14, the mean curves of $E_{(B-V)}$ versus $(V-M_V)$ for four areas indicated in Figure 2.2 are reproduced. The areas are: north, Purgathofer, west, and outside cluster. For comparison, the mean curves

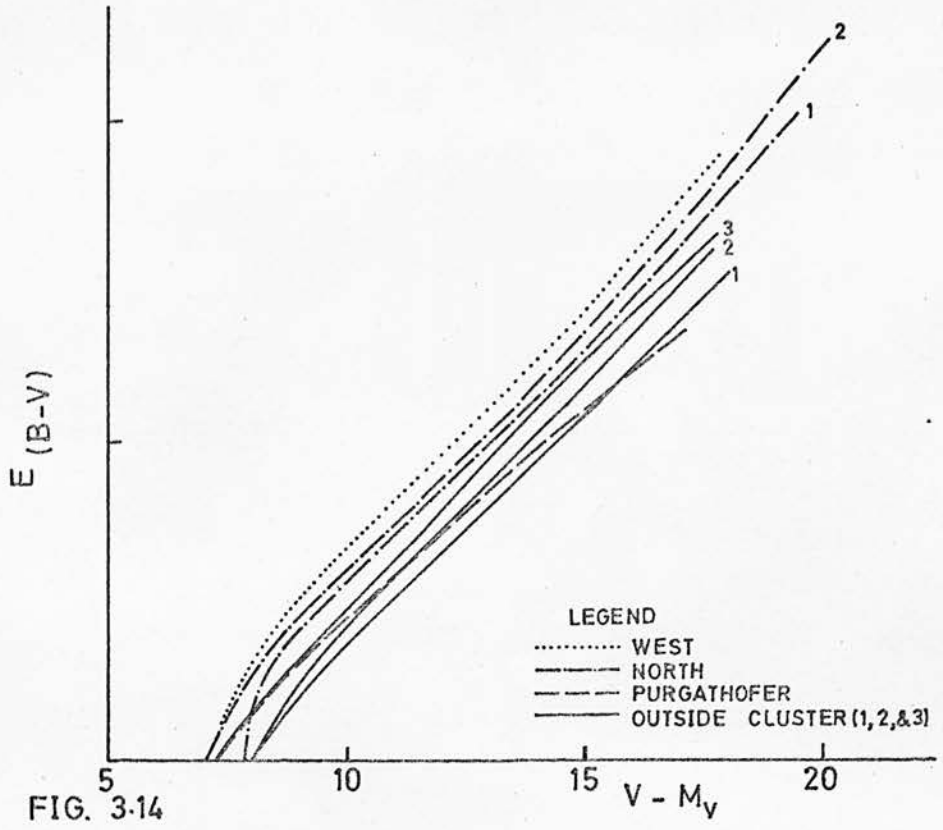

FIG. 3·14

FOR 4 DIFFERENT REGIONS IN THE SCHMIDT- FIELD.

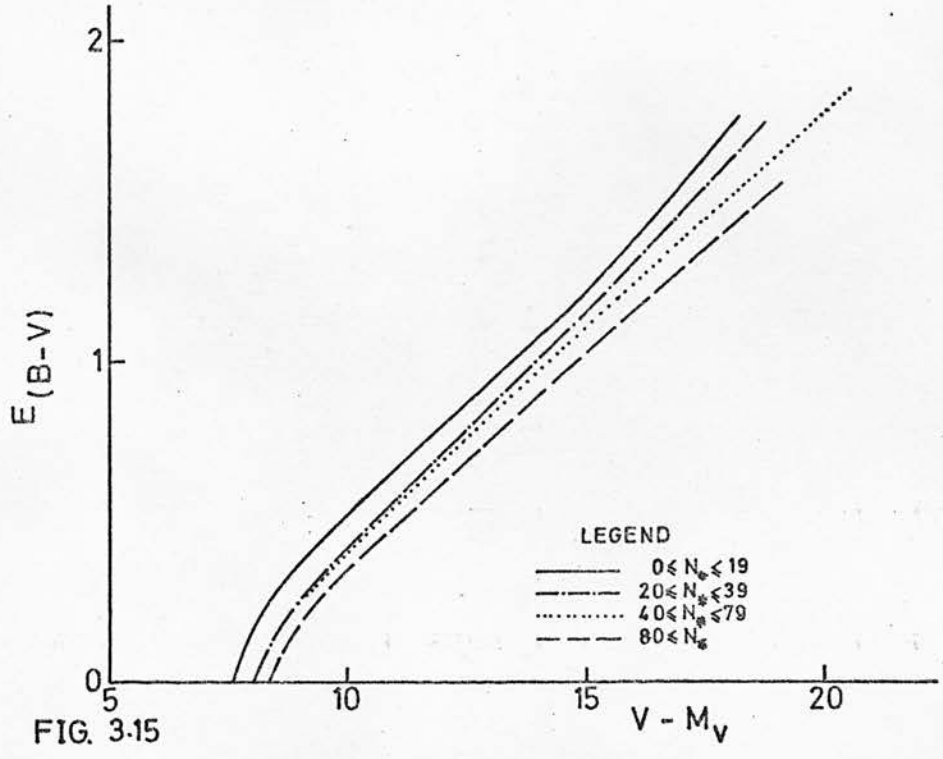

FIG. 3·15

FOR AREAS OF DIFFERENT STAR DENSITIES.

for areas with different star counts (1 to 9, 10 to 19, ..., 80 to 89, more than 89 stars per unit area) are given in Figure 3.15. The number of stars involved is given in Table 3.6.

Table 3.6

Distribution of Stars by Region and Star Counts

Fig. 3.14		Fig. 3.15 (Cluster Region Included)	
Region of Cloud	No. Stars	Star Count Range	No. Stars
North-1	421	0- 9	778
-2	392	10-19	452
Purgathofer	195	20-29	142
West	165	30-39	304
Outside Cluster-1	534	40-49	361
-2	521	50-59	246
-3	478	60-69	379
		70-79	222
		80-89	134
		90	152

Each curve in both figures was drawn as independently as possible. Some idea of the good agreement can be seen in the curves for different star counts (Figure 3.15); the curves coincided for 0-9 and 10-19, for 20-29 and 30-39, for 40-49 to 70-79, and for 80-89

and 90. There are also some disagreements shown in Figure 3.14. The low reddening portions of the curves for north and outside cluster show some scatter. But the interpretation of these figures is not affected: the cloud is most opaque and nearest the Sun at a line through north and west approximately along $b^{II}=-1^{o}$. In the 0-19 range of star counts, the mean distance of stars with zero reddening is 340 pc from the Sun but this distance has increased to 480 pc in the region having more than 80 stars per unit area (the absolute value of these distances may be in error by as much as 10% but the error of the difference in distance between the two regions is smaller). In the west region and a part of north, the cloud begins at 275 pc while in two parts of the outside cluster region is begins at 400 pc. Thus the differences vary from 125 pc to 140 pc depending on the data used.

The cloud has an angular width of 5^{o} perpendicular to the plane; at a distance of 300 pc, this corresponds to 26 pc. But there is no reason to believe that the thickness of the cloud in the plane is also 26 pc; on the contrary, it was shown in Figures 3.6 and 3.8 that the stars between 40^{o} and 50^{o} l^{II} associated with the Cygnus feature just beyond the Sun are at distances between 300 and 1000 pc. Figure 3.16 shows the dust to be distributed in the same way. The opacity is initially very high (equivalent to a=15 mag./kpc) but tapers off near the outer edge of the spiral feature

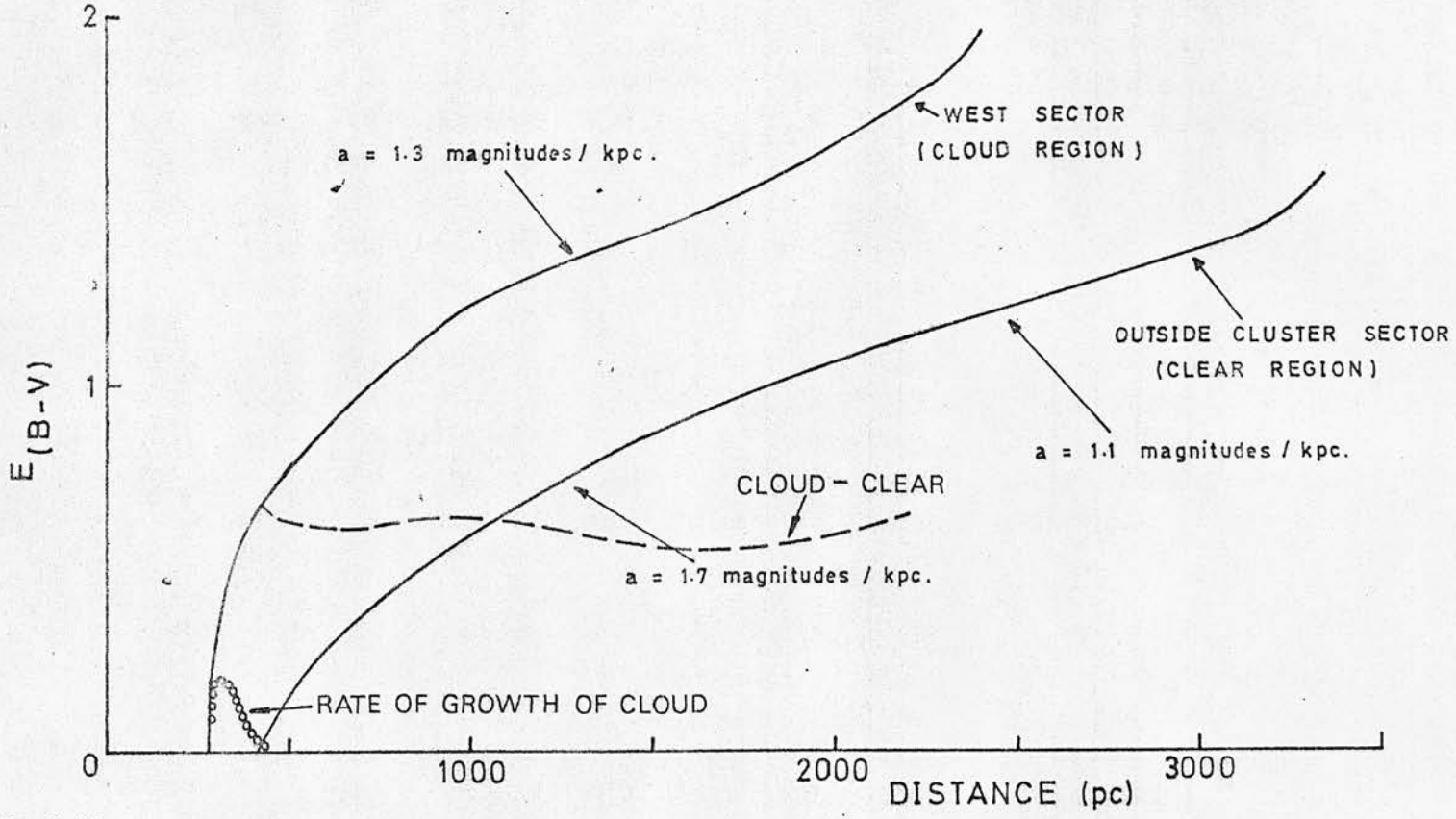

FIG. 3.16

REDDENING WITH DISTANCE IN TWO REGIONS OF THE SCHMIDT FIELD.

until a uniform but high reddening begins: a=1.1 to 1.7 mag./kpc. This uniform reddening extends across the interarm region until it shows a jump between 2 and 4 kpc away for all the regions but the distance cannot be accurately determined due to a paucity of stars. However, it is reasonable to associate it with the intersection of the line-of-sight with the -I arm.

The other regions show similar relations to that in Figure 3.16; "outside cluster" is plotted for comparison. The difference in reddening between the cloud and clear regions allows the determination of the rate of increase in reddening through the cloud. These relations are also given in Figure 3.16 with the latter relation determined for 20 parsec increments through the cloud.

The cloud is effectively defined between 300 and 400 pc and shows the same steep gradient in absorption along the line-of-sight as can be seen in the direction perpendicular to and below the plane in Figure 3.9. Above the plane, there is still a low surface brightness and it is evident from Plate 1 that a great area is covered by an upward sweep of dust.

3.2.2.3 Some Characteristics of the Cloud Summarized

Until now the cloud has been discussed as a single entity but it has considerable structure and really ought to be regarded as a complex aggregate. In spite of the complexity, it is probably homogeneous, being a well-defined physical structure belonging to the outer spur.

If we assume the complex to be an aggregate of clouds all of one kind, it is possible to use the theory developed by Münch (1952) to determine the number of clouds per kpc and their average $E_{(B-V)}$ from the dispersion in the reddening with true distance modulus relation.

Figure 3.17 relates $E_{(B-V)}$ to (V_o-M_v) for the stars in Table 3.4. The high luminosity stars in LS II and IV have been distinguished from those in the Schmidt field to show that they have in general less reddening for a given distance. An example of the use of a reddening solution is also given for the star 190-4.

The average reddening at a distance r is E with a dispersion d. If there are n clouds per kpc, each with a colour excess e, then

$$E = enr$$

and the dispersion is

$$d^2 = e^2nr$$

or

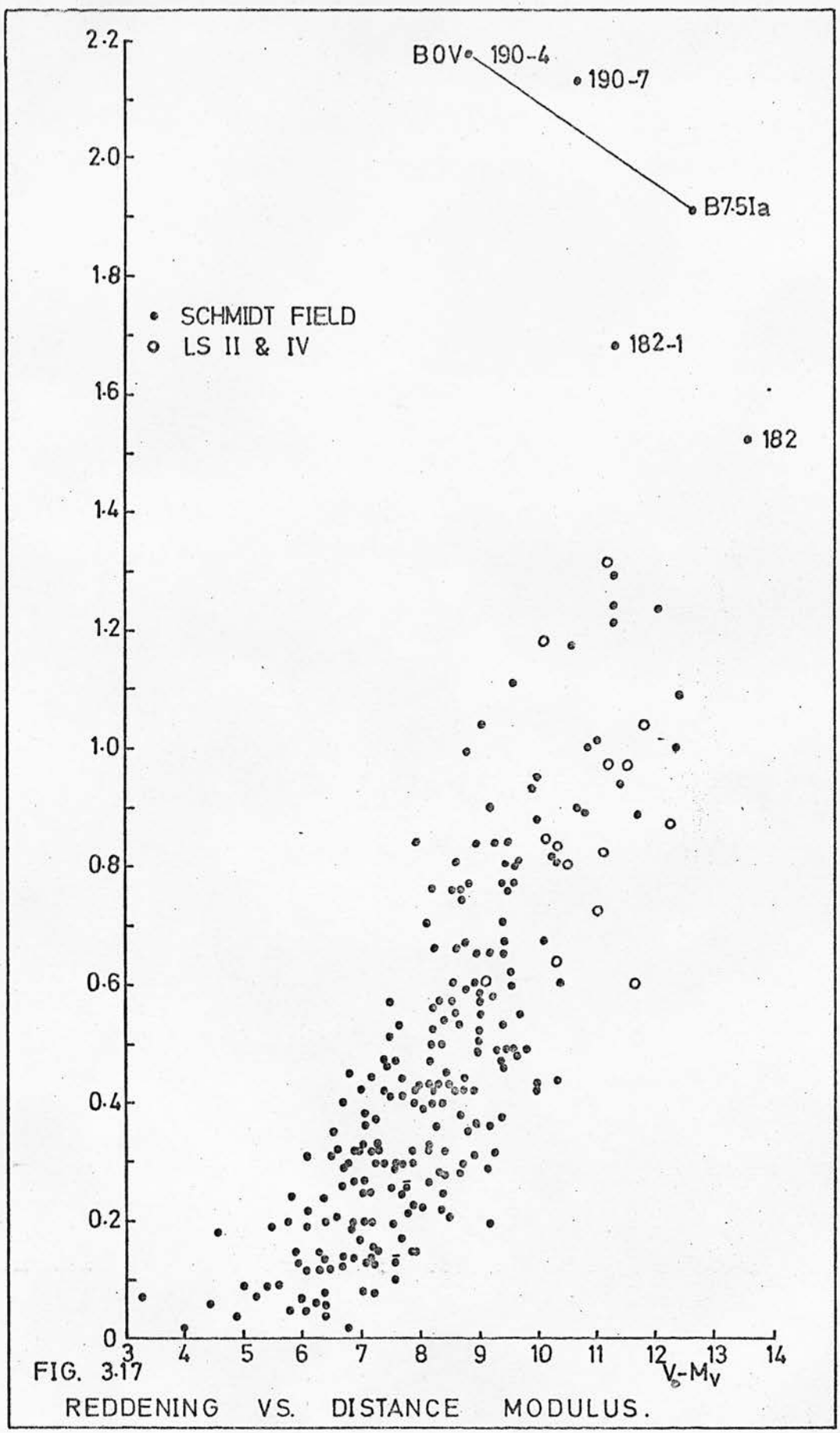

FIG. 3·17

REDDENING VS. DISTANCE MODULUS.

$$d^2 = eE \quad . \qquad \text{(FitzGerald, 1967)}$$

The error in the photometry is so small that the dispersion d was used uncorrected. The results are given in Table 3.7.

Table 3.7

Mean Reddening and Number Density of Clouds between $30^\circ \leq l^{II} \leq 50^\circ$.

Distance r(pc)	$E_{(B-V)}$ E	Dispersion d	$E_{(B-V)}$ e	No. Clouds n(per kpc)
250	$0^m.26$	0.14	$0^m.08$	16.1
398	0.45	0.20	0.09	12.7
631	0.57	0.25	0.11	8.2
1000	0.80	0.26	0.08	9.5
			0.09	11.6

These results may be compared with FitzGerald (1967) who averaged his data over areas of 16 square degrees compared with an area of 400 square degrees for Table 3.7. He found $e=0^m.05$ and n=16 clouds per kpc. The difference is probably not statistically significant on the whole but indicates that for this area, the values in the table are reasonable. The decrease in the number of clouds per kpc with increasing distance may be the result of the selection effect mentioned in Section 3.1.

The distribution of the dust may now be summarized as follows: it is much more restricted to the plane than the O-B2 stars are, having a thickness of about 30 parsecs. The rate of change of reddening with distance suggests that the dust belongs to the inside edge of the outer spur. An optical depth of perhaps 6 is reached in some parts of the cloud but there is no indication from the stellar distributions that the ratio of total to selective absorption, R, is in any way significantly different from 3.2. Small changes (to R=4) would probably not be detected as much of the work was comparative.

Chapter 4

Discussion of the Results and Suggestions for Further Research

4.1 Distribution of Neutral Hydrogen

The distribution of neutral hydrogen in this longitude range has been described by Shane and Bieger-Smith (1966), Kerr (1969, 1970), Weaver (1970), and Shane (1971). Some analysis is contained in these works as well as in that of Burton and Shane (1970). Bok(1971) has summarized the results and only a few points need to be repeated. Kerr's observations point to two spiral arms in the region of interest: the Sagittarius or -I arm and the Cygnus feature starting close to the Sun in the direction $l^{II}=75^{o}$ and gradually bending inward on the far side of the Galaxy. Using neutral hydrogen, the -I arm can be traced over the same longitude range as it can be traced optically. Weaver's data point to the same Sagittarius arm but the Cygnus feature becomes only one of many spurs. Optically, this picture coincides better with Figure 3.8 than does Kerr's picture.

Shane's observations (1971) indicate that the gas near the Sun ($22^{o} \leq l^{II} \leq 42^{o}$) has a width of $\pm 5^{o}$ in latitude, about the same as for the stars (Figure 3.7). The dust would appear as a separate, much narrower

feature of the Cygnus spur while the gas and O-B2 stars would have a common distribution.

Gas in the Sagittarius arm appears to have the same thickness as in the spur but there are too few stars to determine the stellar thickness or the distribution of the dust.

If the radio structure of the Galaxy should consist of two independent arms and the optical structure should consist of an arm and a spur, then the Galaxy could have two separate classifications with the optical one being earlier. Recent work by Schmidt-Kaler and Schlosser (preprint) also suggests that filamentary structure similar to that in the Sb galaxies NGC 2841 and NGC 7331 is prominent in our Galaxy too. Kerr (1969) relates velocity fluctuations to variations in density which occur over 500 to 1000 pc - about the scale being considered here.

Van den Bergh (1972) discussed the question of whether galaxies can change their Hubble type. If the optical structure really differs from the radio structure as has been discussed here and in Chapter 1, the answer would seem to be yes. Which way a galaxy would evolve is difficult to say - presumably in the way dictated by star formation.

4.2 Gas to Dust Ratio

In the previous section, the gas and dust were found to have separate space distributions. This may be confirmed by determining the gas to dust density ratio. The results are dependent on the dust model adopted. Calculations will be made for the classic model by Spitzer first employed for this purpose by Lilley (1955) and for a model by Wickramasinghe (1967).

Distances were derived assuming that the hydrogen gas rotates in circular orbits with a rotational velocity W km/sec according to the rotation curve given by Burton and Shane (1970):

$$W(R) = 250.0 + 4.05\ (10 - R) - 1.62\ (10 - R)^2$$

where R is the distance in kpc from the galactic centre which is 10 kpc from the Sun. The radial velocities and column densities of hydrogen, N_H, were taken from Shane (1971).

From Section 3.2.2, it is known that the dust extends from 0.3 to 1 kpc; this corresponds to a radial velocity range of +4 to +14 km/sec. The average value of N_H in this velocity range between 38^o and 42^o l^{II} is $11.60 \pm 2.06 \times 10^{20}$ cm^{-2} equivalent to $1.0 \times 10^6 \eta_\odot$ per kpc at one kiloparsec.

The value of N_H varies very little between $\pm 5^o$ latitude in contrast with the dust distribution concentrated in the plane but extending also above it. The mean distance of the hydrogen as derived from the radial velocity is 400 ± 40 pc. This distance is just

inside the cloud and from Figure 3.16 corresponds to an absorption of 1.8 magnitudes. From the star counts, an absorption of more than 3.0 magnitudes was obtained. The ratios of gas to dust density will be derived for both cases.

The formulation of the calculation has been given by Lilley (1955) and Garoli and Varsavsky (1966) among others. The part pertaining to dust grain models has been reviewed by Greenberg (1968) and Wickramasinghe (1967). Wickramasinghe described several models but the one used here is the graphite core-ice mantle grain. The graphite core radius is 5×10^{-6} cm and the extinction efficiency $Q_{ext} = 0.849$ was adopted for the visual region from his Appendix 2. The two models are compared in Table 4.1.

Table 4.1

Values of Parameters for the Classical and Graphite Core-Ice Mantle Models.

Parameter	Classical	Ice+Graphite
Grain Radius (cm)	3×10^{-5}	1×10^{-5}
Q_{ext}	2.0	0.849
Grain Density (gm cm^{-3})	1.0	1.1

The results of the calculations are given in Table 4.2 for both models and absorptions of 1.8 and

3.0 magnitudes. The evidence is in favour of a low gas to dust ratio. It is important to emphasize that the results are extremely dependent on the model. Therefore, in order to compare these results with others, the classical model is adopted although the graphite core-ice mantle model is probably more realistic.

Table 4.2

Gas to Dust Density Ratio

Absorption	Classical	Ice+Graphite
$1^{m}.8$	54 : 1	2.5 : 1
3.0	32 : 1	1.5 : 1

Lilley was the first to report a ratio of 100:1 for the anticentre region; he found a good correlation between hydrogen density and absorption. Wesselius and Sancisi (1971) did a statistical study covering most of the Galaxy and found little if any correlation between the presence of gas and dust. Lambrecht and Schmidt (1957) found a positive correlation in the direction of early-type stars and young associations. The mean ratio was 130:1 but significant variations were found which suggested that there was probably no unique value. There appear to be three choices:

i) The gas and dust distributions need not coexist in the same volume of space as was suggested in Section 4.1.

ii) The spin temperature of hydrogen is very low, producing line saturation leading to an underestimate of the amount of hydrogen.

iii) The hydrogen is no longer in an observable form being either in molecular or solid form under the aegis of the grains.

Zimmermann (1968a and b, 1970) has shown that dust particles can be separated dynamically during cloud collisions without being destroyed. The effect may have important consequences for star formation in this part of the Galaxy.

The second and third cases have been discussed by several people including Heiles (1967), Garoli and Varsavsky (1966), and Reddish (1969). Heiles has stated that his high-frequency resolution observations of regions on either side of $l^{II}=40^{o}$ do not indicate line saturation.

If the hydrogen is in molecular form, the percentage can be estimated assuming that: i) the gas to dust ratio (100 or 130 to 1) for low opacity regions is valid everywhere in the Galaxy, ii) there is a strict coupling of the gas and dust whichever way dust clouds of low and high optical depth evolve, and iii) discrepancies between the true or valid ratio and the observed ratio given for the classical model in Table 4.2 is due to the conversion of atomic hydrogen (H) to molecular hydrogen (H_2). These assumptions are not independent but simply relate the

three components, atomic and molecular hydrogen and dust, together. For each of the two "true" values and the two observed values for the classical grain, the percentage of hydrogen atoms in molecular form is given in Table 4.3.

Table 4.3

Percentage of the Total Number of Hydrogen Atoms in Molecular Form (H_2).

True Gas to Dust Ratio	100:1	130:1
Observed Ratio		
54:1	46%	58%
32:1	68%	74%

Where the absorption reaches 6 magnitudes, there would be more than 84% of the hydrogen in molecular form.

4.3 On the Existence of a Pre-Main Sequence Population Associated with the Cloud

There are three T-associations near the region being considered:

Oph T1 at $l^{II}=38^{\circ}$ and $b^{II}=+8^{\circ}$,

Aql T1 at $l^{II}=37^{\circ}$ and $b^{II}=-9^{\circ}$, and

Del T1 at $l^{II}=55^{\circ}$ and $b^{II}=-9^{\circ}$.

Each is between 200 and 300 pc away - about the distance to the cloud - and has about twenty members. Herbig (private communication) has stated that the only certain T Tauri star in the immediate area ia AS 353 ($l^{II}=46^{\circ}$, $b^{II}=-3^{\circ}$) (Merrill and Barwell, 1950); it has a companion about 2 magnitudes fainter at 6" and a Herbig-Haro object at 24". Herbig added that further away is a small group of emission-line and/or variables associated with the dark nebula B 142; V536 Aql (dKe) is one of the stars at $l^{II}=47^{\circ}.8$, $b^{II}=-5^{\circ}.6$. He pointed out that the Aquila cloud probably contains many more T Tauri stars but the large area has discouraged any survey with their small-field equipment. The question then is: have pre-main sequence stars been detected at $l^{II}=40^{\circ}$?

The first evidence for a group of stars associated with the cloud comes in Chapter 2; in Figure 2.7, the frequency distribution of stars as a function of (B-V) is given for nearly equal areas in the clear and cloud regions. It might be expected that the "cloud"

distribution would be somewhat redder than the "clear" distribution. However, the low surface density region has many more stars with (B-V) $0^m.6$ and includes the only stars in the sample with (B-V) $0^m.3$. This is the range in (B-V) for F-G2 spectral types.

To test the hypothesis that there are more F stars per unit area projected against the cloud than against the clear area, the objective prism field was divided approximately along $b^{II}=-1^o$ and the stars of different spectral types (Apriamashvili, 1966) were counted complete to $m_{pg}=12^m.0$.

The frequency distribution is given in Figure 4.1. The effect of interstellar reddening on the B and A distributions is clearly seen but if this effect is removed, then there are between 25% and 50% more F stars in the direction of the cloud than away from it. The frequency distributions for LF1 and LF2 (M^{c}Cuskey, 1949 and M^{c}Cuskey and Seyfert, 1947) for areas in Aquila and Cygnus free from obscuration are nearly the same as the one found here for the clear region.

It does not seem likely that this group of stars has T-Tauri characteristics. The LS II and IV surveys were carried out with H_α objective prism plates as well as the usual blue plates. The limiting magnitude for H_α was probably brighter than $V=12^m$. No emission-line objects were reported for this field.

The inspection of the objective prism plates taken at Cerro Tololo revealed a few suspects, two of which,

180 and 181, were found at the telescope to have close visual companions. Apriamashvili classified the stars as F8 and F6 respectively but 181 probably consists of two reddened stars. No. 141-1 also appears to be an emission object but this could be due to band structure in a very late-type star to judge by its colours.

It was concluded that probably no T-Tauri spectral characteristics are included in this group of pre-main sequence stars. Walker (1972) has discussed the properties of some young, non-T Tauri stars with ultraviolet excess. Herbig (1970) has suggested that T-Tauri characteristics are displayed less than 5% of the pre-main sequence lifetime. The lack of T-Tauri characteristics need not be a major objection to these stars being pre-main sequence stars. A more detailed analysis is required to confirm this: to identify the stars and to determine with greater confidence the differences such as ultraviolet excess and variability.

The photoelectric data in Table 3.4 also suggests the existence of a cloud population with ultraviolet excess (combining the two suggestions: supernumerous F stars with ultraviolet excess). All nine stars having F spectral types and B"photoelectric spectral types" lie in or at the edge of the cloud. It is difficult to allow for the selection of the original stars for observation, but it seems unlikely that this selection could have produced such a result. The average magnitude and colour for eight of the stars

(excluding no. 150, V=$9^{m}.77$) is $11^{m}.85$, $0^{m}.68$, and $0^{m}.10$ for V, (B-V), and (U-B) respectively; individually and in the mean, a small ultraviolet excess is present. The scatter is about $0^{m}.3$ in V. If M_{v} is taken to be between 4^{m} and 5^{m}, typical values for pre-main sequence stars in Orion (Mpg=5^{m}), then the stars are probably located near the front of the cloud, perhaps related to the maximum in neutral hydrogen at 400 pc. This is obviously an uncertain result, but three independent sources of data all suggest that there exists a group of stars associated with the cloud.

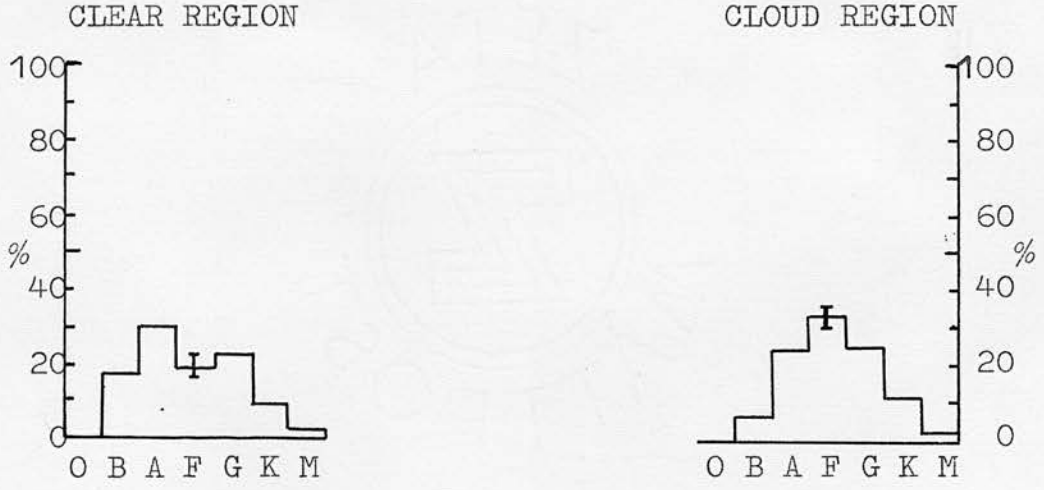

FIG. 4.1

FREQUENCY DISTRIBUTION OF SPECTRAL TYPES IN THE CLEAR AND CLOUD REGIONS OF THE SCHMIDT FIELD.

4.4 Future Work

Several problems have already been mentioned: the low value of the gas to dust ratio and its association with star formation, and a group of stars possibly associated with the cloud. A new determination of the luminosity function and space distribution of stars may relate star formation to the gas and dust density distribution in the cloud.

Much more spectroscopic work is required to determine luminosities and spectral types for some of the bright and suspected pre-main sequence stars found here. The spectrograms should be used to establish more MK types for objective prism classification and to determine radial velocities for kinematic distances. This would be important for some of the "182" and "190" stars.

A much larger area for future research lies in the domain of galactic structure: how has the dust been accumulated so effectively? Theoretical work such as by Roberts (1972) and the observations of high-latitude in-falling clouds such as by Habing (1966) and Oort can be applied together at $l^{II}=40^{o}$. The results may be helpful in assessing the rôles played by density waves and explosions (in galactic nuclei) in producing spiral structure.

Chapter 5

Conclusions

The discontinuity about $l^{II}=40^{o}$ is the result of heavy obscuration reaching over six magnitudes in places. A search for faint OB stars has been successful. These stars lie at the same distance as those stars relatively free from obscuration and do not suggest abnormal extinction.

The dust is located between 300 and 1000 parsecs from the Sun and some patches have extinction as high as 15 magnitudes per kpc. Previous estimates were based on too few stars which were either nearby or out of the galactic plane. The dust has a different distribution from that of the O-B2 stars used as spiral tracers; it is confined much more to the plane and inner edge of the Cygnus feature with a thickness about one tenth that of the stars (30 versus 300 parsecs).

A preliminary result is the probable existence of a pre-main sequence population associated with the dust cloud;the stars do not exhibit extreme T-Tauri characteristics.

The O-B2 spiral tracers have filled in the gap in the Sagittarius arm (-I arm) between $l^{II}=30^{o}$ and 60^{o}. The arm extends up to 7000 parsecs from the Sun with the tangent point occurring near this distance at $l^{II}=50^{o}$. The local or Cygnus arm is probably one of

many spurs and joins the -I arm beyond 2000 parsecs (probably at 4500 parsecs) from the Sun also near $l^{II}=50^{o}$.

Finally, the comparison of optical and radio data suggests small but significant differences in the galactic structure each presents. This has been found in other galaxies and may indicate the relationship between star formation and the evolution of galaxies.

Appendix A

Computer Programmes

A1 FIVE-BY-FIVE

This computer programme summarizes the GALAXY measurements by areas 4.6 arc minutes square, **ie.** 21.23 square arc minutes. Eight of these areas equal one GALAXY zone of 8.192 mm by 4.096 mm. The programme determines the area in which each star appears and adds it to the local statistics. At the end of each zone, these statistics are presented:

i) The number of stars, n(m) (per 21.23 square arc minutes,not per square degree) brighter than magnitude $m+\frac{1}{2}$ for each of V, B, and U where m ranges from 7^{th} to 19^{th} magnitude.

ii) The sum of the intensities of stars in each magnitude interval expressed as a fraction of the intensity of a zero-magnitude star.

iii) The integrated intensities I_V, I_B, and I_U for the area.

iv) Integrated magnitudes and colours derived from these integrated intensities.

Point i) is demonstrated in Section 3.2.2, Figure 3.9, for star counts on the yellow plates. The application of the other points is discussed in Appendix B.

A2 FARBE

This programme was written by Moffat and Vogt (Bochum) and determines (if possible) the intrinsic colour, and hence colour excess, of a star for any luminosity class. To save computer time, the solutions for luminosity classes IV and Iab were not determined. The programme was altered in the course of this work to provide, in addition, the absolute magnitude, the apparent and true distance moduli (for a particular value of R), and the distance in parsecs also for any luminosity.

The programme works in the following way:

i) The intrinsic colours and absolute magnitudes (Schmidt-Kaler, 1965) for each luminosity class were tabulated with a one-to-one correspondence in a form suitable for interpolation.

ii) The ratio $X=E_{(U-B)}/E_{(B-V)}-0.06E_{(B-V)}$ was also given as a function of an independent tabulation of $(B-V)_o$. For OB stars, this solution was taken from Serkowski (1963), while for stars with $(B-V)_o > 0.0$, the relation was from Fernie (1963).

iii) For the chosen luminosity classes (V, III, II, Ib, or Ia), $(B-V)_o$ is obtained by successively subtracting a number of $0^m.05$ steps from the initial (observed) (B-V); $(U-B)_o$ is calculated using the value of X appropriate for $(B-V)_o$.

iv) When the trial crosses the intrinsic relation, the

programme iterates until a solution is obtained meeting a prescribed tolerance ($\pm 0^{m}.005$ in $(B-V)_o$).

v) With this value of $(B-V)_o$, the value of M_V is found for the same luminosity also by iteration. For giants and dwarfs, $(U-B)_o$ was used to find M_V if $(B-V)_o < -0.08$; for all other cases, $(B-V)_o$ was used. The reason for this may be seen in the HR diagram where the M_V versus $(B-V)_o$ relation is very steep for $(B-V)_o < -0.08$ but M_V versus $(U-B)_o$ makes an approximately 45^{o} line in this interval and so is better for interpolation.

vi) The programme continues from step iii) until no further solutions are possible. Up to three reddening solutions are anticipated but more could be accepted.

vii) The determination of $E_{(B-V)}$, $V-M_V$, V_o-M_V, and distance in parsecs is straightforward. The value of R is obtained from Schmidt-Kaler (1965):

$$R = 3.20 + 0.21\ (B-V)_o \quad .$$

This relation allows for changes in effective wavelength.

A3 MODULUS

This is a graph-plotting programme used in conjunction with FARBE. Data is ordered in $E_{(B-V)}$ and plotted against $(V-M_V)$, (V_o-M_V), and/or distance for one or more luminosities. The symbols printed for the different luminosities and reddening solutions are given in Table A3.1.

Table A3.1

Definition of Symbols Used in Modulus.

Luminosity	Reddening Solutions		
	1st	2nd	3rd
Ia	0	A	Ø
Ib	1	B	I
II	2	C	L
III	3	R	G
V	5	V	D

Appendix B

Surface Photometry

The primary purpose of GALAXY is to make the vast amount of information recorded of Schmidt plates available for complete analysis of a region. In general, this is an analysis of the group characteristics since the individual results may have large random errors.

The FIVE-BY-FIVE programme described in Appendix A1 was written to prepare data for group analysis, originally planned to include surface photometry. Unfortunately, the programme was carried out before adequate photoelectric sequences were established with the consequence that the photometry has significant field and colour terms nullifying its usefulness.

Pannekoek (1933) and later with Koelbloed (1949) carried out the first detailed surface photometry of the Milky Way based on extrafocal photographs. The work is quite good but suffers from poor resolution. Elsässer and Haug (1960) did photoelectric photometry in P and V but with even poorer resolution (2° to 5°). Pfleiderer and Mayer (1971) carried out ultraviolet surface photometry with a resolution of 1° to 2°. With GALAXY, the resolution may be varied according to the surface density of stars; in the present work, the resolution of about five arc minutes is adequate.

The early interest in surface photometry was aimed at discovering the structural details of the Galaxy from the appearance of its projection on the observer's celestial sphere (Becker, 1956). This is much the same way as the projection of the hydrogen gas distribution is used to infer the spiral structure. Elsässer and Haug (1960) identified the brighter regions of the Galaxy with the directions along spiral arms. But Behr (1965) took self-absorption into account in the spiral arms and showed by comparison with radio observations of neutral hydrogen that the optical surface brightness corresponded to minima of radio intensity and vice versa. Pavlovskaya and Sharov (1971) confirmed this and further showed that when real inhomogeneities in star and dust distributions are considered, then surface photometry is an unreliable way of studying spiral structure. In fact, Sharov (1971) has shown that the apparent brightness of the Galaxy is determined primarily by dust in the vicinity of the Sun rather than by structural peculiarities.

What then are the reasons for studying surface photometry? There are at least four reasons:

i) Removing the influence of background fog from photographic photometry (such as in the crowded region of NGC 6755). Combined with star counts, the integrated magnitude per unit area may permit an empirical correction to be made. (At the time GALAXY measured the plates, there was no facility for measuring the fog

level on the plate directly.

ii) Synthesizing galaxies. This is probably best carried out with multi-colour, intermediate band photometry. It is more useful than photoelectric surface photometry because the data may be used for other purposes such as determining the spiral structure and luminosity function which when combined yield the observed colours. The effect of reddening can also be studied. Useful comparisons can be made between other galaxies and our own.

iii) Measuring diffuse galactic light. At present, GALAXY measures only star images but the photographic surface photometry may be combined with photoelectric surface photometry with interesting consequences. Integrated sky light at 5577Å for a 100Å wide filter consists of 70.7% airglow, 15.4% zodiacal light, 7.7% star light, and 6.2% diffuse scattered light (Roach and Megill, 1961). In general, the percentage composition varies and it is difficult to make proper allowances. At good sites, air glow corrections can be determined. Zodiacal light is more difficult but its relative variations with time can be determined if one is observing one area (such as the dust cloud at $l^{II}=40^{o}$). The knowledge of the starlight comes from the photographic surface photometry and after allowing for these components in the photoelectric measurements, the diffuse component can be determined.

iv) Measuring the zodiacal light and gegenschein.

This is done in a way similar to that described in iii). The photographic photometry establishes one component of the total signal. The time variations of the signal allow the other components to be taken out.

The first and third points are of definite value. The first will be used when the plates are completely calibrated. The third probably would be best carried out in infrared. Use of UBVI surface photometry might allow an extrapolation to longer wavelengths not affectively reached with photography but perhaps more interesting astrophysically. As a substitute for the missing infrared data, some V and B observations have been made at $l^{II}=40^{o}$ and when reduced will be used for a feasability test of the method.

References

Abt, H.A., Meinel, A.B., Morgan, W.W., Tapscott, J.W. 1968, An Atlas of Low Dispersion Stellar Spectra.

AGK_2 1958, Zweiter Kat. A.G. 13 & 14, Ed. R. Schorr and A. Kohlschütter, Bonn.

Allen, C.W. 1955, Astrophysical Quantities (2^{nd} Ed.), Athlone Press, London, p. 236.

Apriamashvili, S.P. 1966, Bull. Abastumani Obs. 35, 3.

Baade, W. 1963, Evolution of Stars and Galaxies, Ed. C. Payne-Gaposchkin, Harvard University Press, Cambridge.

Becker, W. 1956, Vistas in Astronomy 2, Ed. A. Beer, Pergamon Press, London, p. 1515.

Becker, W., Fenkart, R. 1971, A & Ap Suppl. 4, 241.

Behr, A. 1965, ZfA 62, 157.

Bergh, S. van den 1972, Conference on the Rôle of Schmidt Telescopes in Astronomy, Ed. U. Haug, Hamburg, p. 67.

Bidelman, W.P. 1972, Conference on the Rôle of Schmidt Telescopes in Astronomy, Ed. U. Haug, Hamburg, p. 53.

Blanco, V.M., Demers, S., Douglass, G.G., FitzGerald, M.P. 1968, Photoelectric Catalogue, Publ. U.S. Naval Obs., 2^{nd} Series, XXI.

Bok, B.J. 1937, The Distribution of Stars in Space, University of Chicago Press, Chicago.

Bok, B.J. 1956, AJ 61, 309.

1971, IAU Highlights of Astronomy 2, Ed. C. de Jager, D. Reidel Publ. Co., Dordrecht, p. 63.

Börngen, F., Friedrich, G., Link, G., Richter, L., Richter, N. 1970, IAU Symposium No. 38, Ed. W. Becker and G. Contopoulos, D. Reidel Publ. Co., Dordrecht, p. 69.

Burton, W.B., Shane, W.W. 1970, IAU Symposium No. 38, Ed. W. Becker and G. Contopoulos, D. Reidel Publ. Co., Dordrecht, p. 397.

Connolly, L.P., Montarakis, P.Z., Thompson, L.A. 1972, PASP 84, 61.

Cousins, A.W.J. 1971, Royal Obs. Annals No. 7.

Cousins, A.W.J., Stoy, R.H. 1962, Royal Obs. Bull. No. 49.

Davies, R.D., Gottesman, S.T. 1970, MN 149, 237.

Dewhirst, D.W., Yates, G.G. 1954, Obs. 74, 71.

Elsässer, H., Haug, U. 1960, ZfA 50, 121.

Fernie, J.D. 1963, AJ 68, 780.

FitzGerald, M.P. 1967, PhD Thesis, Case Western Reserve University.

Garoli, S.L., Varsavsky, C.M. 1966, ApJ 145, 79.

Georgelin, Y.P., Georgelin, Y.M. 1970, A & Ap 6, 349.

1971, A & Ap 12, 482.

Gottesman, S.T., Davies, R.D. 1970, MN 149, 263.

Greenberg, J.M. 1968, S & SS 7, Ed. B.M. Middlehurst and L.H. Aller, University of Chicago Press, Chicago, p. 221.

Habing, H.J. 1966, BAN 18, 323.

Hardie, R.H. 1962, S & SS 2, Ed. W.A. Hiltner, University of Chicago Press, Chicago, p. 178.

Heiles, C. 1967, ApJ 148, 299.

Herbig, G.H. 1970, Spectroscopic Astrophysics, Ed. G.H. Herbig, University of California Press, Berkeley, p. 237.

Hiltner, W.A. 1956, ApJ Suppl. 2, 389.

Hoag, A.A., Johnson, H.L., Iriarte, B., Mitchell, R.I., Hallam, K.L., Sharpless, S. 1961, Publ. U.S. Naval Obs., 2nd Series XVII, Part 7, 343.

Humphreys, R.M. 1970, AJ 75, 602.

Jager, G. de, Davies, R.D. 1971, MN 153, 9.

Johnson, H.L., Harris,D.L. 1954, ApJ 120, 196.

Johnson, H.L., Morgan, W.W. 1953, ApJ 117, 313.

Kerr, F.J. 1969, Ann. Rev. A & Ap 7, 39.

1970, IAU Symposium No. 38, Ed. W. Becker and G. Contopoulos, D. Reidel Publ. Co., Dordrecht, p. 95.

Kruit, P.C. van de, Oort, J.H., Mathewson, D.S. 1972, A & Ap 21, 169.

Lambrecht, H., Schmidt, K.H. 1957, AN 284, 71.

Lawrence, L.C., Reddish, V.C. 1965, Publ. Royal Obs. Edinburgh 3, 275.

Lilley, A.E. 1955, ApJ 121, 559.

Lynds, B.T. 1970, IAU Symposium No. 38, Ed. W. Becker and G. Contopoulos, D. Reidel Publ. Co., Dordrecht, p.26.

M^{c}Cuskey, S.W. 1949, ApJ 109, 426.

M^{c}Cuskey, S.W., Seyfert, C.K. 1947, ApJ 106, 1.

Merrill, P.W., Burwell, C.G. 1950, ApJ 112, 72.

Moffat, A.F.J., Vogt, N. 1973, A & Ap 23, 317.

Münch, G. 1955, ApJ 116, 575.

Nassau, J.J., Stephenson, C.B. 1963, Luminous Stars of the Northern Milky Way IV (LS IV), Hamburg-Bergedorf.

Pannekoek, A. 1933, Publ. Astro. Inst. Amsterdam No. 3.

Pannekoek, A., Koelbloed, D. 1949, Publ. Astro. Inst. Amsterdam No. 9.

Pavlovskaya, E.D., Sharov, A.S. 1971, SAJ 14, 849.

Pfleiderer, J., Mayer, U. 1971, AJ 76, 691.

Plaut, L. 1964, S & SS 5, Ed. A. Blaauw and M. Schmidt, University of Chicago Press, Chicago, P. 302.

Pratt, N.M. 1971, Publ. Royal Obs. Edinburgh 8, 109.

Purgathofer, A. Th. 1969, Lowell Obs. Bull. 7, 98.

Reddish, V.C. 1968, Quart. J.R.A.S. 9, 409.

1969, MN 143, 139.

1970, Phys. Bull. 21, 351.

Rhijn, P.J. van 1929, Publ. Kapteyn Astro. Lab., Groningen, No. 43.

Roach, F.E., Megill, L.R. 1961, ApJ 133, 228.

Roberts, M.S. 1962, AJ 67, 79.

Roberts, W.W. Jr. 1972, ApJ 173, 259.

Sandage, A. 1961, The Hubble Atlas of Galaxies, Carnegie Institute of Washington, Washington.

Schmidt-Kaler, Th. 1964, ZfA 58, 217.

1965, Landolt-Börnstein, New Series, Group 6, Vol. 1, Ed. H.H. Voigt, Springer-Verlag, Berlin, p. 284.

1971, Structure and Evolution of the Galaxy, Ed. L.N. Mavridis, D. Reidel Publ. Co., Dordrecht, p. 85.

Schmidt-Kaler, Th., Dachs, J. 1968, ESO Bull. No. 5, 15.

Seitter, W.C. 1970, Publ. Astro. Inst., Dummlers, Bonn.

Serkowski, K. 1963, ApJ 138, 1035.

Shane, W.W. 1971, Dr. of Sci. Thesis, Leiden Obs.

Shane, W.W., Bieger-Smith, G.P. 1966, BAN 18, 263.

Sharov, A.S. 1971, SAJ 14, 942.

Sharpless, S. 1959, ApJ Suppl. 4, 257.

Smith, L.F. 1968, MN 138, 109.

1968b, MN 141, 317.

Stephenson, C.B. 1966, AJ 71, 477.

Stephenson, C.B., Sanduleak, N. 1971, Luminous Stars of the Southern Milky Way, Publ. Warner & Swasey Obs. 1, No. 1.

Stock, J., Nassau, J.J., Stephenson, C.B. 1060, Luminous Stars of the Northern Milky Way II (LS II), Hamburg-Bergedorf.

Tammann, G.A. 1970, IAU Symposium No. 38, Ed. W. Becker and G. Contopoulos, D. Reidel Publ. Co., Dordrecht, p. 236.

Vaucouleurs, G. de 1970, IAU Symposium No. 38, Ed. W. Becker and G. Contopoulos, D. Reidel Publ. Co., Dordrecht, p. 18.

Wackerling, L.R. 1970, Mem. R.A.S. 73, 153.

Walker, G.S. 1971, Publ. Royal Obs. Edinburgh 8, 103.

Walker, M.F. 1972, ApJ 175, 89.

Weaver, H.F. 1949, ApJ 110, 190.

1970, IAU Symposium No. 38, Ed. W. Becker and G. Contopoulos, D. Reidel Publ. Co., Dordrecht, p. 126.

Wesselius, P.R., Sancisi, R. 1971, A & Ap 11, 246.

Wickramasinghe, N.C. 1967, Interstellar Grains, Chapman and Hall, London, p. 51.

Zimmermann, H. 1968a, AN 290, 193.

1968b, AN 290, 211.

1970, AN 292, 17.

1971, AN 293, 71.